Department of Forest Products Technology

Surface-modified nanoparticles for ultrathin coatings

Tiina Nypelö

Aalto University

DOCTORAL DISSERTATIONS

Aalto University publication series
DOCTORAL DISSERTATIONS 12/2012

Surface-modified nanoparticles for ultrathin coatings

Tiina Nypelö

Doctoral dissertation for the degree of Doctor of Science in Technology to be presented with due permission of the School of Chemical Technology for public examination and debate in Auditorium Puu2 at the Aalto University School of Chemical Technology (Espoo, Finland) on the 17th of February 2012 at 12 noon.

Aalto University
School of Chemical Technology
Department of Forest Products Technology
Forest Products Surface Chemistry

Supervisor
Professor Janne Laine

Instructor
Associate Professor Monika Österberg

Preliminary examiners
Dr. Jarkko Saarinen, Åbo Akademi, Finland
Dr. Michael Dickey, North Carolina State University, USA

Opponent
Professor Juan Hinestroza, Cornell University, USA

Aalto University publication series
DOCTORAL DISSERTATIONS 12/2012

ISBN 978-952-60-4498-9 (printed)
ISBN 978-952-60-4499-6 (pdf)
ISSN-L 1799-4934
ISSN 1799-4934 (printed)
ISSN 1799-4942 (pdf)

Unigrafia Oy
Helsinki 2012

Finland

The dissertation can be read at http://lib.tkk.fi/Diss/

441 697
Printed matter

Author
Tiina Nypelö

Name of the doctoral dissertation
Surface-modified nanoparticles for ultrathin coatings

Publisher Aalto University School of Chemical Technology

Unit Department of Forest Products Technology

Series Aalto University publication series DOCTORAL DISSERTATIONS 12/2012

Field of research Forest Products Chemistry

Manuscript submitted 18 October 2011 **Manuscript revised** 17 January 2012

Date of the defence 17 February 2012 **Language** English

☐ **Monograph** ☒ **Article dissertation (summary + original articles)**

Abstract

Nanoparticle modification and their utilization in the modification of planar substrates were examined. Emphasis was placed on two topics: the control of layer structure during formation and the alteration of the wetting characteristics of modified surfaces. Layer formation was investigated by adsorbing nanoparticles with a distinct shape and charge onto a nanofibrillated cellulose (NFC) substrate. In addition, nanosized silica particles and NFC were adsorbed sequentially with an oppositely charged polyelectrolyte onto an NFC substrate in order to explore the structures achievable using layer-by-layer assembly. Evidently, the utilization of nanoparticles in layer formation demands the control of the nanoparticle dispersion stability and particle affinity to the substrate. When combining nanoparticles with other substances, the properties of the particles define the layer structure; large fibrils were able to form a stratified layer, while silica nanoparticles were able to penetrate the preceding layer and transform the structure into a uniform network of polyelectrolyte and nanoparticles.

The effect of nanoparticle surface modification on dispersion properties and on the structure and properties of the layers formed were also of interest. Modification of nanosized silica and precipitated calcium carbonate particles was conducted by treatment with oppositely charged substances. This treatment resulted in stable nanoparticle dispersions able to be further modified with hydrophobic sizing agents. In addition to enhanced stability and functionality, the polyelectrolyte treatment could be used to affect the interaction of the nanoparticles with the other dispersion constituents.

Wetting of a smooth and dense substrate was not affected by the nanoscale roughness caused by the nanoparticle coating on the substrate. In order to affect substrate hydrophobicity, chemical hydrophobicity was deemed necessary. The combination of modified nanoparticles and a hydrophobic emulsion resulted in a nanostructure able to change the wetting characteristics of a planar substrate. Treatment of a smooth substrate with a hydrophobic dispersion resulted in slightly enhanced surface hydrophobicity. On paper, the combination of micron and nanoscale roughness with chemical hydrophobicity resulted in a significant increase in hydrophobicity. The coatings consisted of a thin nanoparticle structure with evenly distributed particles. In addition to use as a paper surface treatment, a layer, consisting of inexpensive particles allowing simple surface modification, could be used to functionalize planar substrates and enable the use of paper as a sustainable substrate, even in applications beyond its traditional use.

Keywords Nanoparticle adsorption, dispersion stability, surface modification, ultrathin coatings, layer-by-layer assembly, wetting

ISBN (printed) 978-952-60-4498-9 **ISBN (pdf)** 978-952-60-4499-6

ISSN-L 1799-4934 **ISSN (printed)** 1799-4934 **ISSN (pdf)** 1799-4942

Location of publisher Espoo **Location of printing** Helsinki **Year** 2012

Pages 163 **The dissertation can be read at** http://lib.tkk.fi/Diss/

Aalto-yliopisto

Tiivistelmä

Aalto-yliopisto, PL 11000, 00076 Aalto www.aalto.fi

Tekijä
Tiina Nypelö

Väitöskirjan nimi
Nanopartikkeleiden pintamodifiointi ja käyttö tasomaisten pintojen muokkaamisessa

Julkaisija Aalto-yliopisto Kemian tekniikan korkeakoulu

Yksikkö Puunjalostustekniikan laitos

Sarja Aalto University publication series DOCTORAL DISSERTATIONS 12/2012

Tutkimusala Puunjalostuksen kemia

Käsikirjoituksen pvm 18.10.2011 **Korjatun käsikirjoituksen pvm** 17.01.2012

Väitöspäivä 17.02.2012 **Kieli** Englanti

☐ **Monografia** ☒ **Yhdistelmäväitöskirja (yhteenveto-osa + erillisartikkelit)**

Tiivistelmä

Tässä työssä tutkittiin nanopartikkeleiden käyttöä tasomaisten pintojen muokkauksessa. Erityisesti keskityttiin nanopartikkelikerroksen rakenteeseen sekä muodostuneen rakenteen vaikutukseen tason pintaominaisuuksiin. Nanopartikkelikerroksen muodostumista havainnoitiin muun muassa tutkimalla kahden ominaisuuksiltaan hyvin erilaisen nanopartikkelimateriaalin asettumista selluloosapinnalle. Nanopartikkelidispersion stabiilisuudella, partikkeleiden ja pinnan varauksella sekä liuoksen väliaineen ominaisuuksilla havaittiin olevan välitön vaikutus muodostuneen pinnan rakenteeseen. Nanopartikkeleiden adsorboimisen lisäksi kerroksen rakentumista hallittiin adsorboimalla nanopartikkelidispersio selluloosapinnalle vuorotellen vastakkaisesti varautuneen polyelektrolyyttiliuoksen kanssa. Tämä niin sanottu monikerrosrakenne muodostui eri tavoin riippuen käytettyjen nanopartikkeleiden koosta ja muodosta. Pienet silikananopartikkelit pystyivät tunkeutumaan polyelektrolyyttikerrokseen, ja monikerrosrakenne tasoittui rakenteeksi, jossa nanopartikkelit olivat jakautuneet tasaisesti polyelektrolyyttimatriisiin. Pitkät nanofibrillit taas muodostivat kerroksellisen rakenteen polyelektrolyyttikerroksen kanssa, eikä huomattavaa kerrosten sekoittumista havaittu.

Nanopartikkeleiden pintaominaisuuksilla on suuri vaikutus muodostuneeseen rakenteeseen. Niinpä nanopartikkeleita modifioitiin adsorboimalla pintaan vastakkaisesti varautunut polyelektrolyyttikerros, jonka avulla dispersioiden stabiilisuutta sekä partikkeleiden pintavarausta pystyttiin muokkaamaan. Lisäksi modifioinnilla pystyttiin joissakin tapauksissa vaikuttamaan nanopartikkeleiden vuorovaikutukseen muiden dispersion ainesosien kanssa.

Nanopartikkeleiden aiheuttama karheus tasolla todettiin hyödyttömäksi nesteiden leviämisominaisuuksien muuttamisessa. Yhdistämällä nanopartikkelit hydrofobisten materiaalien kanssa vesidispersiossa pystyttiin luomaan päällystyskerros, jolla tasaisen pinnan kastumiseen voitiin vaikuttaa. Muodostamalla sama rakenne paperin päälle, siis yhdistämällä mikro- ja nanoluokan karheus kemialliseen hydrofobisuuteen, valmistettiin erittäin vettähylkivä pinta. Vedenkeston lisäksi tällaista hyvin tarkasti määriteltyä nanopartikkelirakennetta, esimerkiksi paperin päällysteenä, voidaan käyttää lisäämään pinnan funktionaalisuutta, ja lisätä niin tämän luonnonmukaisen pohjamateriaalin käyttöä myös muualla kuin perinteisessä tarkoituksessaan.

Avainsanat Nanopartikkeleiden adsorbointi, dispersiostabiilisuus, pintamuokkaus, ohutpäällysteet, nesteen leviäminen pinnalla

ISBN (painettu) 978-952-60-4498-9 **ISBN (pdf)** 978-952-60-4499-6

ISSN-L 1799-4934 **ISSN (painettu)** 1799-4934 **ISSN (pdf)** 1799-4942

Julkaisupaikka Espoo **Painopaikka** Helsinki **Vuosi** 2012

Sivumäärä 163 **Luettavissa verkossa osoitteessa** http://lib.tkk.fi/Diss/

Preface

The work presented in this thesis was performed between the years 2007 and 2011 at Helsinki University of Technology, which in 2010 merged with Helsinki School of Economics and Helsinki School of Art and Design forming Aalto University. The work was carried out at the department of Forest Products Technology in research group of forest products surface chemistry, mostly in research projects "Nanopate" funded by UPM and Tekes, and "Silsurf" funded by KCL and Tekes.

These years at the Forest products department have taught me a lot of science, yet of life too. I'm indebted to many for helping me along this tough journey. The initiative to work at the Department of Forest Products Technology is credit to Professor Ali Harlin, who guided my master thesis work at Tampere University of Technology and saw the potential graduate student in me. He suggested me to contact Professor Laine, who was seeking for new students, and in December 2006 we met with Janne and Monika. Despite the interview, they welcomed me to work in the research group of forest products chemistry.

I am grateful to Janne for accepting me as a graduate student and for guiding me through these years. Working in this group has been the best time of my life. Not only have I learned a lot about science and chemistry, I have also enjoyed working with the best colleagues one could imagine. I am indebted to Monika for the massive amount of work you have conducted to revise my manuscripts and presentations again and again. Without you I would not have been able to finish my work.

I thank my co-authors Jani, Jie, Lei, Mikko, Hanna and Jouni. It was a pleasure working with you. Jani, thank you for the several informal introductions to force measurements, and answers to my many questions on numerous topics. You've always been easy to talk to. Hanna, I will never forget the inspiring start to our joint publication at Wappu few years ago. It took us some time to finish the experiments and the manuscript, yet we succeeded!

It is very difficult to put in writing the words I would like to dedicate to Elli and Laura. I met you both in the very beginning of this thesis work and I have gained two very good friends. We have shared many scientific discussions, but I have to admit, mostly on other topics. Thank you for the continuous support and for making the working days, and several non-working evenings, fun. I hope, and I'm sure, that we'll stay in touch also in the future.

There are several very special men at the department who deserve a massive thank you. Niko, thank you for the lively discussion regarding polymers, not to mention the concept of electrophoretic mobility. Also thank you for the several non-scientific things that I highly appreciate: the Spanish discussions on our own superior level, hearing the

non-existent music with me etc... Hannes, thank you for all the help, support and the questionable jokes, as well as for so many times taking the sharpest edge off from my bad moods. Mikhail, thank you for lending me coins for the coffee machine as well as sharing the Coca-Cola bar in the coffee room. Oh yeah, and thank you for being the most genuine and warm-hearted person I have ever met. Timbe, it was a pleasure to get to know you. Especially I have enjoyed the many occasions being able to share the dance floor with you. Eero, thank you for helping me with data analysis, with journal choices as well as for being so kind and approachable person.

I'm grateful to Miro, Sole, Justin, Marcelo and Ola (and many others), not to mention Profe Rojas, for creating the international atmosphere at the department. It has been an eye-opener for me to get to know you all. Thank you Ola also for helping me with this thesis and whenever I needed your assistance. Ilari and Sole, thank you for the support, help and friendship, I have enjoyed the many memorable evenings spent with you, and of course, I appreciate both of your help at work. Elina, Raili, Katri and Anni, thank you for creating the enjoyable atmosphere at work. Ingrid, thank you for your support and care during the last crucial days before the thesis printing. I want to thank all the members of Teh Band for the many inspiring musical experiences. Tuomas, thank you for giving me the position at the rhythm section, it really meant a lot to me.

Joe, thank you for reading my manuscripts and teaching me many useful things about English grammar, not to mention science. Leena-Sisko, your enthusiasm towards science is catching, after all, you got me to read the articles by guru Tougaard. Huge thanks to you Anna, Paula and Karoliina for the N-club meetings. I will never forget our few, yet utmost inspiring meetings and lab experiments.

My labwork could not have been finished without the excellent assistance of our lab technicians Risu, Anu, Marja, Aila and Rita. In addition to always helping me with measurements, I have felt that I can rely on you in anything. Also Ari, Timo, Kati, Anne J. and Riitta are gratefully acknowledged for helping me with the many practicalities.

The last five years passed so fast, yet when I think back, there have been a massive amount of memorable, fun events and incidents along the way that I will never forget. I truly wish that we'll be able to maintain the friendships gained and stay in touch!

I'm grateful to my family for never questioning my career choice. The other family, Heikki and Anneli, I acknowledge for questioning everything. Tuomas, thank you for believing in me and being my best friend, every day.

Helsinki, January 8th, 2012.
Tiina Nypelö

List of publications

This thesis is a summary of the author's work regarding exploitation of nanoparticles in ultrathin coating layers. The thesis is mainly based on the results presented in five publications, which are referred to by Roman numerals in the text. Some previously unpublished data is also presented.

Paper I

Nypelö, T., Pynnönen, H., Österberg, M., Paltakari, J. and Laine J. Interactions between inorganic nanoparticles and cellulose nanofibrils. Accepted to *Cellulose*.

Paper II

Salmi, J., Nypelö, T., Österberg, M. and Laine, J. (2009) Layer structures formed by silica nanoparticles and cellulose nanofibrils with cationic polyacrylamide (C-PAM) on cellulose surface and their influence on interactions. *BioResources* 4(2), 602-625.

Paper III

Nypelö, T., Österberg, M., Zu, X. and Laine, J. (2011) Preparation of ultrathin coating layers using surface modified silica nanoparticles. *Colloids and Surfaces A: Physicochemical and Engineering Aspects* 392(1) 313-321.

Paper IV

Nypelö, T., Österberg, M. and Laine, J. (2011) Tailoring surface properties of paper using nanosized precipitated calcium carbonate particles. *ACS Applied Materials & Interfaces* 3(9), 3725-3731.

Paper V

Dong, L., Nypelö, T., Österberg, M., Laine, J. and Alava, M. (2010) Modifying the wettability of surfaces by nanoparticles: experiments and modeling using the Wenzel law. *Langmuir* 26(18), 14563-14566.

Author's contribution

I, III-IV

Tiina Nypelö was responsible for the experimental design with the co-authors, performed the experimental work and analyzed the results. She wrote the manuscript with the co-authors (responsible author).

II

Tiina Nypelö was responsible for the experimental design with the co-authors, performed the QCM-D measurements, analyzed the corresponding results and wrote the corresponding part of the manuscript.

V

Tiina Nypelö was responsible for the experimental design with the co-authors, performed the experimental part of the measurements, analyzed the corresponding results and wrote the corresponding part of the manuscript.

List of key abbreviations

AFM	atomic force microscopy
AKD	alkyl ketene dimer
A-PAM	anionic polyacrylamide
ASA	alkenyl succinic anhydride
CMC	carboxymethyl cellulose
C-PAM	cationic polyacrylamide
DLVO	Derjaguin, Landau, Verwey and Overbreek
LbL	layer-by-layer
nanoPCC	nanosized precipitated calcium carbonate
NFC	nanofibrillated cellulose
PAH	poly(allylamine) hydrochloride
PCC	precipitated calcium carbonate
PEI	polyethyleneimine
PVAm	polyvinylamine
QCM-D	quartz crystal microbalance with dissipation monitoring
rms	root mean square
SNP	silica nanoparticles
XPS	x-ray photoelectron spectroscopy

Table of contents

1 Introduction and objectives of the study

A demand for higher efficiency in business operations accompanied with the challenging state of the global economy has led to radical changes in industries worldwide. Increasing competition and balancing between costs and pricing has resulted in the companies' urge to develop corporate strategies as well as to reassess product portfolios. Consequently, improved efficiency is sought, among other things, by applying existing competence to new products outside the common product range. Like others, the forest products industry has been exposed to the need to reform its ways of working (Koepenick 2003, Moon et al. 2006).

In a variety of disciplines nanotechnology has been considered to have the potential to improve existing products and to boost the development of new ones (Koepenick 2001, Wegner & Jones 2006). The increased interest towards research in nanotechnology has arisen from the unique properties of nanoparticles, that is, quantum effects, length scales smaller than the visible light, size-dependent properties and large surface area to volume ratio. Nanotechnology has been employed in various applications with hopes of new and improved properties accompanied by reduced costs (Atalla et al. 2005, Kamel 2007).

The rise of nanotechnology has led to increasing development of cellulose nanomaterials, particularly cellulose nanofibrils (Herrick et al. 1983, Turbak et al. 1983, Pääkkö et al. 2007, Siro & Plackett 2010, Eichhorn et al. 2010) and nanocrystals (Hamad 2006, Habibi et al. 2010). These organic materials have been suggested to be suitable as strength promoters and barrier materials (Taniguchi & Okamura 1998, Azizi Samir et al. 2004, Ahola et al. 2008a, Henriksson et al. 2008, Syverud & Stenius 2009, Aulin et al. 2010a, Guimond et al. 2010), as well as in advanced applications, for example, in preparing transparent flexible films (Yano et al. 2005, Nogi et al. 2009, Okahisa et al. 2009), magnetic or superabsorbent aerogels (Kettunen et al. 2011, Korhonen et al. 2011, Olsson et al. 2011) and films with tunable optical properties (Beck et al. 2011). However, progress related to cellulose nanomaterials is still very much on the research and development level, and larger scale utilization is yet to emerge.

In addition to the progress and use of organic nanomaterials, development of inorganic nanoparticles has led to their exploitation in various applications, including paper related products. Nanoparticles are, among others, used to enhance the barrier properties of coatings (Sun et al. 2007) and the thermal stability of cellulose fibers (Lin et al. 2008). Although grades of nanosized pigment particles exist, their utilization in paper coatings has not yet been greatly studied. Paper is mainly coated to affect its appearance

and printing properties. The coat weight of a typical paper coating prepared using micrometer sized particles fluctuates from a few to tens of grams per square meter. Consequently, the thickness of the coatings is, even at its lowest, in the micrometer range. Hence, the development of nanosized pigments and their controlled exploitation in coatings can enable preparation of ultrathin coatings with a consequent decrease in the coat weight. This can lead to further reduced material costs.

The objective of this study was to explore how nanoparticles can be used to change surface characteristics of planar substrates by applying an ultrathin coating layer. The coatings prepared were even as thin as the submonolayer range. Within this thesis work these thin coatings are referred to as "coatings" or "surface treatments" and should be distinguished from the concept of traditional coatings. The inorganic nanoparticles used in this study were of silica, precipitated calcium carbonate and montmorillonite. The choice of these materials stems from interest in the development of nanoscale venues for paper surface treatments. However, the experiments performed also have a bearing in developing new nanotechnology solutions combining inorganic and organic materials.

A major part of the work was devoted to examine nanoparticle layer formation on planar substrates and the structures formed. The effect of the adsorption medium and particle properties on nanoparticle layer growth is presented in **Paper I,** and adsorption through layer-by-layer (LbL) assembly with polyelectrolytes is compared to polyelectrolyte/nanoparticle complex adsorption in **Paper II.** In order to obtain a thin coating layer with uniformly distributed particles, dispersion stability was considered an imperative. The aim was to reduce aggregation of the nanoparticles and to prepare stable nanostructures containing nanoparticles by particle surface treatment using a simple and upscalable method. Hence, nanoparticle surface modification by the adsorption of oppositely charged polyelectrolytes is evaluated in **Papers III** and **IV**. Throughout the experimental work, the wetting characteristics of the substrates were measured. Hence, as surface roughness has been found to have an effect on the wetting of surfaces (Bico et al. 2001, Bico et al. 2002, Callies & Quere 2005, Hsieh et al. 2005, Yoshimitsu et al. 2002, Spori et al. 2008), the role of surface roughness caused by nanoparticles is evaluated in **Paper V**.

This work attests that nanoparticle dispersion properties and particle interactions with a substrate are the determining factors when controllably constructing coating layers using nanoparticles. A stable dispersion is necessary for uniform particle distribution on a substrate. Dispersion stability can be enhanced by modifying particles with polymers. Furthermore, it is shown that nanoparticles in surface treatments enable a change in the surface characteristics of porous and nonporous substrates already with a submonolayer coating. These observations provide an interesting starting point, considering development of future paper-based products combining low-cost with high functionality.

2 Background

Nanotechnology is employed in a variety of industries exploiting materials with dimension from a few to hundreds of nanometers. Nanoparticles are considered to be a potential material in many applications due to reduced material consumption with respect to the benefits gained. In traditional industries manufacturing bulk products with high raw material consumption, such as paper, nanotechnology can provide substantial improvements. In paper industry nanoparticles are presently employed, for example, in flocculation and retention systems (Solberg & Wågberg 2003), in pigment and filler applications (Juuti et al. 2009, Koivunen et al. 2009) and in coatings (Neumann et al. 2005, Syverud & Stenius 2009).

2.1 Interactions and stability of nanoparticles in dispersions

Nanoparticles are often prepared, modified and applied as an aqueous dispersion, that is, a system where an aqueous medium carries immiscible particles, for example, liquid drops or solid particles. In a nanoparticle dispersion, the dispersion properties are dominated by the particle interactions. These interactions depend on the particle surface properties, their shape, size and the distance between them (Jiang et al. 2009). Additionally, the properties of the medium influence the dispersion properties (Metin et al. 2011).

One of the most important particle property is particle surface charge. It originates from the ionization of functional groups or adsorption of ions and charged molecules on the particle surface. In the case of minerals, for example, clay, the substitution of surface cations with lower valence cations contributes to the development of surface charge (Hu & Liu 2003, Cadene et al. 2005). The particle surface charge largely affects the interactions between dispersion constituents, and hence, the stability.

Due to their characteristic properties nanoparticles typically have a high tendency to aggregate, and hence, the dispersions are unstable. Firstly, the Brownian motion of the particles in a dispersion causes collisions, which leads to aggregation due to electrostatic interactions or chemical bonding. Secondly, the high surface area and low surface potential further enhances nanoparticle aggregation (Evans & Wennerström 1999, Kallay 2002). Thirdly, an equivalent surface-to-surface distance between particles is reached with a lower nanoparticle concentration than in a sub-micron particle dispersion. In

concentrated dispersions the distance between particles decreases, increasing the possibility of particle coagulation (Kamiya & Iijima 2010). By changing the particle surface properties, and consequently, the particle interactions, one can control dispersion stability and aggregate size.

In general, a particle dispersion is stable when particle-particle interactions are repulsive. The forces between sub-micron particles in a liquid medium can be described by the theory proposed by Derjaguin & Landau (1941) and Verwey & Overbreek (1948), also known as the DLVO theory. This theory considers the total interaction between similar particles to be the sum of attractive van der Waals forces and repulsive electrical double-layer forces (Fig. 1).

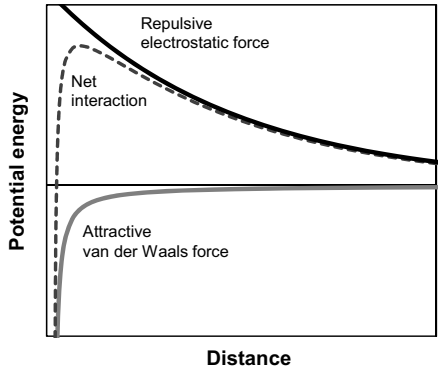

Figure 1. The DLVO theory. Schematic illustration of the energy to particle separation regarding repulsive double-layer, attractive van der Waals and their net interaction.

The van der Waals forces originate from the polarization of the electron clouds of atoms creating permanent and induced dipoles, where the Keesom interaction takes place between permanent dipoles, the Debye interactions between a permanent dipole and an induced dipole, and the London interaction between induced dipoles. The potential energy of interaction (V_{vdW}) between two spheres (with radii R_1 and R_2) can be calculated using the Hamaker method (1937),

$$\Delta V_{\mathrm{vdW}} = -\frac{A}{6D}\frac{R_1 R_2}{R_1+R_2} \qquad (2.1),$$

where D is the particle separation and A is the Hamaker constant, which is dependent on the material and can be calculated using, for example, Lifshitz theory (1956). These forces are attractive between identical particles in liquid.

Charged particles in liquid are surrounded by a cloud of oppositely charged counter-ions, which form an electrical double-layer (Fig. 2): In the inner layer (Stern layer) the ions are strongly bound to the surface and they move with the particle as it travels in the liquid, while ions in the outer layer are not bound to the particle surface and do not follow the particle. The counter-ion concentration gradually decreases with increasing distance from the particle surface, and in the bulk the counter-ion and the co-ion concentration is equal. When two particles of similar charge approach, their double-layers overlap causing an increase in the counter-ion concentration between the particles, and therefore, result in repulsion between the particles. The magnitude of the electrostatic repulsion depends on the surface potential and the thickness of the double-layer. The Debye length, κ^{-1}, can be used to characterize the thickness of the double-layer, that is, the distance at which the effective interaction is appreciable:

$$\kappa^{-1} = \sqrt{\frac{\varepsilon\varepsilon_0 kT}{e^2 I}}, \qquad I = \sum_{i=1} n_i z_i^{\,2} \qquad (2.2),$$

where ε is the dielectric constant of the medium, ε_o the permittivity of vacuum, k the Boltzmann constant, T temperature and e the elementary charge. I denotes the ionic strength where n_i is the ion concentration and z_i the valence of the counter-ions. It is evident that an increase in the ionic strength decreases the Debye length, and hence, affects the interaction of the particles upon collision, that is, the extent of repulsion.

The double-layer interaction between two charged particles in liquid originates from the increase in the ion concentration in the region where their double-layers overlap. The interaction energy can be calculated by a Poisson-Bolzmann equation. However, defining the repulsive electrical double-layer forces is complex and is not dealt with in detail here. In short, the potential energy of repulsive interaction between two identical spheres of radius R and separation D, can be expressed as:

$$\Delta V_{el} = 2\pi\varepsilon_0\varepsilon R\Phi_0^2 \exp^{-\kappa D} \qquad (2.3),$$

where π is the solvent permeability, Φ surface potential and κ a function of ionic composition. When considering the stability of ideal particles in a dispersion, the surface potential, valence, the ion concentration, and particle size are important.

The repulsive force is strongly dependent on changes in the surface potential, which affects the magnitude of repulsion. In practice, instead of the surface potential, the ζ-potential value is often used. It describes the properties of the slipping plane in the outer layer of the electrical double-layer (Fig. 2). A ζ-potential value is estimated by measuring

the mobility of the particles in an applied electric field. The electrophoretic mobility, U_e, is converted to a ζ-potential value using the Henry equation:

$$U_E = \frac{2\varepsilon\varepsilon_0\zeta f(\kappa a)}{3\eta} \qquad (2.4),$$

where η is the solvent viscosity and $f(\kappa a)$ is Henry's function, which in water is typically approximated to be 1.5. The ζ-potential value can be used to determine the magnitude of the repulsive electrostatic forces between particles. In general, it is a good tool to evaluate the stability of bare particles because the magnitude of repulsion between the particles determines their coagulation tendency (Cosgrove 2005). However, it is important to recognize that due to the compression of the electrical double-layer, an increase in ionic strength affects the mobility, and hence, the ζ-potential. Therefore, when non-surface potential determining ions are added into a dispersion, the electrophoretic mobility is changed even though surface potential remains constant. Also, especially with platey nanoclay, the ζ-potential value needs to be handled with caution due to the difference in the basal and edge charge properties causing overlap of the two potentials (Chang & Sposito 1996).

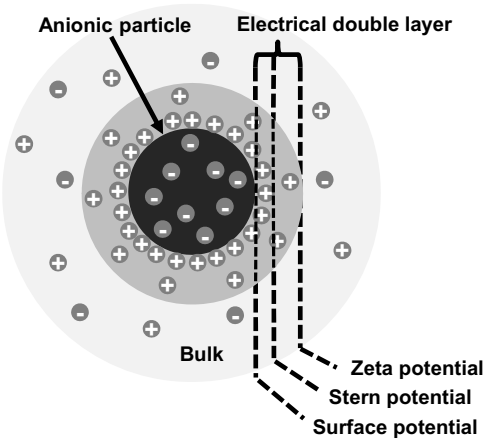

Figure 2. Electrical double-layer surrounding a charged particle in liquid.

In addition to the DLVO forces, interactions originating from polymers adsorbed on particle surfaces are, especially in practical systems, important regarding the stability of the particles in a dispersion. *Steric forces* are important when a polymer is adsorbed on a particle, causing a thick layer to extend from the particle surface into the solvent (Fleer et al. 1993). Consider when two polymer covered particles approach; overlap of the polymer layers leads to repulsion due to loss in entropy as the polyelectrolyte chains lose

their conformational freedom. This repulsion is determined by solvent-polymer, solvent-surface, polymer-surface and polymer-polymer interactions. Typically steric forces provide resistance towards coagulation, even when the dispersion electrolyte concentration increases (Ohshima 1995). However, if a polymer only partially covers a particle, the polymer tails and unoccupied surface sites can attract one another leading to flocculation through bridging (Åkesson et al. 1989, Miklavic et al. 1990, Biggs et al. 2000).

When a polymer carries charged groups it is possible that a given system is stabilized neither by electrostatic nor steric forces alone. The term *electrosteric force* is used to describe the situation where both steric and electrostatic forces are present (Fritz et al. 2002). This is the case when highly charged polyelectrolytes are used for particle stabilization.

In addition to the interactions described above, a few other forces can affect nanoparticle dispersions. *Hydration forces* are short-range structural forces, which originate from changes in the water medium between the approaching particles. Hydration forces are repulsive and originate from the energy required for the dehydration of the interacting surfaces containing adsorbed hydrated cations (Israelachvili & Pashley 1983, Pashley & Israelachvili 1984, Argyris et al. 2011). Evidently these forces are of importance with mineral surfaces (Yotsumoto & Yoon 1993) and are related to, for example, the swelling of clay (Pashley & Quirk 1984). *Hydrophobic forces* are long-ranged attractive forces between hydrophobic substances in water. These forces are often studied in surfactant systems (Yoon & Ravishankar 1996, Yoon et al. 1997). The hydrophobic effect is caused by hydrophobic substances interrupting the structure of the water medium. Reorientation of water molecules would balance the energy, but a loss in entropy of the system prevents this. Hydrophobic forces are important, for example, in emulsions when oil droplets in water can self-organize and coalesce (Israelachvili & Pashley 1984, Claesson & Christenson 1988). In papermaking, hydrophobic forces are utilized to control deposits (Wallqvist et al. 2006, Wallqvist et al. 2007). *Hydrodynamic forces* are caused by particles' movement in a liquid. A moving particle creates a flow in the dispersion, which generates a hydrodynamic repulsive force (Evans & Wennerström 1999). Hydrodynamic forces only affect the dynamics of the solution, not the equilibrium distribution.

2.2 Inorganic nanoparticles and their modification

Within this thesis work, various grades of inorganic nanoparticles were studied with respect to their use in the modification of planar substrates. The nanoparticles used were precipitated calcium carbonate, clay and silica. These materials are briefly introduced in this chapter.

Micrometer sized grades of PCC are typically used in paper coatings. Although nanosized grades are available, their use in coatings is limited and seldom reported. Nanostructures from PCC have been reported to change optical properties (Juuti et al. 2009) and to affect liquid absorption in paper (Gane & Rigway 2005). Studies about modification of papermaking PCC particles are exiguous, yet examples exist regarding particles being rendered hydrophobic (Domka 1994, Tang et al. 2006). Modification with fatty acids seems to be a particularly common way to modify surface hydrophobicity of these particles (Hu et al. 2009, Hu & Deng 2010). The poor acid resistance of the particles can be improved by surface treatment with fluosilicic acid (Kim & Lee 2002).

Clay particles are used, in addition to paper coating pigments, in applications providing improved barrier properties of paper (Sun et al. 2007) and enhancing the thermal properties of neat cellulose (Cerruti et al. 2008) and cotton (Delhom et al. 2010). Clay has also been combined with methyl cellulose to prepare films for food packaging (Tunc & Duman 2010). Additionally, nanosized grades have been used to prepare nanocomposites with polysaccharides (Chivrac et al. 2009). Clay has also been combined with nanofibrillated cellulose (NFC) to form paper coatings to improve paper properties important in printing (Mörseburg & Chinga-Carrasco 2009). Furthermore, a few studies report preparation of thin nanopaper from clay and NFC (Sehaqui et al. 2010, Liu et al. 2011a).

Silica particles are widely used in a plethora of applications, for example, in catalysts, paints and coatings (Bergna & Roberts 2006). In paper coatings, silica particles are used in inkjet coatings (Hladnik & Muck 2002). For variety of applications, silica particles are, in addition to stability, modified to prepare hydrophobic or functional particles (Bagwe et al. 2006). Hydrophobicity is commonly achieved by silylation (Goodwin et al. 1990, Tolnai et al. 2001) as schematically presented in Figure 3. Treatment with amino-organosilane, among others, can be used to functionalize particles (Vrancken et al. 1995). In addition to chemical modification, examples of particle modification by adsorption (Okubo & Suda 1999, Liufu et al. 2005, Janhom 2010), polymerization (Radhakrishnan et al. 2006, Lan 2007) or treatment with surfactants (Goloub et al. 1996, Lu et al. 2008) exist.

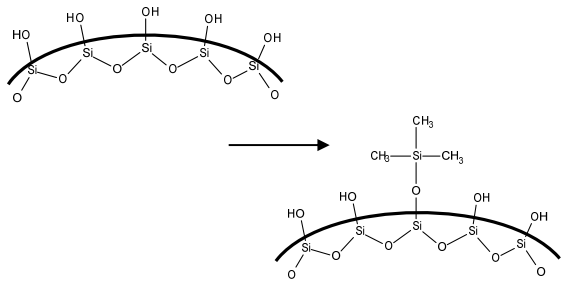

Figure 3. Schematic presentation of fully hydroxylated silica surface and its silylation (adapted from Bergna & Roberts 2006).

Modification of particles by the adsorption of polymers or surfactants is a facile way to alter particle surface characteristics (Lourenco et al. 1996, Schwarz et al. 2000, Studart et al. 2007). This method was also used in this thesis and is therefore briefly covered here. As already discussed, a polymer layer on the particle surface can generate steric repulsion between the modified particles, and hence, enhance stability. The adsorption of polymers on surfaces is, among others, affected by the adsorption energy and the polymer-solution interactions. In the case of polyelectrolytes, that is, charged polymers, adsorption in aqueous solutions is also affected by the polyelectrolyte charge, the surface charge density and the ionic strength (Fleer et al. 1993). The adsorption of a polyelectrolyte onto an uncharged substrate is weak if no chemical affinity exists. On a substrate with a charge of the same sign, adsorption is negligible at low ionic strength, but increases with increasing salt concentration due to decreased repulsion between the polyelectrolyte segments and the surface. Modification by oppositely charged substances, however, was used in this thesis to modify the silica and PCC nanoparticles. Polyelectrolyte adsorption on an oppositely charged substrate is driven by electrostatics. In general, an increase in the charge density of a polyelectrolyte decreases adsorption as less polyelectrolyte is required for charge compensation (Rojas 2002). When adsorption is purely electrosorption, that is, no chemical affinity exists, increasing the salt concentration can result in competing adsorption of counter-ions, which eventually leads to desorption of the polyelectrolyte at high ionic strength (van de Steeg et al. 1992). Conversely, in the case of a polyelectrolyte with high charge density, adsorption can increase due to internal screening of charges, hence enabling a more coiled structure to form. In the case of some polyelectrolytes, the solution pH affects the dissociation of the polyelectrolyte, and consequently, the charge, leading to high adsorption as the charge density decreases (Claesson et al. 1997, Notley & Leong 2010).

2.3 Nanoparticles for surface treatment of planar substrates

The work done in this thesis was focused on exploring the modification of surface characteristics of both smooth and porous planar substrates with nanoparticles. In fact, a few such applications already exist regarding, for example, the treatment of a paper substrate with nanoparticles to enhance hydrophobicity (Teisala et al. 2010) or antibacterial properties (Ghule et al. 2006) as well as to alter the wetting of smooth and dense substrates (Han et al. 2005, Bravo et al. 2007). In this study the emphasis regarding the use of nanoparticles as substrate modifiers was placed on two topics: control of the structure of the layer and control of surface wetting. Phenomena related to these subjects are discussed in Chapters 2.3.1 and 2.3.2.

2.3.1 Nanoparticle adsorption, layer-by-layer (LbL) assembly and adsorption of complexes

In order to modify planar surfaces using nanoparticles, it is essential to consider the nanoparticle layer build-up and the parameters affecting the structures formed. Adsorption of nanoparticles on a substrate is affected by, among other factors, particle-particle interactions and affinity towards the substrate. Alteration of the particle surface charge can be used to decrease particle aggregation, as well as to tune the attraction between the substrate and the particles. For example, the silica and clay nanoparticles used in this thesis both possess a pH-dependent charge due to the presence of silanol groups (Bergna & Roberts 2006), and therefore, adsorption can be affected by changing the pH. Also the electrolyte concentration and polydispersity have been shown to affect the resulting particle distribution (Hanarp et al. 2001). In theory, nanoparticles can form a thin rigid monolayer on a substrate. However, in practice the aggregation of nanoparticles often results in a layer constructed of stacks of nanoparticles instead. In such a case the unique properties of individual nanoparticles cannot be utilized.

In addition to creating structures using solely nanoparticles, they can be adsorbed onto surfaces as sequential layers with oppositely charged substances, typically polyelectrolytes. Early work on the matter was presented by Iler (1966). Later the subject has been studied by, among others, Kotov et al. (1995) exploring sequential adsorption of a cationic polyelectrolyte and negatively charged semiconductor particles. Especially silica nanoparticles have been widely used in LbL assembly (Ariga et al. 1997, Lvov et al. 1997, Sennerfors et al. 2002). In a structure combining nanoparticles and polyelectrolytes, it is worth noting, that unlike particles, polyelectrolytes can change their conformation (loops, tails and trains) depending on the solution properties (Shiratori & Rubner 2000, Messina

et al. 2004, Notley et al. 2005). The structure of the polyelectrolyte layer is also affected by properties such as molecular weight and charge density.

LbL assembly with nanoparticles and polyelectrolytes has been reported to form a stratified layer (Ariga et al. 1997, Lvov et al. 1997). This is in accordance with the commonly accepted concept of multilayering pioneered by Decher (1997). However, formation of a layer consisting of a uniform matrix of the particles and polyelectrolyte instead of a stratified structure is possible (Sennerfors et al. 2002). Studies exploring LbL formation often discuss the role of the substrate on the layer formation and many of these studies show that the substrate can be used as a tool to affect layer formation (Buron et al. 2007, Aulin et al. 2008, Wågberg et al. 2008). However, as the layer-by-layer assembly proceeds, the outer adsorbed layer determines the layer growth (Wang et al. 2011).

Lately efforts have been made to investigate multilayer formation involving cellulose nanofibrils as one of the components (Wågberg et al. 2008, Aulin et al. 2010b). Such systems as well as LbL formation with cellulose nanofibrils of varying charge (Eronen et al. *in press*), are suggested to provide a way to build bionanomaterials. In addition to fundamental studies typically performed on planar substrates, the LbL technique has found more practical applications, and has been employed in treating cellulosic fibers to improve fiber properties, fiber matrix strength and fiber adhesion (Wågberg et al. 2002, Eriksson et al. 2006, Lingström et al. 2006, Enarsson & Wågberg 2007, Lingström et al. 2007, Hyde et al. 2007a).

Besides using LbL assembly, structures containing multiple constituents can be prepared using colloidal complexes. Complexes are formed by combining two counterparts carrying opposite charges, which leads to spontaneous formation of the complex structure. Typically complexes are formed of two oppositely charged polyelectrolytes but particles and polyelectrolytes can also be used (Ulrich et al 2004). Complex formation is entropically driven due to the release of counter-ions, causing an entropy gain favoring complexation (Bucur et al. 2006, Xiao et al. 2009). The properties of complexes naturally vary significantly depending on the building blocks, preparation method and component properties (Holappa et al. 2003, Saarinen et al. 2008, Ankerfors et al. 2010). The charge density, molecular weight of the polyelectrolytes and the charge ratio affect their properties (Mende et al. 2002, Salmi et al. 2007a).

The adsorption of complexes on a planar substrate differs from LbL formation because ready-made structures are adsorbed onto the substrate instead of the constituents being sequentially adsorbed (Fig. 4). Depending on the coverage and charge of the outermost layer, multilayer formation can continue, while with complexes adsorption is limited to the available adsorption sites on the substrate. The layer formed by the complexes can then bind water in the structure making the layer dissipative and hindering adsorption of more “layers”. Moreover, it has been proposed that an increase in the

thickness of a complex layer is hindered by the large complex size in comparison to the Debye length. Hence, only a small amount of the complex interacts with the substrate and contributes to the entropy gain (Ankerfors et al. 2009). Shovsky et al. (2011) reported that complex adsorption is highly affected by the complex charge, and therefore, by electrostatic interactions.

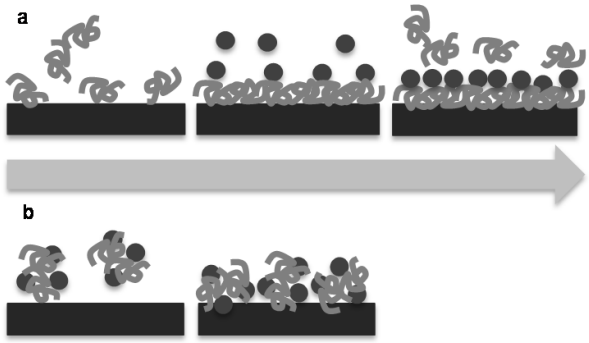

Figure 4. Layer formation by (a) layer-by-layer and (b) complex adsorption.

Few studies comparing the difference between multilayer and complex adsorption have been conducted. Saarinen et al. (2008) found that with a low amount of polyelectrolyte complexes a fairly thick and loose layer can be constructed, while with multilayer assembly, a high amount of polyelectrolytes was deposited and a dense layer was formed. Ankerfors et al. (2009) have reported that the adsorbed amount in complex structures is low in comparison to multilayer formation. These conclusions are logical considering the differences in the layer formation between the two techniques: multilayer assembly enables a more ordered structure to be formed on the surface than complex adsorption.

2.3.2 Effect of nanoparticles on wetting of dense and porous substrates

Throughout the thesis work the wetting characteristics of the created nanoparticle layers were assessed. Although advances in nanoparticle research have increased the number of applications concerning control of the wetting of substrates using small particles (Shibuichi et al. 1996, Quéré 2005, Feng & Jiang 2006), the wetting of nanoparticles or wetting affected by nanoparticles is still a seldom examined phenomenon. In studies of nanoparticle induced hydrophobicity the surface layer described often consists of a packed (Yan et al. 2007, McConnell et al. 2009) or an unevenly covered surface structure of nanoparticles, causing roughness greater than the monolayer range (Hsieh et al. 2005, Yüce & Demirel 2008). Therefore, in paper V, the effect of nanoparticles, and more

specifically, of nanoscale roughness on the wetting of a planar substrate was examined. The related phenomena are discussed in this chapter. Additionally, the wetting of paper is briefly reviewed, as nanoparticle coatings were also applied on paper substrate in Papers III and IV.

The wetting of a substrate is determined by its surface energy, the adhesion, that is the affinity between the substrate and the drop of the wetting liquid, and the geometry of the drop and the surface, among other factors. When the adhesion between the wetting drop and the substrate exceeds the cohesion of the liquid, the drop spreads on the substrate. Otherwise the drop will form a contact angle with the substrate. When the contact angle is above 90°, the surface is said to be hydrophobic. Materials with contact angle above 150° are commonly referred to as superhydrophobic. The movement of the contact line between the drop and the solid, that is, the spreading of the drop is defined by the competition between the interfacial energies for solid-vapor, solid-liquid and liquid-vapor interfaces.

In the simplest case of wetting, a smooth and uniform surface is wetted by a droplet (Fig. 5a). Wetting of such surface can be described by Young's equation:

$$\cos\theta_{\mathrm{Y}} = \frac{\gamma_{SV} - \gamma_{SL}}{\gamma_{LV}} \qquad (2.5),$$

where θ_Y is the equilibrium contact angle and γ_{SV}, γ_{SL} and γ_{LV} are the solid-vapor, solid-liquid and liquid-vapor surface energies, respectively. Silica surfaces used in this thesis are smooth enough to enable their wetting to be described using Young's model. Variation in the substrate geometry, that is, in roughness or in chemical composition complicates the wetting phenomenon and makes the prediction of the equilibrium contact angle challenging. A wetting model by Wenzel (1936) takes surface roughness into account (Fig. 5b) by introducing a roughness factor R_w,

$$\cos\theta_{\mathrm{W}} = R_{\mathrm{W}}\cos\theta_{\mathrm{Y}} \qquad (2.6).$$

With contact angles below 90°, the contact angle in the Wenzel model (θ_W) is lower than that of Young's prediction, while the opposite is true with angles above 90°. When the surface roughness is even higher, wetting is predicted with the Cassie-Baxter model (1944). The Cassie-Baxter model describes the case where air pockets are trapped under the droplet (Fig. 5c),

$$\cos\theta_{\mathrm{C}} = R_{\mathrm{F}}F\cos\theta_{\mathrm{Y}} + (1-F)\cos\theta_{\mathrm{A}} \qquad (2.7).$$

The Cassie-Baxter contact angle (θ_C) is a function of the area fraction of the solid wetted by liquid (F) under the drop, the roughness ratio of the wetted area (R_F) and the Young contact angle (θ_Y). As $\cos\theta_A$ denotes the contact angle of droplet in air (θ_A=180°) the equation (2.7) can be simplified into:

$$\cos\theta_C = R_F F \cos\theta_Y + F - 1 \qquad (2.8).$$

Wetting of superhydrophobic substrates can be described with the Cassie-Baxter wetting model. Their difference to hydrophobic surfaces is the ability of the wetting droplet to roll off the surface already at a low sliding angle. This effect originates from micrometer scale roughness accompanied by nanoscale roughness enabling low adhesion between the drop and the substrate (Feng et al. 2002, Martines et al. 2005, Bhushan et al. 2009a, Bhushan et al. 2009b).

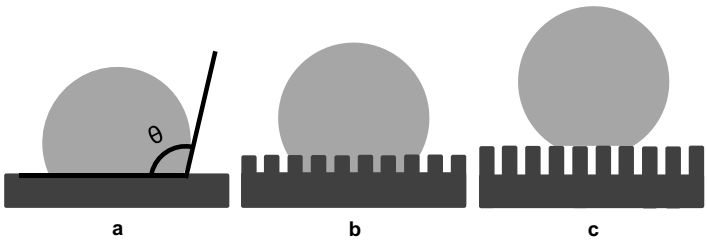

Figure 5. Illustrations of the (a) Young, (b) Wenzel and (c) Cassie-Baxter approaches to describe wetting.

Unlike smooth and well-defined substrates such as the silica wafers, paper is a heterogeneous and rough substrate. The roughness is generated from its surface heterogeneity and the fact that paper is constructed of a fiber network containing empty spaces between the fibers. Consequently, wetting of paper is affected by the rough and porous structure. Additionally, wood fibers, the main raw material of paper, adsorb water eagerly and swell, further complicating the definition of the wetting process. Because high liquid adsorption causes problems, for example, during the printing process as ink can penetrate into the porous paper and spread along the fiber matrix, controlling wetting of paper is of concern. In order to increase paper's resistance to wetting it is typically coated with hydrophobic substances, often called sizing agents (Hubbe 2006). Internal sizing is added to the pulp prior to web formation whereas surface sizing can be used as a pretreatment for coated papers, or as a finish. Surface sizing binds particles on the paper surfaces, increases strength and decreases water absorbance (Wilson 2005).

Wetting of paper by a liquid drop has been shown to take place in two stages; first, a pseudo-equilibrium contact angle is reached, and then the drop adsorbs into the structure, causing a decrease in the contact angle (Modaressi & Garnier 2002). In general,

paper roughness affects wetting in two ways; it influences the adhesion between the wetting drop and the substrate and alters the spreading dynamics of the drop. In the latter case the wetting drop experiences roughness as a horizontal restriction for spreading (Cazabat 1987, Cazabat 1989, Decker & Garoff 1997, Moulinet et al. 2002). Meanwhile, porosity affects the penetration of water into the structure. For a cylindrical pore, it is affected by the contact angle, the liquid-vapor interfacial tension and the radius of the pore. In the case of paper, the rate of penetration is an intricate combination of pore size, pore connectivity and the chemical properties of the surface and pores (Alleborn & Raszillier 2004). A few studies (Hyväluoma et al. 2006) state that despite the complexity, the liquid penetration in paper can be described using the simplified models, such as the well-known theory by Lucas (1918) and Washburn (1921). Nevertheless, claims also exist that a model describing the wetting of a single capillary is not adequate to predict wetting of paper (Schoelkopf et al. 2002). For example, in the case of ideal capillaries, spontaneous wetting takes place only when contact angle is less than 90° (Cazabat 1989, Schoelkopf et al. 2000, Ridgway & Gane 2006). However, with commercial paper grades, the often heterogeneously distributed sizing agents allow water vapour uptake on hydrophilic spots even on hydrophobic paper (von Bahr et al. 2004). It is also recognized that pore size has an effect on paper wetting and presence of fine pores is known to increase the penetration rate in comparison to large pores (Schoelkopf et al. 2000). This can be described by the adaptation made to the Washburn theory by Bosanquet (1923) regarding the notion that pores of optimal diameter will fill very fast, while larger ones are bypassed by the liquid. The parameters and their combination have been described in several studies related to wetting regarding paper coatings and printing (Gane et al. 2000, Schoelkopf et al. 2000, Ridgway & Gane 2002, Daniel & Berg 2006, Ridgway & Gane 2006).

3 Experimental

An overview of the materials and methods used in this thesis is presented in this chapter. Some theoretical principles as well as the advantages and disadvantages of the main methods are briefly discussed. A detailed description of the materials and methods used can be found in the attached Papers I-V.

3.1 Materials

3.1.1 Inorganic nanoparticles

Inorganic nanoparticles of silica, precipitated calcium carbonate and montmorillonite clay were used throughout the experimental work. Among other uses, these materials are of interest as pigments for paper surface treatments. The nanosized particles were used in this thesis for constructing nanostructures on planar silica, cellulosic and paper substrates. Progress in the utilization of nanosized pigments in surface treatments can enable preparation of ultrathin coating layers. Moreover, incorporation of an organic substance with inorganic nanoparticles can lead the way to the development of hybrid materials. The silica sol used in Papers II, III and V was of commercial grade (Bindzil 40/130, Eka Chemicals AB, Sweden) containing hydrophilic silica nanoparticles (SNP) with a diameter of 25 nm and average specific surface area of 130 $m^2\ g^{-1}$. Hydrophobic fumed silica with a diameter of 16 nm and average specific surface area of 130 $m^2\ g^{-1}$ (Aerosil R972, Degussa, Germany) diluted in a water/ethanol (1/1) solution was used to tune lignin substrate hydrophobicity (unpublished data). The particles were negatively charged and were used as received. The charge of the silica particles originates from the dissociation of silanol groups (Bergna & Roberts 2006). The nanosized precipitated calcium carbonate (nanoPCC) used in Papers I and IV was donated by Schaefer Kalk (Diez, Germany) as a ~12% dispersion containing no dispersant. The average particle diameter was 50 nm. The properties of the calcium carbonate particles are suggested to be controlled by the ratio of Ca^{2+} and CO_3^{2-} ions (Foxall et al. 1979), the cationic net charge being dominated by Ca^{2+} ions. Hydrophilic bentonite nanoclay (Nanocor Inc., Arlington Heights, USA) was supplied in powder form (Paper I). This sodium montmorillonite aluminosilicate mineral consisted of platy particles with thickness of only one nanometer

and length and width of hundreds of nanometers (aspect ratio 150-200). The basal planes of the clay particles have a permanent anionic charge due to isomorphous substitution in the structure, whereas their edges can possess positive charges at low pH and negative charges at high pH (van Olphen 1977). The net charge of the particles is always negative.

3.1.2 Other substances

Nanofibrillated cellulose (NFC) is a cellulosic nanomaterial prepared by disintegration of wood pulp fibers, which liberates the nanofibrils from the fiber matrix (Herrick et al. 1983, Turbak et al. 1983, Pääkkö et al. 2007). NFC has been used as a model material for studying cellulosic interactions (Ahola et al. 2008b), in multicomponent assemblies (Wågberg et al. 2008) and as a dispersion stabilizer (Andresen & Stenius 2007, Xhanari et al. 2011), to name a few. Recently industrial applications have also started to emerge. In this thesis NFC was used in ultrathin films as a cellulosic substrate for surface sensitive interaction studies (Papers I and II), as a layer-by-layer building block (Paper II) and as a dispersion medium (Paper IV). NFC was studied in order to explore its potential as dispersion stabilizer, in the preparation of materials combining organic and inorganic substances as well as in surface treatments of planar substrates. The NFC grades used were mainly prepared according to the procedure described by Pääkkö et al. (2007) utilizing a high-pressure fluidizer.

Sodium carboxymethyl cellulose, CMC (CP Kelco, Äänekoski, Finland) with a molecular weight of 80 000 g mol^{-1} was used in Paper I to modify NFC. CMC is a cellulose derivative with carboxymethyl groups introduced into the cellulose chain. Modification of NFC by adsorption of CMC increases the surface charge (Liu et al. 2011b), yet preserves the fibrillar structure (Eronen et al. 2011a). Prior to use CMC was diluted in water and dialyzed. It was negatively charged, having charge density of 3.8 meq g^{-1} as determined by polyelectrolyte titration against polybrene (5.35 meq g^{-1}).

Polyelectrolytes were used in LbL assembly, in complex preparation and to modify nanoparticles. A cationic polyacrylamide, C-PAM, (Kemira, Espoo, Finland) with a molecular weight of 1.4 million g mol^{-1} and a charge density of 1.8 meq g^{-1} (17 mol-%) was used in paper II as a LbL and complex structure constituent. Polyacrylamides are commonly used as retention aids in papermaking, and hence, they are relatively inexpensive and easily available. Poly(allylamine hydrochloride), PAH (Sigma-Aldrich, Weinheim, Germany) with a molecular weight of ~56 000 g mol^{-1} and branched polyethyleneimine, PEI (Polysciences Inc., Warrington, USA), with a molecular weight of 50 000 – 100 000 g mol^{-1} (containing primary, secondary, and tertiary amine groups, 1/2/1) were used in Paper III for surface modification of the anionic SNPs. Both PAH and PEI are commonly used with silica particles either for modification (Lindquist & Stratton

1976, Qin et al. 2009, Sörensen et al. 2009, Xia et al. 2009, Janhom 2010) or as a template for particle formation (Patwardhan et al. 2002). Anionic pectin from citrus peel with a molecular weight of 30 000 – 100 000 g mol^{-1} (degree of esterification ~60%), low viscosity alginic acid sodium salt from brown algae (Sigma-Aldrich Chemie GmbH, Steinheim, Germany) with a molecular weight of 75 000 – 100 000 g mol^{-1} and anionic polyacrylamide, A-PAM (Kemira, Espoo, Finland), with a molecular weight of 0.5 – 1 million g mol^{-1} were used for nanoPCC particle modification (Paper IV). In addition to their anionic character pectin and sodium alginate were chosen as modifiers because of their specific interaction with calcium (Fang et al. 2008). Molecular structures of the substances described above are presented in Figure 6.

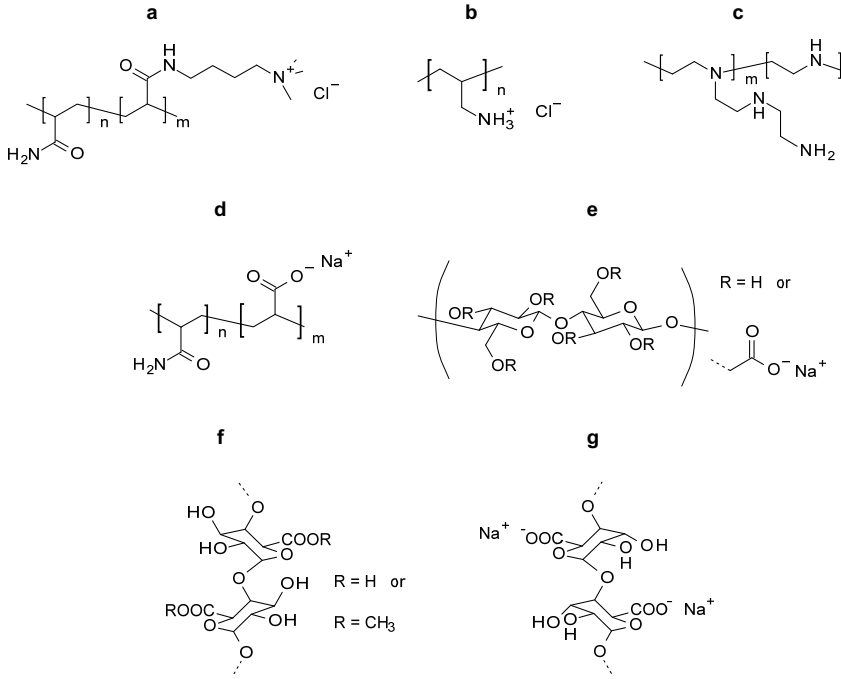

Figure 6. Molecular structure of (a) C-PAM, (b) linear PAH, (c) schematic structure of PEI, (25% primary, 50% secondary, and 25% tertiary amines), (d) A-PAM and (e) sodium CMC. Schematic structures of (f) galacturonate unit of pectin and (g) guluronate unit of alginate are redrawn from Braccini & Perez, 2001.

Hydrophobic substances, alkyl ketene dimer, AKD (Ciba Finland Oy), with solidification temperature of ~20°C and alkenyl succinic anhydride, ASA (Kemira, Espoo, Finland), were used in Papers III and IV, respectively, to prepare hydrophobic coating layers. These substances were emulsified with water in a blender prior to use. No

stabilizers were used in the emulsions. The molecular structures of the sizing agents and their hydrolysis reactions in water are presented in Figure 7.

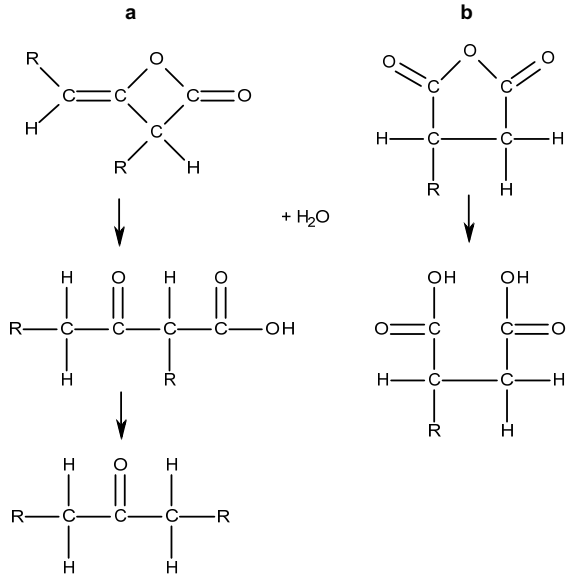

Figure 7. Molecular structure of (a) AKD and (b) ASA and their hydrolysis reaction in water. AKD hydrolyses to its β-keto acid and into a ketone by decarboxylation. ASA hydrolyses to form a dicarboxylic acid (adapted from Roberts 1997).

3.1.3 Lignin and cellulose substrates

LbL assembly and adsorption of colloidal complexes is often examined using devices with specific demands for the adsorption substrate. With a majority of such equipment, a substrate such as paper cannot be used as an adsorption substrate. Hence, model substrates have been developed when the use of rougher and thicker substrates is impossible. In this work NFC and lignin model substrates were used to observe nanoparticle layer formation, the effect of nanoparticles on substrate wetting and substrate-nanoparticle interactions. Unlike pure cellulose model substrates that can be prepared, for example, by the regeneration of a film of trimethylsilylcellulose spin coated on a mica substrate (Kontturi et al. 2003), the NFC substrates are cellulosic model surfaces as they also contain some amounts of hemicelluloses (Eronen et al. 2011b). Hence, whereas cellulose model films prepared from dissolved cellulose provide a good model to study cellulose molecular interactions with other constituents, fibril model substrates are regarded as much more relevant models for cellulose fibers and paper surfaces (Ahola et al. 2008b). Lignin model substrates can be prepared by spin coating

dissolved lignin onto a silica substrate (Norgren et al. 2006, Tammelin et al. 2006) and have, similarly to the cellulose substrates (Saarinen et al. 2009), been used to provide information on polyelectrolyte and polyelectrolyte complex adsorption (Norgren et al. 2007).

The cellulosic films were prepared from NFC according to the procedure described by Ahola et al. (2008b). The NFC gel was diluted to 1.67 g dm^{-3} and disintegrated with an ultrasonic microtip, a Branson Sonifier S-450 D (Danbury, USA), for 10 min at 25% amplitude. The dispersion was then centrifuged with an Optima L-90K Beckman Coulter ultracentrifuge (USA) at approximately 8000 G (10 400 rpm) for 45 min; the supernatant was then spin coated onto silica coated crystals (Q-Sense AB, Sweden) or onto silica substrates cut from silicon wafers (Okmetic, Espoo, Finland). In Paper II 3-aminopropyltrimethoxysilane and in Papers I and IV poly(vinyl amine) were used as anchoring polymers. The spin coated surfaces were rinsed with water, dried gently with nitrogen gas and heat-treated in an oven at 80°C for 10 min. This procedure leads to uniform films with a thickness of approximately 10 nm and to a crystallinity of the cellulose I surface of approximately 60% (Aulin et al. 2009). Lignin films were used in Paper V as substrates for hydrophilic nanoparticle coatings. The substrates were prepared by spin coating milled wood lignin dissolved in 1,4-dioxane onto a silica wafer according to the procedure described by Tammelin et al. (2006). Prior to spin coating the lignin layer, an anchoring layer of polystyrene dissolved in toluene was spin coated onto the surface.

3.2 Methods

3.2.1 Dispersion and complex preparation

Polyelectrolyte/nanoparticle complexes were prepared in Paper II to compare their adsorption behavior on a planar substrate to LbL assembly of the separately adsorbed constituents. Complexes of C-PAM/SNP and C-PAM/NFC with a mass ratio of 1:1 were prepared by adding the polyelectrolyte stock solution to water, followed by an NFC or SNP dispersion (Paper II). The concentration of the complex dispersions was 100 mg dm^{-3}.

In order to tune nanoparticle surface properties and dispersion stability, the nanoparticles were modified using the polyelectrolytes introduced in Chapter 3.1.2. The nanoparticle modifications were conducted in water-phase by the adsorption of oppositely charged polyelectrolytes. SNPs were modified to be cationic and nanoPCC particles anionic in Papers III and IV, respectively. Throughout the experiments nanoparticle disintegration and modification was assisted using an ultrasonic bath and the Branson sonifier. The minimum modifier concentration required to saturate a particle surface was

determined by measuring the mobility of the dispersion as a function of the polyelectrolyte concentration to nanoparticle ratio (Kleimann et al. 2005). The cationically treated SNPs were washed by centrifugation using the Optima L-90K Beckman Coulter ultracentrifuge at 10 400 rpm for 45 min in order to remove any excess polyelectrolyte. The dispersions of polyelectrolyte treated nanoparticles were combined with AKD (Paper III) and ASA (Paper IV) to prepare dispersions able to change the wetting characteristics of a given substrate. After the addition of the AKD emulsion or the ASA emulsion to a nanoparticle dispersion, the dispersion was sonicated using the Branson sonifier with an amplitude of 25%.

3.2.2 Dispersion characterization

Changes in dispersion *turbidity* were observed using a Turbiscan Ma 2000 instrument (Formulaction, Toulouse, France), which has a pulsed near-infrared light source with a wavelength of 850 nm and two sensors measuring the transmitted (0° from the incident beam) and backscattered (135° from the incident beam) light flux relative to external standards as a function of the sample height. An increase in turbidity is detectable as a decrease in light transmission and as an increase in backscattering (Mengual et al. 1999a, Mengual et al. 1999b, Lemarchand et al. 2003, Daoud-Mahammed et al. 2007). A rapid change in turbidity indicates flocculation and sedimentation of the particles.

In addition to turbidity measurements, *ζ-potential measurements* were utilized in exploring dispersion stability and efficiency of particle modification. A ζ-potential value characterizes the properties of the diffuse part of the electrical double-layer, hence it can be used to evaluate the dispersion coagulation tendency. A sufficiently high ζ-potential value, the magnitude which is characteristic to a given system, is known to provide electrostatic dispersion stability (Li & Tian 2002). Surface modification of particles with oppositely charged substances, for example, polyelectrolytes, can be detected as charge reversal of the ζ-potential value (Okubo & Suda 1999, Schwarz et al. 2000). A Coulter Delsa 440SX Electrophoretic Light Scattering Analyzer (Coulter Electronic Ltd., USA) was used to calculate the ζ-potential values by determining electrophoretic mobility of the samples.

Colloidal titration (Mütek PCD 03, Mütek Analytic GmbH, Germany) was used to determine the *charge densities* of the polyelectrolytes. *Particle sizes* were determined by dynamic light scattering using an N5 Submicron Particle Size Analyzer (Beckman Coulter Inc., USA). The particle size analyzer detects interference patterns caused by the Brownian motion of particles. Fluctuation in the interference determines the rate of diffusion, which is used to determine average particle size. An intensity analysis using the software supplied by the manufacturer was used to determine the particle size distributions.

X-ray photoelectron spectroscopy was used to characterize the silica nanoparticles (Paper III). XPS is a surface sensitive method able to characterize the chemical composition of the topmost region of a sample as the maximum sensing depth is 10 nm. XPS is based on the emission of electrons from core orbitals of a substance exposed to monochromatic electromagnetic radiation in the X-ray range. The emitted photoelectrons are distinguished by their specific kinetic energies. The kinetic energy of the photoelectrons emitted is dependent on the irradiation energy and the original binding energy of the photoelectron in its inner core orbital (Koopmans 1933). In the case of thin or only partially covering films on a substrate, the XPS signal consists of both the underlying and the top layer signals. In such a case, the surface distribution can be evaluated either by comparing the atomic ratios coming from a known substrate or by comparing the shapes and intensities of the backgrounds tailing each elemental signal (Tougaard 1996, Tougaard 1998). The XPS analyses in Paper III of the SNP dispersions after freeze-drying were performed using a Kratos AXIS 165 electron spectrometer with monochromatic $Al_{K\alpha}$ X-ray source (Manchester, UK). The polyelectrolyte treatment was monitored by the nitrogen N1s signal, while the AKD treatment was followed by observing increasing carbon C1s and decreasing silicon Si2p signals.

3.2.3 Layer build-up and multilayer characterization

Examination of pigment particle layer formation in Paper I, multilayer build-up in Paper II and the dispersion counterpart affinity in Paper III was carried out using *a quartz crystal microbalance with dissipation monitoring* E4 equipment supplied by Q-sense AB (Västra Frölunda, Sweden). QCM-D was the main method used throughout the experimental work and is therefore introduced here with in detail.

QCM-D is an acoustic method enabling observation of the adsorption of substances on a given substrate. Presently, QCM-D is routinely used to study thin film formation. The equipment measures a change in the frequency and dissipation of an oscillating quartz crystal. A voltage applied to the quartz crystal sets it to oscillate at a fundamental resonance frequency, 5 MHz, with odd overtones of 15, 25, 35, 45, 55 and 75 MHz. Measuring multiple overtones allows the analysis of vertical variations in the layer due to a decreasing detection range from the sensor surface with increasing overtone number. Adsorption of substances on a crystal changes the resonance frequency. A change in the adsorbed mass (Δm) can be evaluated from the frequency response using the Sauerbrey equation (Sauerbrey 1959, Höök et al. 1998a),

$$\Delta m = \frac{-C\Delta f}{n} \qquad (3.1),$$

where C is a device specific constant (0.177 mg m^{-2} Hz^{-1}), Δf the change in oscillation frequency of the crystal and n is the overtone used. This equation is valid for thin and rigid layers. For viscoelastic layers the Sauerbrey equation tends to underestimate the mass as it is calculated directly from the change in the frequency of one of the overtones. Hence, a model taking the properties of the adsorbed layer into account by utilizing frequencies of multiple overtones and their variations has been proposed to be suitable for calculating the mass of viscoelastic layers. For a full description of the model the reader is referred to the original publication on the matter (Johannsmann et al. 1992) and to a simplified description of the equations (Naderi & Claesson 2006). In short, the model utilizes the concept of an equivalent mass *(m*)*:

$$m^* = -\frac{\sqrt{\rho_q \mu_q}}{2f_0}\frac{\Delta f}{f} \qquad (3.2),$$

where ρ_q is the specific density and μ_q the elastic shear modulus for quartz, f_0 the fundamental frequency of the crystal in air, Δf the frequency response and f the resonant frequency of the crystal in the solution. The intercept of the equivalent masses of several overtones plotted against the squares of their resonance frequencies gives the adsorbed mass.

The frequency change detected in QCM-D only indicates changes in the mass of the sensor. Hence, this response is a sum of phenomena taking place during adsorption and it is impossible, for example, to differentiate a change caused by swelling, that is, binding of water in the layer, from a change caused by adsorption of other substances. However, the dissipation of the adsorbed layer is measured simultaneously with frequency change. By turning off the driving voltage for a short moment and monitoring the decay of the oscillation, the dissipation at several frequencies is collected. Dissipation is defined as,

$$D = \frac{E_{\text{lost}}}{2\pi E_{\text{stored}}} \qquad (3.3),$$

where E_{lost} is the dissipated energy and E_{stored} is the total energy stored in the oscillator. Dissipation response can be used to reveal layer properties such as viscosity, elasticity and thickness.

A ratio of dissipation to frequency change (*Df*) is often used to examine the intrinsic layer properties (Plunkett et al. 2003, Du & Johannsmann 2004). Changes in the *Df*-ratio can indicate changes in the adsorption kinetics (Höök et al. 1998b), layer viscosity, that is, if the layer is loose or rigid (Saarinen et al. 2008) and in swelling of the layer in question (Plunkett et al. 2002, Ahola et al. 2008b). In the case of the adsorption of spherical nanoparticles, the layer may have uneven coverage and a heterogeneous

structure. A few recent publications discuss the effect of particle size and shape as well as the layer structure (coverage) on QCM-D response. Johannsmann et al. (2009) show that the ratio of the frequency change Δf and the bandwith change $\Delta\Gamma$ (equivalent to dissipation, ΔD) develops differently in the case of homogeneous and heterogeneous films. In the case of rigid nanosized objects (e.g. nanoparticles) adsorbing on a surface, the interaction of the particles with the surrounding aqueous phase affects the dissipation response and the *Df*-ratio due to the water trapped inside the layer. Tellechea et al. (2009) furthermore suggest that the *Df*-ratio can be used to determine particle size and the surface coverage of the adsorbing layer.

A typical QCM-D measurement was performed using either a silica coated quartz crystal (Paper III) or the quartz crystal coated with an NFC film (Papers I and II) as the oscillating adsorption substrate. Prior to measurements the NFC substrates were allowed to swell in a corresponding buffer overnight. The measurements were started by pumping the buffer through the measurement chambers of the QCM-D followed by an adsorbent solution at a 0.1 mL min^{-1} flow rate. When a plateau in the Δf curve was reached, the buffer was pumped through the chambers to rinse the substrates. In LbL formation, the surface was rinsed after each layer. The frequency change values (in Hz) discussed in this thesis have been normalized with the corresponding overtone numbers by the Qsoft401 software (version 1.4.4.130, Qsense, Västra Frölunda, Sweden). The amounts adsorbed were calculated using the Sauerbrey (Eq. (3.1)) and Johannsmann (Eq. (3.2)) models after reaching a plateau in the Δf curve and rinsing with the buffer solution.

QCM-D has been extensively used to study multilayer build-up (Ariga et al. 1997, Lvov et al. 1997, Saarinen et al. 2008, Wågberg et al. 2008) and in studies of cellulosic nanomaterials (Ahola et al. 2008c, Aulin et al. 2009, Song et al. 2009). Studies regarding nanoparticle deposition with QCM-D also exist (Ariga et al. 1997, Lvov et al. 1997, Lvov et al. 1998, Chen & Elimelech 2008, Fatisson et al. 2009, Jiang et al. 2010, Xu et al. 2010). Although QCM-D is an advantageous method for studying the deposition of polyelectrolytes and nanoparticles and their layer build-up, the QCM-D response is a combination of phenomena taking place during adsorption. For example, water bound to a layer cannot usually be differentiated from the adsorbed substances, and hence QCM-D is often combined with other complementary techniques such as surface plasmon resonance (Plunkett et al. 2003, Ahola et al. 2008c, Tehrani-Bagha & Holmberg 2008), stagnation point adsorption reflectometry (Enarsson & Wågberg 2008a,b) and ellipsometry (Halthur & Elofsson 2004, Aulin et al. 2009). In this thesis, in addition to QCM-D, *Atomic force microscopy* was used to analyze substrates by imaging in all Papers I-V, and by measuring surface forces in Paper II. The AFM, developed in the 1980s (Binnig et al. 1986), is a commonly used analysis method in surface science. AFM imaging is based on detecting the interaction of a sharp tip attached to a cantilever with a sample. The AFM can operate

in contact or in dynamic mode; dynamic mode is more applicable in studying cellulose samples. The dynamic mode is further divided into tapping mode and non-contact mode, in which either the frequency of the oscillation is kept constant and the change in amplitude is detected, or the amplitude is constant and the changing frequency provides information about the sample, respectively. In this thesis, tapping mode was used. A laser is directed on the cantilever and the movement of the reflected light is detected indicating the movement of the cantilever. Usually the interaction is kept constant and the topographical image is developed by monitoring the feedback from the scanner moving the sample to keep the frequency (or amplitude) constant. Additionally, the phase lag between the oscillation of a free cantilever and the cantilever in contact with a sample is monitored.

In addition to morphological characterization, AFM is commonly used to measure forces between the tip, which can be modified with a probe, and a substrate (Ducker et al. 1991, Butt et al. 2005). The forces between a surface and a probe are detected from the cantilever deflection when the sample is moved towards or away from the probe by a piezoelectric translator. During the approach the cantilever can bend upwards or downwards depending on the interaction (repulsive or attractive) between the tip and the surface. A force measurement results in a measure of the cantilever deflection versus position of the piezo. The deflection of the cantilever (Δz) is converted to surface force (F) according to Hooke's law using the spring constant of the cantilever (k),

$$F = k\Delta z \qquad (3.4).$$

Steric forces commonly affect the interactions between cellulose surfaces due to swelling, compressibility and the tails of cellulose chains (Neuman et al. 1993, Rutland et al. 1997, Carambassis & Rutland 1999). Nevertheless, some studies also report that only the electrical double-layer forces are present between cellulose surfaces when a cellulose probe is used (Rutland et al. 1997, Zauscher & Klingenberg 2000). Force measurements have been exploited to study the effect of polymers on cellulose interactions regarding flocculation and strength additives (Holmberg et al. 1997, Zauscher & Klingenberg 2000, Salmi et al. 2007b). Moreover, force measurements have commonly been used to study polyelectrolyte multilayer build-up (Blomberg et al. 2004, Aulin et al. 2010b) and complex adsorption (Estel et al. 2000, Salmi et al. 2007a).

A Nanoscope IIIa Multimode scanning probe microscope (Digital Instruments Inc., Santa Barbara, USA) was used for the AFM measurements. The high resolution morphological characterization of surfaces in Papers I-V was done in tapping mode in air using silicon cantilevers, producing both topographical and phase contrast images (MicroMasch, Estonia). The AFM images were analyzed using Nanoscope software

(version 6.13R1, Digital Instruments, Inc.). The Scanning Probe Image Processor (SPIP) software (version 4.0.6.0, Image Metrology, Lyngby, Denmark) and its grain analysis with threshold detection method was used to determine substrate coverage values. In surface force measurements a cellulose sphere was used as the probe. It was precipitated from a viscous process and glued to the tipless end of an AFM cantilever with a reported spring constant of 0.06 N m^{-1} (Veeco Instruments, USA). The spheres are described in detail elsewhere (Rutland et al. 1997). The forces were studied during LbL and complex adsorption.

3.2.4 Preparation and characterization of the ultrathin coating layers

One of the aims of this thesis was to be able to prepare ultrathin nanoparticle coating layers on planar substrates. Preparation of a thin layer with a thickness as low as monolayer scale is challenging and not many techniques are available. Many such techniques, for example, atomic layer deposition or the Langmuir-Schaefer method are laborious and not suitable for large scale production. On the other hand, very few other methods enable preparation of nanoscale coatings. However, the *spin coating* technique was used in Papers III, IV-V for coating the nanoparticle dispersion onto silica, cellulosic and paper substrates. Commonly the technique is used to prepare thin films on solid substrates by evaporation of the spinning solvent (Emslie et al. 1958). The centripetal acceleration together with the viscosity and concentration of the spinning solution affect the film thickness (Meyerhofer 1978, Bornside et al. 1993). The technique is suitable for coating smooth and rigid substrates. Because evaporation of the spinning solution is one of the key parameters affecting formation of the layer, clearly the technique is not optimal for coating paper substrates, which eagerly absorb water. Nonetheless, with paper substrates the technique was only used as a way to apply nanoparticles on the topmost layer and to avoid penetration of particles into paper structure.

Throughout this thesis, wetting of the ultrathin coating layers was monitored using a CAM 200 (KSV Instruments Ltd., Helsinki, Finland) contact angle goniometer. Contact angle is a quantitative measure of wetting of a solid by a liquid, assessed by measuring the angle formed between the substrate and the tangent to the drop surface. This value reflects the thermodynamics of the liquid/solid interaction. An immobile drop, that is, a static "advanced" contact angle, was used to determine wetting characteristics. The contact angle of water on the substrate was calculated based on a numerical solution of the full Young-Laplace equation by the software supplied by the manufacturer. Measurements were performed at room temperature with at least three parallel measurements recorded per sample.

4 Results and discussion

In order to create nanotechnological advances applicable on the industrial scale, it is necessary to develop simple and upscalable procedures. The experimental work presented in this thesis discusses exploitation of nanoparticles in surface treatments of planar substrates. In addition to preparing thin nanoparticle coatings, particle modification and layer build-up are examined. Only the main findings of the experimental work related to this thesis are summarized and discussed. A full description of all the results can be found in the attached Papers I-V.

4.1 Layer formation using nanoparticles

4.1.1 Effect of nanoparticle shape, charge and substrate charge

Deposition of nanoparticles on a substrate has distinct characteristics in comparison to their micrometer sized analogs. This is due to the apparent discrepancy between micro and nanometer sized particles, mainly related to their size and surface area. This chapter presents observations regarding layer build-up by nanoparticles on a planar substrate.

Layer formation solely by nanoparticles was examined by observing adsorption of nanosized pigment particles, nanoPCC and nanoclay, on a nanofibrillated cellulose substrate used as a model for cellulosic materials. The nanoPCC particles are cubic and slightly cationic, while nanoclay particles are plate-like anionic particles (under the conditions used). In addition to particle shape and size, the particle-particle and particle-substrate interactions were expected to be important in considering layer formation.

The particle-particle interactions define dispersion stability, which was hypothesized to be an imperative to obtain a uniform distribution of particles on a substrate as well as in a dispersion. Dispersion stability is achieved by increasing the electrostatic repulsive forces between the particles, the magnitude of which depends on the particle surface potential and the thickness of the electrical double-layer (Evans & Wennerström 1999). In these experiments the particle interactions were changed by altering the electrolyte concentration of the medium. Additionally, the particle substrate interactions were altered by changing the NFC substrate surface charge by pre-adsorption of CMC.

The NFC model surfaces used in this thesis were constructed of slightly anionic cellulosic nanofibrils disintegrated from wood (Ahola et al. 2008b). To enable preparation of smooth films, the fibril material is sonicated and centrifuged and only the finest fraction is used for film preparation. Even though the films are very smooth with roughness of only a few nanometers, they are chemically heterogeneous. The films contain both crystalline and amorphous cellulose with crystallinity of approximately 60% (Aulin et al. 2009). In addition to cellulose the material contains some amounts of hemicelluloses (Eronen et al. 2011b), and therefore, rather than being models for pure cellulose, these films are cellulosic model substrates. The structure of the fibril film resembles the surface of a wood fiber hence making the film a relevant model for wood fibers as well (Myllytie 2009).

The nanoparticle layer build-up on an NFC substrate was explored in aqueous phase and hence few words about its behavior in water are needed. Like cellulosic fibers, the fibril films have a strong interaction with aqueous solutions causing softening and swelling of the thin film in liquid. Swelling is dependent on pH and ionic strength of the medium. At high pH, dissociation of the carboxyl groups causes swelling. Increase in electrolyte concentration first increases swelling, yet further increasing concentration causes deswelling (Ahola et al. 2008b).

The NFC films can be modified by adsorption of polymers (Ahola et al. 2008c) or hemicelluloses (Eronen et al. 2011b) affecting, among others, their charge. In this thesis the films were used as they were or modified by adsorption of CMC. It is recognized that CMC adsorption can be used to change cellulose film surface charge (Liu et al. 2011b), and hence for simplicity, a CMC layer was used instead of carboxymethylated fibril material (Walecka 1956, Wågberg et al. 2008).

The nanoPCC dispersion properties were adjusted by altering the $CaCl_2$ concentration. The presence of additional calcium ions was expected to affect the nanoparticle surface charge (Huang et al. 1991) and therefore the stability. The affinity of the nanoPCC dispersion for a neat NFC substrate increased with increasing $CaCl_2$ concentration noted as a decrease in the frequency and an increase in the dissipation of the QCM-D response. The frequency change is further converted to adsorbed mass in Fig. 8a. With increasing $CaCl_2$ concentration, the particle-particle interactions of the nanoPCC dispersion were simultaneously altered, noted as an increase in the ζ-potential value from approximately +9 to +35 mV. Indeed, the charge determining ions of PCC present in the PCC dispersion may adsorb on the particle surface increasing their cationic charge. Hence, the increased adsorption on NFC can be attributed to the particle charge. These observations correlate with findings regarding the affinity of calcium carbonate fillers with cellulose fibers, stating that the driving force for the constituent affinity is the charge (Fimbel & Siffert 1986, Vanerek et al. 2000). The increase in adsorption was also detected

as an increase in the substrate coverage from 30% (with 0 and 0.1 mM $CaCl_2$) to 40% (with 1 and 10 mM $CaCl_2$).

Although the nanoclay dispersion and the NFC substrate were both negatively charged, nanoclay was able to adsorb on NFC detected as a change in the frequency and dissipation response of QCM-D. Similarly to the nanoPCC adsorption, the nanoclay adsorption increased with increasing $CaCl_2$ concentration, reaching a maximum (Δf ~43 Hz corresponding to Johannsmann mass of ~8.2 mg m^{-2}) at 1 mM concentration (Fig. 8a). Evidently, this is due to reduction in repulsion between the substances caused by the increasing electrolyte concentration. However, at 10 mM $CaCl_2$ the dispersion started to flocculate, and consequently, adsorption was restricted.

The electrolyte concentration of the nanoclay dispersion was adjusted with NaCl in addition to $CaCl_2$. Interestingly, adsorption of nanoclay particles on NFC was strongly affected depending on the electrolyte chosen to adjust the ionic strength. In comparison to the maximum adsorption recorded when the electrolyte concentration was controlled with $CaCl_2$ (8.2 mg m^{-2}), the change in frequency at 10 mM NaCl was high, ~208 Hz, which corresponds to rather high Johannsmann mass of ~38 mg m^{-2} (Fig. 8b). Assuming a clay layer density of 2.4 g cm^{-3} the layer thickness (adsorbed mass divided by density) would be approximately 16 nm. It is possible that the vast decrease in the frequency change at 10 mM NaCl compared to 1 mM $CaCl_2$ is dependent on an optimal ionic strength able to decrease the repulsive interaction, yet not able to flocculate the particles. However, the difference in the masses adsorbed was large and might not be only due to the effect of ionic strength on dispersion flocculation. The possible differences between Ca^{2+} and Na^{+} ion adsorption on the nanoclay particle surface and interlayers (Norrish 1954, Pashley & Quirk 1984, Delville & Laszlo 1990), a property exhibited by the high cation exchange capacity of the material, is likely to be important. It seems that the choice of the electrolyte can be used to tune nanoclay affinity towards the NFC substrate, an important factor regarding construction of barrier materials from cellulose and clay (Liu et al. 2011a).

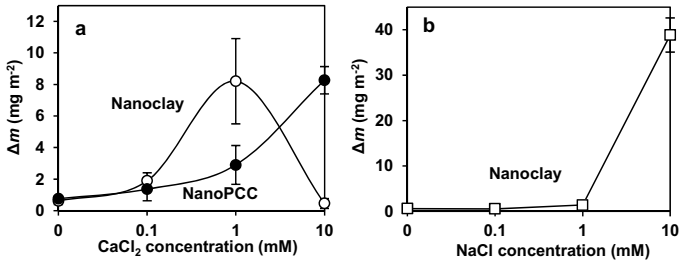

Figure 8. (a) Adsorbed mass of nanoPCC (●) and nanoclay (○) on a neat NFC substrate as a function of $CaCl_2$ concentration and (b) nanoclay adsorption as a function of NaCl concentration (□). The adsorbed mass values were calculated using the Equation 3.2. The lines are only guides for the eye. (Paper I).

The benefit of observing adsorption with QCM-D is the ability to simultaneously monitor the adsorbed mass and the layer properties. Especially, observation of the ratio of frequency, indicating the adsorbed mass, and dissipation, indicating the intrinsic layer properties, can distinguish viscoelasticity (Saarinen et al. 2008) and swelling of the layer in question (Plunkett et al. 2002, Ahola et al. 2008b). Moreover, the *Df*-ratio is also applicable in examining the behavior of solid particles unable to swell in a similar way as, for example, polyelectrolytes (Tellechea et al. 2009). In the case of a homogeneous layer formed by solid particles, the *Df*-ratio should be unaffected by the layer thickness.

The QCM-D responses of the nanoPCC and nanoclay adsorption presented as the *Df*-ratio as a function of time show that the adsorption behavior of the nanoparticle dispersions differ from one another (Fig. 9). In the case of nanoPCC adsorption, the ratio decreases with time indicating layer rearrangement along the adsorption or changes in the layer coverage. Conversely, the ratio remained constant during nanoclay adsorption at 10 mM NaCl. This is indicative of adsorption of a layer with particles adsorbing face down on the substrate, causing a low effect on the response in depth direction, or adsorption of a fully covering layer. However, at 1 mM $CaCl_2$, a small decrease in the *Df*-ratio was detected in the beginning of the adsorption. This is probably due to the more aggregated structure of the nanoclay dispersion at 1 mM $CaCl_2$ than at 10 mM NaCl. These observations correlate well with notions regarding AFM topography images of the NFC substrates after nanoclay dispersion adsorption, suggesting that particles deposit in a thin conformation on the substrate, yet the substrate is not fully covered by the particles (presented in Paper I).

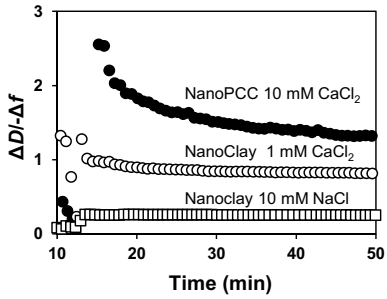

Figure 9. The dissipation to frequency ratio of the 3rd overtone as a function of time of the adsorption of nanoPCC at 10 mM $CaCl_2$ (●), nanoclay at 1 mM $CaCl_2$ (○) and nanoclay at 10 mM NaCl (□) on an NFC substrate. The dispersions were prepared at 1 mM $NaHCO_3$. (Paper I).

As already stated, the surface charge of the adsorption substrate, the NFC film, was also assumed to affect the nanoparticle layer build-up. Hence, the NFC substrate was modified by adsorbing CMC on the fibril film. Adsorption of CMC on cellulose is known to be assisted by sufficient $CaCl_2$ concentration (Laine et al. 2000, Liu et al. 2011).

Consequently, in a 10 mM $CaCl_2$ medium, CMC adsorption on NFC substrate caused a frequency decrease of approximately 60 Hz. The corresponding Johannsmann mass is approximately 10.5 mg m^{-2}. At 1 mM electrolyte concentration the change in frequency was lower and a plateau of adsorption could not be determined because rinsing of the layer with buffer caused desorption of the layer. The permanence of a CMC treatment has been suggested to be dependent on the adsorption pH; in pH 4.5 (Eronen et al. 2011a) the layer has been reported to adsorb irreversibly, whereas in pH 8 the layer desorbs during rinsing (Ahola et al. 2008c). Increasing the NFC substrate charge by CMC pre-adsorption (the graphs are presented in Paper I) was noted to increase the adsorbed mass of the cationic nanoPCC particles (at 1 mM $CaCl_2$), from 2.9 to 7.3 mg m^{-2}, calculated using the Equation 3.2, while nanoclay adsorption decreased from 8.2 to 2.9 mg m^{-2}. These observations confirm that the NFC substrate charge and electrostatic interactions affect the nanoparticle layer build-up. NanoPCC adsorption increases due to enhanced attraction, while nanoclay adsorption decreased due to the increased repulsion between the anionic substrate and the anionic particles. Hence, possibly instead of increasing the anionic charge of NFC substrate, cationic fibrils could be used to enhance the affinity between the anionic particles and NFC (Lin et al. 2008, Dong & Hinestroza 2009, Olszewska et al. 2011).

Figure 10 presents the AFM images of the CMC-modified NFC substrates after adsorption of the nanoparticles. The observed particle morphology highlights the difference in the layer structure formed by the two nanopigment grades. The spherical nanoPCC particles adsorb leaving a substrate covered with particle islands, while the nanoclay particles form a thin layer. Moreover, the adsorption kinetics of the two nanoparticle materials was distinct. In comparison to the adsorption of nanoclay on the NFC substrate (with or without the pre-adsorbed CMC), nanoPCC adsorption was slower and detection of a clear plateau in the adsorption was often not possible. This is presumably due to continuous adsorption of particles forming increasingly larger particle islands on the substrate.

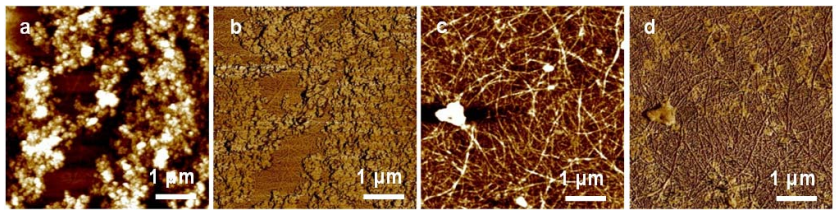

Figure 10. AFM topography and phase contrast images (25 µm²) of nanoPCC (a) and (b), and nanoclay (c) and (d), adsorbed on CMC-modified NFC substrate. (Paper I).

These experiments clearly show that the two nanoparticles form very distinct surface structures upon adsorption. It is therefore highly probable that the physical properties of the particles as well as the electrostatic affinity with the adsorption substrate determine the layer structure. Based on the observations regarding the affinity between the nanosized pigment particles and NFC, the key elements that control these interactions are the dispersion stability and the charge of both the particles and the substrate. However, it is important to keep in mind that while the affinity between substances is beneficial regarding formation of a nanoparticle layer on the planar NFC substrate, when considering the preparation of a dispersion of a cellulose nanofibril network with uniformly embedded nanoparticles, the increased affinity between the substances can lead to flocculation. In such a case the stability of the nanoparticles as well as the formation of a uniform network of fibrils and particles are essential.

4.1.2 Layer-by-layer assembly with polymers

Besides adsorbing nanoparticles directly, it is possible to form a layered structure using nanoparticles accompanied with substances of opposite charge (Iler 1966, Decher 1997). In such a case, alternating layers of the two constituents can form a well-organized structure. LbL assembly was examined by alternating adsorption of C-PAM with either silica nanoparticles or nanofibrillated cellulose on an NFC substrate. The NFC used as the layer constituent was more charged than the substrate NFC material due to carboxymethyl pretreatment (Wågberg et al. 2008).

Layer formation with SNPs and NFC sequentially with C-PAM clearly gave rise to non-linear layer growth (Fig. 11). A similar tendency has been often reported in multilayer experiments (Dubas & Schlenoff 1999, Lavalle et al. 2002, Wågberg et al. 2008, Elzbieciak et al. 2009, Rahim et al. 2011). Adsorption of the first cationic polymer layer caused a fairly low, yet clear change in the frequency (5-10 Hz) indicating that a layer was formed. Adsorption of both of the nanoparticles, SNP and NFC, on this layer induced a significant change in the frequency implying that a layered structure was formed. When C-PAM was added the second time, a seemingly higher amount adsorbed on the NFC layer than on the SNP layer. With both systems layer formation was enhanced with an increase in the electrolyte concentration (1 mM $NaHCO_3$ vs. 1 mM $NaHCO_3$ + 10 mM NaCl).

In comparison to NFC, SNP adsorption caused a high change in the frequency, yet the dissipation response was low. This suggests that a large amount of SNPs is adsorbed, but the layer viscosity does not change. The dissipation upon NFC adsorption was high. This was expected, and has been reported with this water-binding material (Aulin et al. 2008, Aulin et al. 2009, Eronen et al. *in press*, Olszewska et al. 2011). Moreover, adsorption of NFC induced a deviation in the frequency shift of the several measured

overtones indicating variation in the layer properties in the depth direction. This effect was not detected with the SNP adsorption. Fairly recently Eita et al. (2011) have reported a layer-by-layer assembly using both silica nanoparticles and NFC in the structure. Similarly, they reported that in comparison to silica particles, the NFC fibril matrix was able to bind large amount of water.

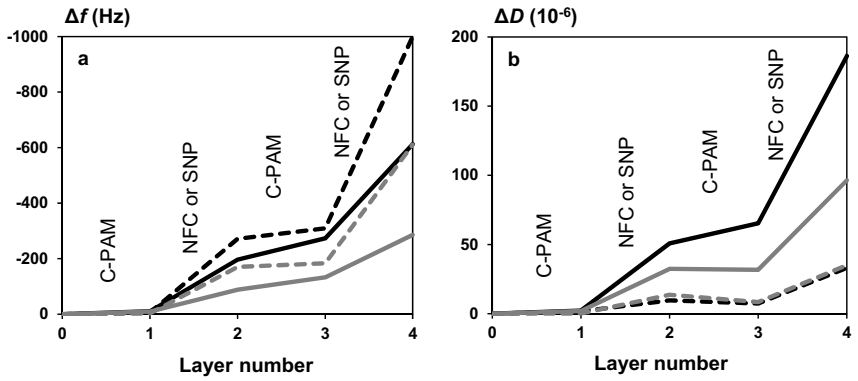

Figure 11. The effect of LbL formation with C-PAM and SNP (dashed lines) and C-PAM and NFC (solid lines) on a change in (a) the frequency and (b) the dissipation at 1 mM (grey) and 11 mM (black) electrolyte concentration on NFC substrate. (Paper II).

It is worth noting that especially with LbL assembly of SNP and C-PAM the adsorption of the second C-PAM layer induced a drop in the dissipation, along with a decrease in the frequency, implying removal of water and densification of the layer (Ahola et al. 2008c). This is shown in Figure 12, which represents the QCM-D frequency and dissipation response during the layer build-up. Such a behavior suggests that the LbL assembly of the SNPs with C-PAM does not necessarily lead to the growth of separate layers, but the particles might be able to penetrate inside the polyelectrolyte layer.

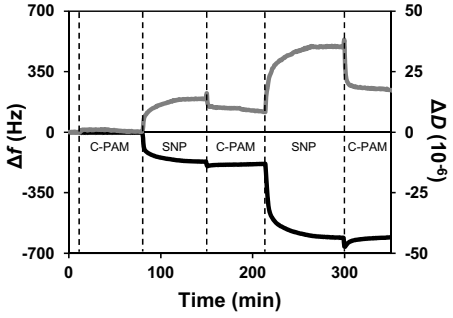

Figure 12. The frequency (black) and dissipation (grey) change (3rd overtone) during sequential adsorption of C-PAM and SNP at 1 mM $NaHCO_3$ on NFC substrate. (Paper II).

In addition to QCM-D experiments, the layer build-up was monitored by measuring changes in the surface forces during LbL assembly (presented in Paper II). The interaction between the NFC substrate and a cellulose sphere before addition of the layer substances was repulsive as also observed elsewhere (Salmi et al. 2007b). During the LbL assembly of C-PAM and SNP the repulsion increased monotonically. Interestingly, the electrolyte concentration affected the interaction and in low electrolyte concentration (1 mM $NaHCO_3$) the increase in the repulsion upon adsorption of SNP on the C-PAM layer was lower than at the 11 mM electrolyte concentration (1 mM $NaHCO_3$ + 10 mM NaCl). In both cases the second addition of C-PAM again increased repulsion. The observed repulsions did not follow DLVO theory, and thus, they were concluded to be mainly of steric origin.

Adsorption of an NFC layer on a C-PAM layer resulted in a long-ranged repulsion. This is due to ability of fibrils to form an extended layer (Aulin et al. 2010b, Eronen et al. *in press*, Ahola et al. 2008b). Considering the size and shape of NFC, it was not expected that the layer of NFC could penetrate inside the C-PAM layer. Both the increase in the repulsion observed in the force measurements and the continuous layer growth observed using QCM-D support this conclusion. Smooth and well-defined multilayers using microfibrillated cellulose and polyelectrolytes have also been reported elsewhere (Wågberg et al. 2008).

4.1.3 Adsorption of complexes

Besides adsorption of SNPs and NFC sequentially with C-PAM, the constituents were mixed together by adding SNPs or NFC to a dilute C-PAM solution leading to the formation of complexes. The resulting complex dispersions were anionic, verified by the ζ-potential measurements presented in Paper II.

Adsorption of the C-PAM/SNP complexes on the NFC substrate was fast. This was seen as crowding of the data points in the $\Delta D/\Delta f$-plot indicating when the adsorption plateau was achieved (Fig. 13). The adsorption of the C-PAM/NFC complex, however, caused a steady increase in the frequency and dissipation indicating a slow settling of the layer. In contrast to the layered structures (Fig. 11), adsorption of the preformed complexes showed a higher change in the frequency in lower electrolyte concentration.

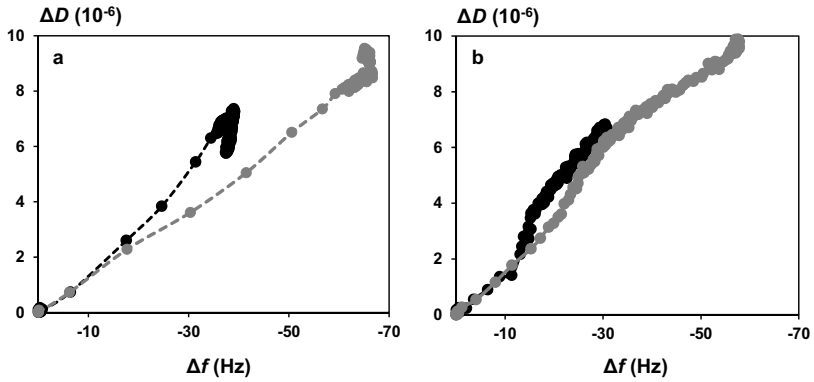

Figure 13. The dissipation change during adsorption of (a) C-PAM/SNP and (b) C-PAM/NFC complexes at 1 mM (grey) and 11 mM (black) electrolyte concentration as a function of the frequency change. (Paper II).

AFM imaging was also used to characterize the complex and LbL structures. Conclusions regarding the layer build-up using NFC could not be done as the fibrils originating from the adsorbing solution were not distinguishable from the substrate covered with the fibrils (images are presented in Paper II). However, the SNPs were observable on the NFC substrates. As extensively proven by many groups, LbL assembly can be used to form well-organized structures (Iler 1966, Ariga et al. 1997, Decher 1997, Lvov et al. 1997). Not surprisingly, sequential adsorption of C-PAM-SNP-C-PAM layer (at 1 mM $NaHCO_3$) resulted in a uniformly covered substrate, verified by AFM imaging (Fig. 14a). In contrast, complex adsorption led to a substrate covered with particle clusters leaving the substrate partly uncovered (Fig. 14b). Similarly, complexes have been noted elsewhere to form only a partially covered surface (Maximova et al. 2004, Ankerfors et al. 2009), while multilayer adsorption containing silica particles and a cationic polyelectrolyte has been reported to form a packed layer (Ariga et al. 1997, Lvov et al. 1998, Sennerfors et al. 2002).

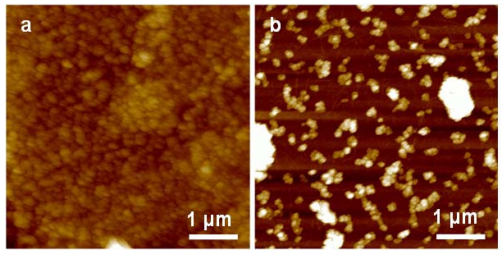

Figure 14. AFM topography images (25 µm²) of NFC substrates after C-PAM/SNP (a) sequential and (b) complex adsorption at 1mM electrolyte concentration. (Paper II).

The AFM observation of the fully covering SNP/C-PAM layered structure and the notion of the discontinuous increase in the dissipation detected with QCM-D suggest that, in LbL assembly, the SNPs are able to penetrate inside the C-PAM layer. This conclusion deviates from previously proposed models stating that colloidal particles form separate layers in the multilayer structure (Lvov et al. 1997). However, formation of a uniform layer instead of a stratified structure has been also seen by Sennerfors et al. (2002). Furthermore, the observations differ from those made by Eita et al. (2011), stating that the layered structure of SNPs, NFC and polyelectrolyte was more viscoelastic than a comparative structure without SNPs, an effect claimed to originate from a stratified layer structure.

4.2 Nanoparticle surface modification

As shown in Chapter 4.1, nanoparticle surface properties affect their interactions in the dispersion as well as during adsorption on a given substrate. Besides altering the surface charge properties (Pham et al. 2007), nanoparticles can be modified to improve their compatibility with other substances (Rong et al. 2006), to functionalize the particles (Goodwin et al. 1990, Vrancken et al. 1995) and to improve their stability (Bagwe et al. 2006, Kamiya & Iijima 2010). Stability is of major concern due to the stronger tendency of the particles to aggregate in comparison to microparticles.

Although nanoparticle modification is indispensable for many applications, a major hindrance regarding the processes used for surface modification is their complexity. This, in combination with the fact that most of the surface treatments cannot be performed on-site, increases the expense. Industries where large quantities of chemicals or bulk raw materials are used strive for simple processes integrable with existing production lines. Therefore, an approach to particle surface treatment in a facile way, to modify nanoparticles in water, was conducted. The nanoparticles of interest were SNPs and nanoPCC particles. Precipitated calcium carbonate particles are commonly used papermaking pigments and some, yet few, examples of the use of their nanostructured grades exist (Tang et al. 2006, Juuti et al. 2009). Silica nanoparticles, on the other hand, are widely used, among other uses, in surface treatments aiming for hydrophobicity (Gu et al. 2006, Bravo et al. 2007). In coatings, both PCC and silica particles can be used in ink jet applications where the aim is to fix the ink color onto the surface layer of paper and to absorb the solvent in the paper structure (Hladnik & Muck 2002).

In these experiments, the anionic silica particles and slightly cationic nanoPCC particles were modified by the adsorption of oppositely charged polyelectrolytes. A nanoparticle dispersion was considered to be saturated with the modifying agent when a

plateau in the ζ-potential was reached (Kleimann et al. 2005). Treatment of the silica particles with PAH and PEI led to charge reversal from negative to positive with a polyelectrolyte concentration of approximately 30 mg g^{-1} (Fig. 15). The PAH and PEI-modified particles reached ζ-potential values of +55 and +17 mV, respectively. The cationic SNP dispersions were washed via centrifugation (Caruso et al. 2001) resulting in ζ-potential values of approximately +57 and +25 mV for SNP-PAH and SNP-PEI, respectively. The particles in both dispersions were larger than the unmodified particles. A comparable measured particle size of the unmodified SNPs was 40 ± 20 nm (the value reported by the manufacturer was 25 nm). The average particle size of the PAH treated SNPs (120 ± 50 nm) was lower than that of the PEI treated SNPs (190 ± 90 nm). However, both dispersions were stable and no phase separation, even when the dispersions were stored, was detected.

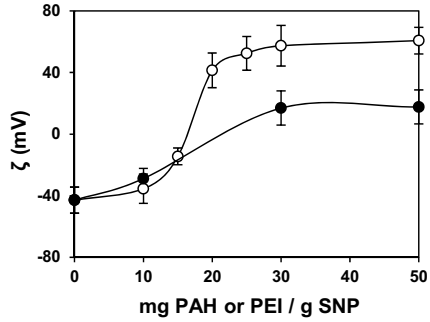

Figure 15. The ζ-potential as a function of PAH (○) and PEI (●) concentration relative to SNP concentration. (Paper III).

The modification of SNPs with the cationic polyelectrolytes was further monitored using QCM-D. Because the steric forces and steric stabilization of particles originate from the polymer layer adsorbed on a particle, with the extended polymer chains able to repel similarly treated particles (Evans & Wennerström 1999), the efficiency of the steric stabilization is largely related to the properties of the adsorbing polymer layer. If only a small amount of polyelectrolyte is adsorbed and the particle is not fully covered by the polymer, a polymer chain can bridge two surfaces, causing particle attraction, that is, bridging flocculation (Biggs et al. 2000). Hence, it is extremely important to verify that the modification is complete.

PAH is a linear polymer, while PEI has a branched structure. Due to the presence of non-quaternary amine groups, their charge is pH-dependent. As expected, with both polyelectrolytes the amount adsorbed decreased with increasing charge density (i.e. decreasing pH) of the polyelectrolyte correlating with studies regarding polyelectrolyte

adsorption on solid surfaces (van de Steeg et al. 1992, Saarinen et al. 2009). Polyelectrolytes with high charge densities adsorb in a flat conformation because of their form in solution. This decreases the amount required for charge compensation (Shiratori & Rubner 2000, Rojas et al. 2002, Notley & Leong 2010). The adsorbed mass of PAH was low within the pH range used. Hence, it seems probable that PAH adsorbs in flat conformation forming a thin layer. The change in adsorbed mass of PEI with respect to charge density was steeper as also seen elsewhere (Lindquist & Stratton 1976, Claesson et al. 1997).

In dispersion the SNPs were treated with PAH and PEI at a pH of ~4 and ~ 9 corresponding to charge densities of ~10 and ~7 meq g^{-1}, respectively. The particle treatment in these conditions resulted in an adsorbed mass of the polyelectrolyte layer of ~70 μg m^{-2} and ~310 μg m^{-2} for PAH and PEI, respectively. Evidently the adsorbed PEI layer is thicker, probably due to PEI's lower charge density and the branched structure of the polymer, in accordance with findings regarding the difference in layer properties between adsorbed linear and branched polyelectrolytes (Claesson et al. 1997, Ondaral et al. 2006).

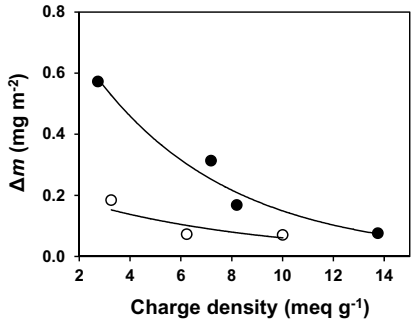

Figure 16. Adsorbed mass of PAH (○) and PEI (●) on a silica sensor as a function of the polyelectrolyte charge density. (Paper III).

In addition to steric stabilization, modification of SNPs with the cationic polyelectrolytes enables alteration of their surface charge. Cationicity of silica particles can be beneficial for printing applications, increasing the affinity between the coating particles and paper or dye (Neumann et al. 2005, Daniel & Berg 2006, Kettle et al. 2010). Typically cationic character is introduced by cationic additives mixed in the coating color (Bugner 2002). However, addition concentration is limited due to the effect of the additives on the coating color viscosity (Ryu et al. 1999). It is recognized that use of particles with cationic surface may overcome this problem, and thus, particles treated to be cationic using, for example, aminosilanes can be exploited (Neumann et al. 2005). The approach described here provides an easy way to use polymers to irreversibly modify the silica particle surface

cationic. The layer formed can be affected by the choice of the polyelectrolyte, and by the treatment pH to some extent (Fig. 16).

In contrast to SNP modification with cationic polyelectrolytes, the nanoPCC particles were modified with anionic substances. Modification with pectin, alginate and A-PAM led to a change in the ζ-potential from positive to negative (Paper IV). The amount of modifier required to saturate the dispersions was approximately 10 mg per gram of nanoPCC in all cases. With this addition the ζ-potential of the particles modified with alginate, A-PAM and pectin was -23, -16 and -14 mV, respectively. Particles modified with pectin were stable and in comparison to the unmodified particles, no changes in dispersion turbidity were noted. Also using A-PAM the stability of nanoPCC particles was improved; no phase separation was detected, yet a slight increase (~8%) in light transmission was observed. This is possibly due to bridging flocculation induced by the polymer's large molecular weight (0.5 – 1 million g mol^{-1}).

The stabilizing effect of pectin and alginate was not very different, yet indications of flocculation were noted with alginate-modified particles. Both pectin and alginate are known to have a specific interaction with calcium (Braccini & Perez 2001, Fang et al. 2008), possibly assisting particle modification and affecting the adsorbed polyelectrolyte layer. Although the difference between the ability of pectin and alginate to stabilize the nanoPCC dispersion was not drastic, an adsorption experiment was performed using the QCM-D to elaborate this difference. As it was not possible to prepare a fully covering nanoPCC layer on a QCM-D crystal, the differences of alginate and pectin were studied by adsorbing them (at 1 mM $NaHCO_3$) on a polyvinylamine layer spin coated onto a silica crystal, representing a cationic particle substrate (Fig. 17). A higher decrease in frequency change, that is, a higher adsorbed mass, was detected when pectin was adsorbed on the cationic substrate. It is possible that, despite the similar molecular weight of the substances, pectin is able to form a more extended layer enabling more efficient steric stabilization. The layers formed were further exposed to the nanoPCC dispersion (at 1 mM $NaHCO_3$ and 1 mM $CaCl_2$) to observe any possible difference in the nanoparticle amount adsorbed, yet such an effect was not detected.

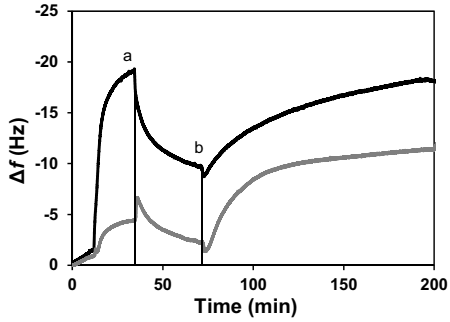

Figure 17. QCM-D frequency response of (a) adsorption of pectin (black) and alginate (gray) on a cationic substrate (PVAm) followed by rinsing and (b) adsorption of 1 g dm^{-3} nanoPCC dispersion (at 1 mM $CaCl_2$). The dispersions were prepared at 1 mM $NaHCO_3$. (Unpublished data).

Dispersions of both modified and unmodified SNPs and nanoPCC were spin coated on a planar substrate to observe the effect of the modifications on layer uniformity. As hypothesized, modification of the particles increased their stability and the cationic silica particle dispersions spin coated on a mica sheet formed a layer much more uniform than the unmodified particles (Fig. 18a). Clearly the PAH treated particles formed a layer consisting of individual particles or clusters of a few particles (Fig. 18b) in contrast to the PEI treated particles, which formed a less uniform layer, but consisted of larger clusters (Fig. 18c). The average coverage of the PAH-SNP layer was approximately 45% and the PEI-SNP layer approximately 30% (SPIP image analysis). The particles are possibly electrosterically stabilized, and due to its branched structure, treatment with PEI results in weak bridging. This leads to a substrate covered by particle clusters instead of individual particles.

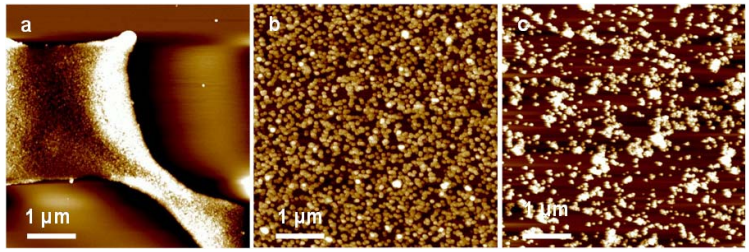

Figure 18. AFM topography images (25 μm^2) of (a) unmodified, (b) PAH-modified and (c) PEI-modified SNP spin coated on a silica substrate. The dispersion concentrations were 5 g dm^{-3}. (Paper III).

The effectiveness of the pectin treatment on the nanoPCC dispersion stability was apparent when the dispersion was spin coated on an NFC substrate (Fig. 19a and b). The modified particles were uniformly distributed, forming a layer consisting of clusters of a

few particles with a coverage of 5%. The unmodified dispersion formed a layer with large particle clusters resulting in a substrate with large uncovered areas and areas packed with nanoparticle clusters.

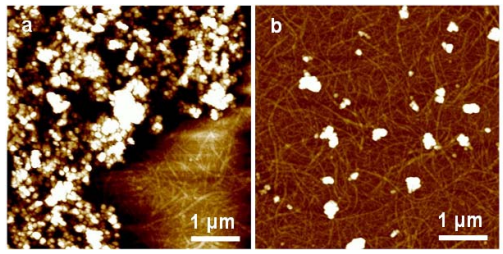

Figure 19. AFM topography images (25 µm²) of (a) unmodified and (b) pectin-modified nanoPCC spin coated on NFC substrate. The dispersion concentrations were 1 g dm^{-3}. (Paper IV).

As already pointed out, nanoparticles aggregate if not modified. In a liquid medium, the particles can, to some extent, be dispersed. However, in air the adhesion of particles is high and they may aggregate irreversibly. In order to evaluate the effect of the particle modification on redispersibility, the dispersions of PAH and PEI-modified SNPs and pectin-modified nanoPCC were freeze-dried resulting in uniform powder-like residues. After drying, the unmodified nanoparticles could not be dispersed in water by sonication, and most of the particles settled at the bottom of a test tube. The polyelectrolyte treated particles were, however, redispersible in water, although a small amount of sediment was detected. The upper phase of the redispersed SNP-PAH particles spin coated on a substrate formed a layer with low coverage, 3% (Fig. 20a), while the coverage of the SNP-PEI layer was ~26% (Fig. 20b). The redispersed pectin-nanoPCC dispersion formed a layer with a coverage of ~12%.

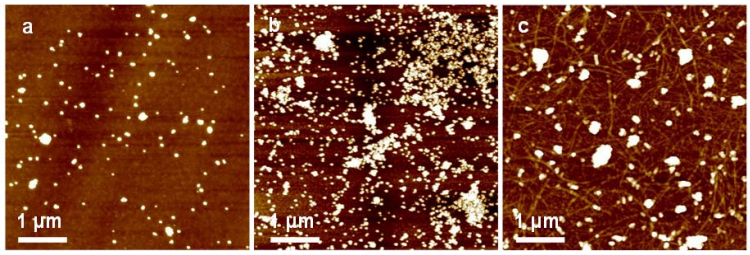

Figure 20. AFM topography images (25 µm²) of redispersed (a) PAH-modified SNP, (b) PEI-modified SNP and (c) pectin-modified nanoPCC spin coated on either a silica or cellulosic fibril substrate. The dispersions were redispersed to a 5 g dm^{-3} concentration. (Paper III and unpublished data).

These results indicate that the modified particles can be dried for transportation in contrast to the unmodified particles. This effect is important when considering utilization

of particles on an industrial scale where expenses can be reduced by transporting dry chemicals to be dispersed on-site.

4.3 Modification of planar substrates with nanoparticles

4.3.1 Effect of nanoparticle surface properties and layer roughness on substrate properties

The modification of the nanoparticles with oppositely charged polyelectrolytes improved dispersion stability, and consequently, allowed preparation of nanoscale structures on a substrate. As shown in the Chapter 4.1, structures of the layers formed by nanoparticles can be significantly affected by the nanoparticle dispersion properties, other constituents present during deposition, and by the affinity between the particles and the substrate. In order to examine the effect of nanoparticle surface properties on the layers formed, silica nanoparticles without surface modification and treated with dimethyldichlorosilane were spin coated on to a lignin film. Silylation of the particles induce surface hydrophobicity (Tolnai et al. 2001), and consequently, with increasing silanized particle concentration, the water contact angle of the substrate increased (Fig. 21a). In fact, spin coating a 20 g dm^{-3} dispersion on the substrate produced a layer with such strong water repellency that a water drop manually descended on the substrate could not spread on the substrate (Fig. 21b). This behavior differs notably from the wetting characteristics of the lignin substrate coated with hydrophilic silica particles, where an increasing dispersion concentration of these particles decreased the water contact angle of the substrate.

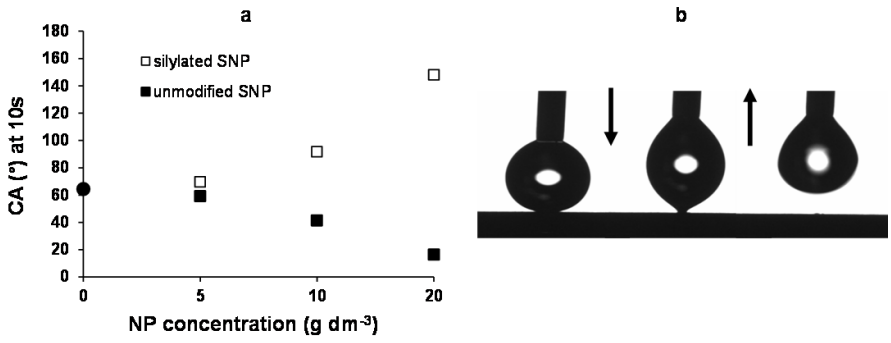

Figure 21. (a) Wetting of a lignin substrate coated with hydrophilic (■) and silylated (□) silica nanoparticles of varying dispersion concentrations. The filled circle (●) represents the water contact angle of the neat lignin substrate. The standard deviations of the data points were less than ± 3°, except for the substrate treated with 20 g dm^{-3} hydrophobic particle dispersion, for which it was ± 12°. (b) A water drop descended manually on this substrate was unable to spread on the substrate. (Unpublished data).

Evidently, nanoparticle surface modification can affect the hydrophobicity of the surface layer. However, considering the generally accepted effect of surface roughness on wetting (Bico et al. 2001, Bico et al. 2002, Yoshimitsu et al. 2002, Callies & Quere 2005, Hsieh et al. 2005, Spori et al. 2008), it is worth considering if nanoscale roughness, per se, can affect wetting. Nanoparticle induced roughness is typically utilized in superhydrophobic surfaces where it is combined with micrometer scale roughness (Feng et al. 2002, Feng & Jiang 2006, Bhushan et al. 2009a). A few studies also exist concerning the alteration of substrate wetting properties using nanoparticles, yet in the majority of these studies the surface layer under investigation consist of a packed or unevenly covered surface structure (Yan et al. 2007, McConnell et al. 2009).

In order to explore the effect of nanoroughness on the wetting of a smooth substrate, hydrophilic silica nanoparticles were spin coated onto a lignin film and the experimental contact angle values were combined with theoretical modeling (Paper V). The surface energy contrast between the SNPs and lignin enabled a change in contact angle with SNP coverage. An increasing coating dispersion concentration was noted to increase the particle coverage on the lignin substrate (Fig. 22a-d). Consequently, with increasing hydrophilic particle coverage on the lignin substrate, the water contact angle decreased. The increase in the coverage also affected the surface roughness, which was determined using image analysis. Initially, an increase in the particle coverage resulted in nanostructures. That increased the surface root mean square roughness (rms) from a few to approximately 10 nm. However, with full particle coverage, the roughness decreased to a few nanometers again.

In the theoretical approach, the rms roughness *(w)* for the nanoparticle coated substrates was expressed by,

$$w = h\sqrt{c(1-c)} \qquad (4.1),$$

derived from the definition of root mean square roughness. The nanoparticle coverage on the substrate is denoted by c and the height of the particles with h. Despite the fact that with the intermediate nanoparticle dispersion concentrations the nanoparticles were not perfectly evenly distributed on the substrate the theoretical and experimental values of the roughness of the nanoparticle coated substrate were congruent (Fig. 22e). The basis for the theoretical approximation of the contact angle of a nanoparticle coated substrate was the Wenzel approach (Eq. (2.6)). The addition of nanoparticles changes the area in contact with the wetting drop, and therefore, the area will change depending on the nanoparticle coverage and the nanoparticle shape. The shape was defined by a shape factor *(A)*. Therefore, the apparent contact angle in equilibrium can be described by,

$$\cos\theta_{\text{app}} = (1-c)\cos\theta_{\text{s}} + Ac\cos\theta_{\text{NP}} \qquad (4.2),$$

where θ_{s} is the contact angle of the lignin substrate and θ_{NP} the contact angle of the nanoparticles. The modified Wenzel equation (Eq. (4.2)) was fitted to the experimental contact angle values in order to enable extraction of the shape factor from the fit (Fig. 22f). By doing this a shape factor of ~1, accompanied with a small offset was noted to give the best fit between the model and the experimental values. Hence, although nanoparticles were noted to affect the substrate surface roughness (at the nanometer scale), the wetting of the lignin substrate seemed to be unaffected by these roughness changes. The effect is probably due to the small size of the particles in comparison to the droplet size (Marmur & Bittoun 2009), enabling the nanoparticles to be considered only as noise during drop spreading.

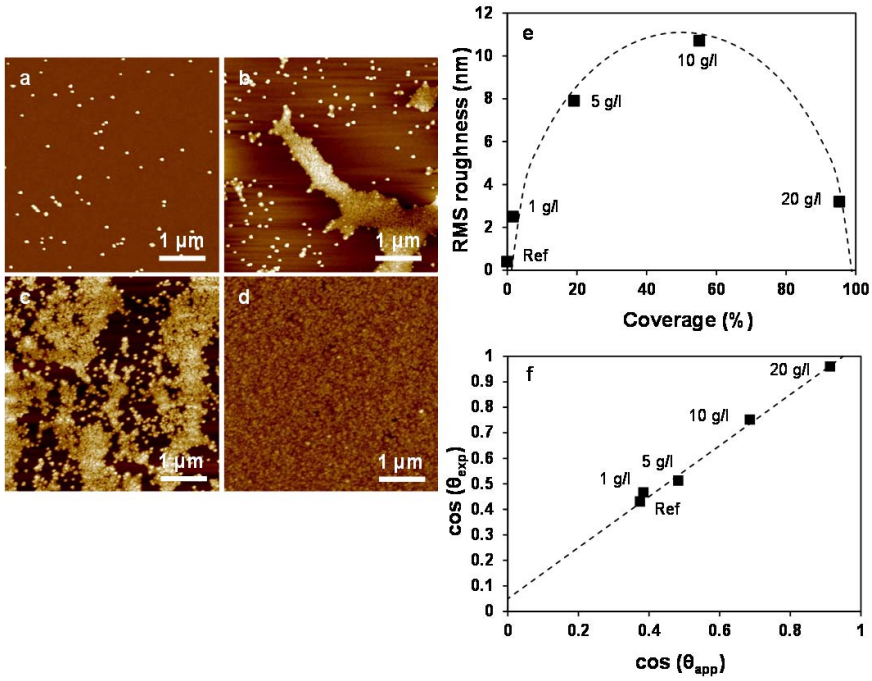

Figure 22. AFM topography images (25 µm²) of lignin substrate spin coated with (a) 1 g dm^{-3}, (b) 5 g dm^{-3}, (c) 10 g dm^{-3} and (d) 20 g dm^{-3} SNP dispersion. (e) Comparison between the experimental (■) and theoretical (dashed line) rms roughness calculated using Eq. (4.1). (f) The relation of the experimental (■) and modeled (dashed line) contact angles calculated using Eq. (4.2). (Paper V).

Evidently, nanoscale substrate roughness is not the critical factor for controlling the wetting or dewetting properties of planar substrates. As was shown in Figure 21,

chemical modification of nanoparticles can be used to prepare hydrophobic particles. However, such chemical treatments (e.g. silylation) of particles do not meet the criteria for creating simple pathways to preparing hydrophobic particles in water-phase, even, on-site. Therefore, in order to be able to affect the hydrophobicity using polyelectrolyte-modified nanoparticles, paper sizing agents AKD and ASA were combined with the cationic SNP and the anionic nanoPCC dispersions, respectively.

4.3.2 Preparation of coating dispersions combining nanoparticles and hydrophobic substances

The concept of a stable emulsion or a hydrophobic colloid is complex. In general, a colloidal dispersion is never thermodynamically stable, leading to continuous decrease in its free energy by, for example, reduction in its interfacial area. This means that the particles coagulate. Moreover, in such dispersions hydrophobic particles experience long-ranged attractive forces leading to coalescence of the substances, and eventually, to drastic changes in the dispersion properties, that is, to phase separation. The stability of such emulsions can be affected by introducing a third phase into the oil-in-water system. One way to do this is to stabilize the emulsion by introducing solid particles into the system (Pickering 1907, Aveyard et al. 2003, Binks & Horozov 2005). In such emulsions the particles can be located in the fluid medium or settle at the interface of water and the hydrophobic substances. The interactions between these constituents and, for example, the particles contact angle with the fluid affects their assembly (Kruglyakov & Nushtayeva 2004).

It was hypothesized that using the sizing agents, dispersions able to form a hydrophobic coating layer could be constructed. However, as pointed out above, preparation of a hydrophobic dispersion is not straightforward. Hence, the interactions between the cationic SNP modifiers and the AKD emulsion were studied using QCM-D (Fig. 23). First, PAH and PEI were adsorbed on the silica coated QCM-D crystal and then the AKD emulsion was adsorbed on the polyelectrolyte layers. The emulsion adsorbed on the PEI layer caused a considerably high decrease in the frequency, 350 Hz. The adsorption of AKD on PAH was significantly lower, 60 Hz. Additionally, the adsorption kinetics of the two systems was different: AKD adsorption on the PAH layer reached the equilibrium quickly while on the PEI layer the QCM-D response reached a plateau more slowly. Although adsorption on PEI was substantially higher than on PAH, the adsorption ratio correlated fairly well with the difference between the amount of the polyelectrolyte adsorbed. Hence, one can state that with the underlying cationic polyelectrolyte, the affinity towards AKD can be adjusted.

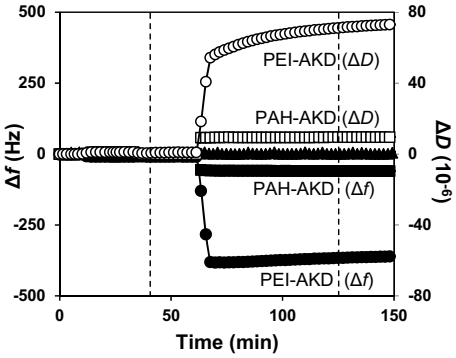

Figure 23. Adsorption of AKD on a PAH coated (■), PEI coated (●) and plain (▲) silica QCM-D crystal. The frequency (left y-axes) and dissipation (right y-axes) response are illustrated by filled and open symbols, respectively. The dashed lines represent the rinsing steps. (Paper III).

AKD was added to the SNP dispersion at a weight ratio of 3:10, AKD to polyelectrolyte-modified SNP, which was the maximum possible AKD amount added resulting in a turbid one-phase dispersion. A higher AKD concentration led to charge reversal, but also to phase separation into clear and opaque phases. The dispersions containing SNP-PEI or SNP-PAH and AKD were freeze-dried and analyzed using XPS. Freeze-drying of the neat emulsion without the particles formed a viscous residual resembling the neat AKD product, while drying of the dispersions containing particles resulted in powder-like residues. It seems that addition of nanoparticles in the dispersion is able to change the structure so that upon drying no separation of the constituents takes place. These observations indicate that the nanoparticles contribute to the dispersion stability.

Due to the amine content of the modifying polyelectrolytes, the nitrogen intensity of the dried dispersion in XPS analysis (Table 1) was noted to increase with the modification. The relative change was higher with PEI-modified particles than with the PAH-modified particles. Similarly, the silicon intensity decreased more, by ~25%, with the PEI treatment, while the change was minor with the SNP-PAH particles. It is apparent, as seen also in the QCM-D experiments (Fig. 16), that the particles are covered by a cationic polyelectrolyte layer, and that the PAH layer is thin (thinner than the analysis depth of XPS, 10 nm), while PEI forms a thicker layer. In comparison to the initial silicon intensity, addition of AKD to the SNP-PEI and SNP-PAH dispersions decreased the intensity by ~70%, accompanied by an increase in the carbon content. This suggests that AKD is preserved in the dispersion and is therefore assumed to affect the dispersion properties as well as to contribute to the properties of the coating layer formed.

Table 1. Atomic percentages (XPS) for dried unmodified and modified silica particle dispersions. (Paper III).

Material	C	O	N	Si
SNP	3	69	-	27
PAH	70	7	12	-
SNP-PAH	8	65	1.3	26
SNP-PAH-AKD	73	19	0.7	7
PEI	67	-	33	-
SNP-PEI	24	45	11	20
SNP-PEI-AKD	62	20	7	9

The hydrophobic dispersions spin coated on a silica substrate showed slightly varying structures depending on the polyelectrolyte used to modify the SNPs. The dispersion of PAH-modified particles formed a layer with coverage varying between 4 and 30%. Figure 24a represents an area with a moderate coverage of 10%. A close-up shows the individual particles (Fig. 24b). The dispersion of PEI-modified SNPs and AKD formed a layer with a constant coverage of ~20% (Fig. 24c). In contrast to the PAH-modified dispersion, the particles formed clusters (Fig. 24d).

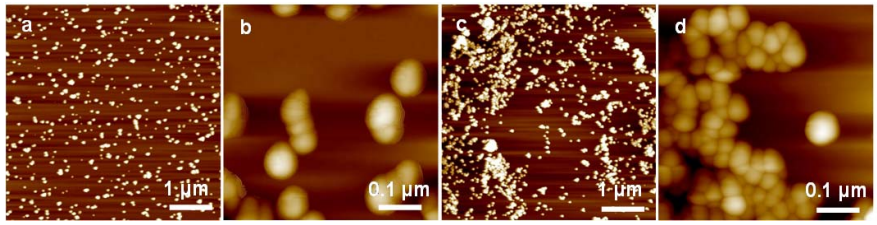

Figure 24. AFM topography images of (a) 25 µm² and (b) a close-up of SNP-PAH-AKD dispersion spin coated on a silica substrate. The corresponding images of SNP-PEI-AKD dispersion are presented in (c) and (d). (Paper III).

When considering the practical use of any dispersion, it is essential to examine its lifetime. The layers shown in Figure 24 were spin coated within few hours after dispersion preparation. However, in many applications longer time scales are also of interest. Therefore, the prepared dispersions were stored for 2 months and applied again on a silica substrate. A clear discrepancy was noticed between the substrate spin coated with the fresh SNP-PAH-AKD (Fig. 25a) and the stored dispersion (Fig. 25b). The latter consisted of larger particle islands than the more uniform coating with the fresh dispersion.

Examination of the 25 μm² images showed various surface structures, an example of which is presented in Figure 25c. The SNP-PEI-AKD dispersion, however, seemed to stay intact during the storage and the 100 μm² topography images of the coating of the fresh and stored dispersion (Fig. 25d and 25e), as well as the 25 μm² images (Fig. 25f and 24c) were similar.

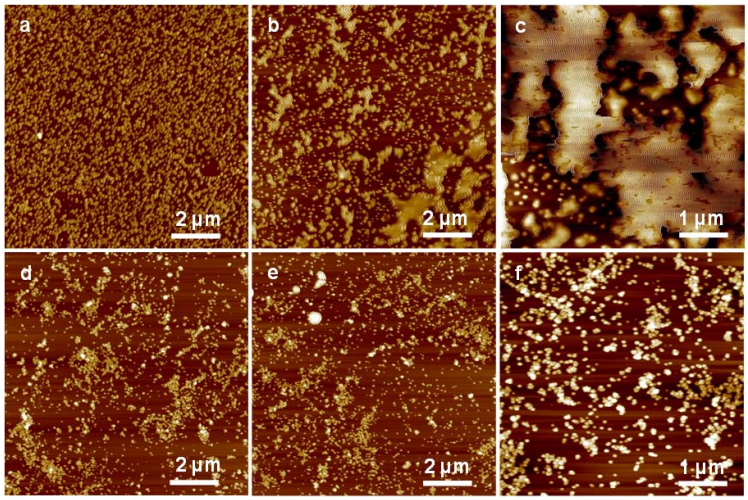

Figure 25. AFM topography images of 100 μm² of a silica substrate spin coated with (a) the fresh and (b) the stored dispersion of SNP-PAH-AKD, and (c) a 25 μm² image of a substrate spin coated with the stored dispersion. The corresponding images of SNP-PEI-AKD dispersion are presented in (d), (e) and (f). (Unpublished data).

Although based on the measurements conducted in this thesis, it is not possible to undoubtedly verify the structures of the nanoparticle dispersions formed with AKD. Based on the properties and interactions of the dispersion components, a few suggestions regarding the structures are presented. In the emulsion combining nanoparticle dispersions, due to a relatively low amount of AKD or ASA in the dispersion, the dispersions contain oil dispersed in water. In a dispersion combining nanoparticles and emulsion droplets the nanoparticles can be located either in the continuous phase, or at the interface of the droplets and the medium. Although the strong affinity between the cationic polyelectrolytes and AKD (Fig. 23) suggest that this interaction can be utilized to form multilayers on particles, energetically it is not likely that the dispersion constituents would organize in such a manner that a hydrophobic layer covers the more hydrophilic particles in an aqueous environment. However, the noted attraction between the dispersion components is likely to cause organization of particles during mixing. Adsorption of PEI induces a thicker polyelectrolyte layer on the silica particle than PAH (Fig. 16) leading to a stronger affinity between PEI and AKD. This interaction can enable

the SNP-PEI particles to settle at the boundary between water and AKD, stabilizing the AKD emulsion, whereas the SNP-PAH particles are possibly located freely in the water phase. This hypothesis is supported by a suggestion that flocculation of the stabilizing particles at the oil-water interface increase stability due to packing of the particles (Midmore 1998, Binks & Lumsdon 1999, Binks et al. 2007) and would hence explain the better stability of the SNP-PEI-AKD dispersion during storage. In addition to the above mentioned dispersion structures, presumably there are some amounts of the free constituents present. The presence of free polymer in an emulsion can induce steric stabilization (Fleer et al. 1972, Sadovoy et al. 2011). The dispersions probably also contain mixtures of polyelectrolyte and AKD, as well as silica nanoparticles covered by these mixtures.

Similarly to the SNPs combined with AKD, the nanoPCC particles were combined with ASA. In comparison to the dispersions containing oppositely charged SNPs and AKD, it is likely that in the dispersion of hydrophilic, anionic pectin-nanoPCC particles with hydrophobic ASA droplets, the constituents do not mix, but the ASA emulsion is interrupted by the particles. However, it needs to be noted that unlike the AKD dispersions, the concept in this case was not primarily to form a hydrophobic dispersion for a nanoparticle coating on a planar substrate, but to be able to control the interaction between ASA and the nanoPCC particles. As depicted in Figure 7, in aqueous solution ASA undergoes hydrolysis to form a dicarboxylic acid (Gess & Rende 2005). Hydrolyzed ASA can further dissociate and is then able to bind Ca^{2+} and form insoluble substances (Lindfors et al. 2005). As predicted, addition of ASA emulsion to a nanoPCC dispersion caused the mixture to aggregate and phase separate. However, the mixture of the pectin-modified particles with ASA remained stable (presented in paper IV). Furthermore, even an increase in the ASA concentration did not cause aggregation in the dispersion and clearly, the pectin treatment was beneficial regarding formation of a uniform dispersion structure. The dispersions of pectin-modified nanoPCC particles combined with ASA spin coated on an NFC substrate resulted in evenly distributed particle clusters, yet at low coverage ranging from ~7% to ~2% (Fig. 26a-c). An increase in the nanoparticle concentration increased coverage, as expected (Kontturi et al. 2007), and the coverage reached ~19 and ~35% for 5 and 10 g dm^{-3} pectin-nanoPCC concentration, respectively (Fig. 26d and e). Spin coating the most concentrated pectin-nanoPCC dispersion (10 g dm^{-3}) with elevated ASA concentration (0.5 g dm^{-3}) produced a uniform layer with ~30% coverage (Fig. 26f). The height of particles of this structure was approximately 240 ± 70 nm denoting that the layer consisted of groups of a few nanoparticles clustered together. Clearly the nanoparticle modification enables the particle concentration to be increased without the formation of considerably aggregated layer as was the case with the

unmodified particles shown in Figure 19a. This is beneficial for the construction of nanoparticle layers with high coverage yet low thickness.

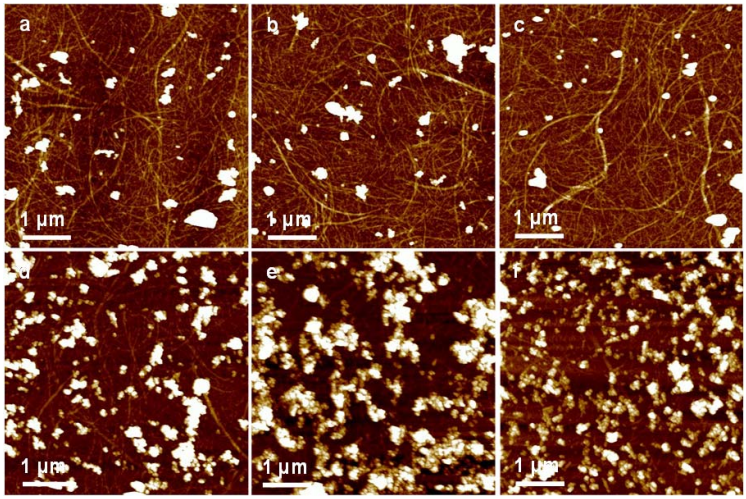

Figure 26. AFM topography images (25 µm²) of NFC substrate spin coated with dispersion containing (a) 1 g dm^{-3} pectin-nanoPCC dispersion with 0.25 g dm^{-3} ASA, (b) 1 g dm^{-3} pectin-nanoPCC dispersion with 1 g dm^{-3} ASA, (c) 1 g dm^{-3} pectin-nanoPCC dispersion with 3 g dm^{-3} ASA, (d) 5 g dm^{-3} pectin-nanoPCC dispersion with 0.25 g dm^{-3} ASA, (e) 10 g dm^{-3} pectin-nanoPCC dispersion with 0.25 g dm^{-3} ASA and (f) 10 g dm^{-3} pectin-nanoPCC dispersion with 0.5 g dm^{-3} ASA. (Paper IV).

Clearly, it is possible to combine hydrophobic substances and nanoparticles in a dispersion in aqueous medium. Nanoparticles can improve the lifetime of such dispersions and nanoparticle surface modification can be used to affect the interactions between the particles and the hydrophobic substances. Since hydrophobic particles tend to attract each other in an aqueous medium, it is clear that the emulsion droplets will eventually coalesce and that the dispersions are only kinetically stable. However, the life-time of the dispersions is always related to the time-span that they are used. If the aim is to develop an easy and upscalable dispersion modification procedure to be conducted on-site, then the described system is feasible.

4.4 Ultrathin coating layers

As shown in the previous chapter, the hydrophobic silica nanoparticle and precipitated calcium carbonate dispersions were successfully applied on a planar substrate forming a nanoparticle coating with uniformly distributed particles (Figs. 24 and 26). Unlike most examples of nanoparticle coatings mainly utilizing packed nanoparticle structures (McConnell et al. 2009, Yan et al. 2007), these surfaces were truly of nanoparticle size and

some of them even at the monolayer scale. In addition to characterizing these ultrathin coating layers using AFM, their wetting characteristics were evaluated by water contact angle measurements. Besides smooth NFC and silica substrates the coatings were applied onto paper. The smooth substrate for the nanoPCC particles was the NFC film, while the SNPs were spin coated on silica substrates. It is recognized that NFC model surfaces have a unique chemical character that cannot be mimicked by silica surfaces, yet due to their corresponding properties (anionic charge, hydrophilicity, OH-groups) silica has been widely used as a model for cellulose substrates.

When the SNPs were applied on the substrates, on both silica and paper the water contact angle increased with the treatment (Table 2). Regardless of the low coverage of the substrates treated with cationic SNPs and AKD, on both substrates the water contact angle increased approximately 50° in comparison to wetting of the bare substrate. The SNP-PAH-AKD coating resulted in a slightly higher water contact angle than the SNP-PEI-AKD coating. Interestingly, the coating layer of the PEI-modified SNPs without AKD clearly increased the contact angle of the substrate in comparison to the respective PAH-modified particles. Moreover, plain PAH spin coated on the silica substrate did not affect the water contact angle, while a PEI layer increased the contact angle to approximately 40°. Water contact angle values for PAH and PEI films have been reported in several studies, yet with discrepancy. PAH is known to be a fairly hydrophilic polymer (Lowack & Helm 1995) and a film has been reported to reach a maximum contact angle of 40° on mica (Kolasinska et al. 2008). PEI film on an aluminium wafer, on the other hand, has been reported to show a contact angle of approximately 70° (Ren et al. 2003). However, observations of slightly higher contact angle of a PAH compared to a PEI film have also been reported (Kolasinska & Warszynski 2005, Hänni-Ciunel et al. 2007).

As shown in the previous Chapter 4.3, nanoparticles are too small to affect wetting by structural roughness. Consequently, the resulting water contact angle values were not ultimately high on the smooth substrates coated with nanoparticles. On the rough paper substrate, on the other hand, the treatment enhanced water-repellency up to very high contact angle values. On paper, the combination of micro and nanoscale roughness can have an impact on the hydrophobicity (Feng & Jiang 2006, Hyde et al. 2007b, Bhushan et al. 2009a).

Table 2. Effect of the nanoparticle coatings on water contact angle of dense silica and porous paper substrates at t=1s. (Paper III).

Material	CA (°) on nonporous silica substrate	CA (°) on porous paper substrate
Ref.	20 ± 2	74 ± 6
SNP-PAH	19 ± 1	69 ± 3
SNP-PAH-AKD	77 ± 3	136 ± 2
SNP-PEI	30 ± 1	108 ± 3
SNP-PEI-AKD	66 ± 1	127 ± 2

Wetting of the coatings containing pectin-modified nanoPCC particles was also evaluated. Because of the hydrophilic character of both the nanoPCC particles and pectin, the modified particles did not increase the hydrophobicity of a given substrate. Therefore, as hypothesized, the ASA concentration in the nanoparticle dispersion was the determining factor for hydrophobicity. This is clearly illustrated by the water contact angle depicted as a function of ASA concentration in Figure 26a. With low nanoparticle concentration (1 g dm^{-3}) accompanied with increasing ASA concentration the water contact angle increased reaching a value of 85 ± 7° and 135 ± 5° on the NFC and the paper substrate, respectively (Fig. 27a). Consequently, an increase in nanoparticle concentration decreased the water contact angle (Fig. 27b), an effect that could again be compensated for by an increase in the ASA concentration. The nanoparticle layer formed by a 10 g dm^{-3} dispersion containing 0.5 g dm^{-3} ASA (the structure with coverage of ~30% shown in Figure 26f) produced a coating with a water contact angle of 65 ± 5° and 125 ± 2° on NFC and paper substrates, respectively.

It is noteworthy that the pectin treatment of the nanoPCC particles enabled an increase in the coverage of the nanoparticle coating, yet the resulting layer was still very uniform and was not constructed of large aggregate clusters (Fig. 26). Hence, with the approach presented, it is possible to form a smooth nanoparticle coating with a tunable particle coverage and, very importantly, with tunable wetting characteristics.

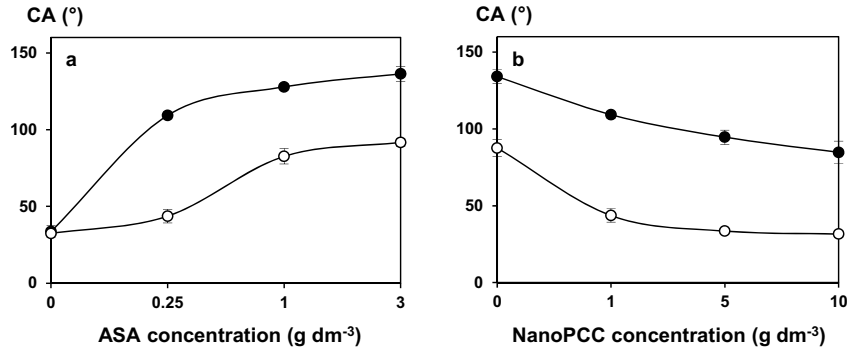

Figure 27. Water contact angle of pectin-nanoPCC/ASA coating with (a) increasing ASA or (b) increasing pectin-nanoPCC concentration on NFC (○) and paper (●) substrates. The nanoPCC concentration in (a) was 1 g dm^{-3} and the ASA concentration in (b) 0.25 g dm^{-3} except for the reference point for which it was 1 g dm^{-3}. (Paper IV).

As discussed in Chapter 2.3.2, besides contact angle, wetting of paper is defined by the penetration of water into the porous structure (Cazabat 1989, Schoelkopf et al. 2000, Ridgway & Gane 2006). In addition to increased contact angle, as demonstrated in Figure 27 and Table 2, both the silica and nanoPCC coatings were able to enhance the resistance of the paper surface to water penetration into the structure, seen as the unchanged contact angle as a function of time (shown in detail in Papers III and IV). Evidently the nanostructured coatings were able to alter the characteristic bipartite wetting behavior of the paper substrate where first a pseudo-equilibrium contact angle is reached, followed by water adsorption into the structure (Modaressi & Garnier 2002). The ability to tune this behaviour is important in variety of applications seeking ways to decrease liquid imbibition into the base substrate, which can lead to, for example, decreased substrate strength properties.

The proposed coating concept differs significantly from traditional coatings. Instead of preparing coatings with a coat weight above several grams per square meter, a controlled nanostructure was formed. It is clear that the evenly distributed and thin nanoparticle coatings presented are not comparable with traditional coating layers where the coating covers paper with a layer that has a minimum thickness in the micrometer scale. However, some of the procedures presented could be beneficial in traditional coating applications. Treating silica particles to be cationic using cationic polyelectrolytes increases the affinity between the particles and paper or dye (Neumann et al. 2005, Daniel & Berg 2006, Kettle et al. 2010), a concept that is exploitable in coatings for inkjet printing. Additionally, stabilization of PCC with pectin provides a tool to control deposit problems and to increase the PCC particle charge. It is also possible to affect material

consumption by using a controllably constructed coating with a minimal amount of particles.

The traditional coating methods are not necessarily suitable for using such dispersions. For example, in blade coating, force is applied on the coating dispersion which might cause nanoparticles to penetrate into paper structure. Thus, prior to utilizing the introduced approach in industrial scale coatings, a proper technique needs to be developed to complement the methodology to prepare a truly nanoscale coating. With a proper method there is, without a doubt, the possibility to use these relatively inexpensive particles allowing facile surface modification, to provide a way to alter the surface properties of paper, a substrate of sustainable material. Such an approach could enable modification of the paper substrate for applications demanding surface functionalization.

5 Concluding remarks

The work presented in this thesis was devoted to exploring the use of nanoparticles in the surface treatment of planar substrates. One of the objectives was to provide an approach exploitable in industrial processes, that is, a simple approach reproducible in large quantities. In addition to the practical aspect, the fundamental understanding of the interactions governing dispersion stability and the adsorption behavior of the substances during particle modification was emphasized. A combination of surface sensitive and bulk methods provides important insight not available otherwise.

One of the main objectives of the study was to explore layer build-up using nanoparticles. This was done by observing the layer deposition in an aqueous environment. Moreover, layer formation of nanoparticles sequentially added with oppositely charged polyelectrolytes and the adsorption of separately prepared complexes of those same constituents were compared. The physical properties of the nanomaterials were noted to significantly affect the layers formed. Nanosized spherical silica particles were able to penetrate the preceding layer, while nanoparticles with high length to width ratio, nanofibrils, formed a stratified layer. A detailed analysis of the layer build-up and the changes in the surface forces provides information not only beneficial in the preparation of surface treatments, but also in any process utilizing nanoparticle-polyelectrolyte interactions. Additionally, adsorption and organization of a nanopigment layer on a cellulosic nanofibril substrate was investigated with respect to dispersion conditions and particle properties. It is clear that the adsorption behavior and the layer structure formed are distinct depending on the nanoparticle shape and charge. Such detailed study regarding the possibilities of creating layered structures of nanoparticles is of significant importance concerning the preparation of highly ordered surfaces. In addition to exploring nanoparticle layer formation, analysis of nanopigment adsorption with QCM-D widens the perception of the interactions occurring in a dispersion containing pigments, that is, in traditional coating colors as well as provides information important in development of hybrid materials combining organic and inorganic substance.

One hypothesis was that coating dispersion stability is necessary for uniform particle distribution on a substrate. Therefore, a significant amount of work was devoted

to examine dispersion stability. Especially with nanoparticles, the importance of dispersion stability cannot be over-estimated. In the majority of existing applications and literature evaluating nanoparticle usage, this fact is often left unconsidered. However, in order to exploit individual nanoparticles instead of larger aggregates the dispersion properties must be understood. An approach to modify inorganic nanoparticles through adsorption of oppositely charged components was presented. The polyelectrolyte properties were shown to strongly affect the layer structure formed as well as the particle interactions. Cationicity of silica nanoparticles enhanced their interaction with an anionic hydrophobic sizing agent. This enabled preparation of dispersions combining emulsion droplets and nanoparticles. With PCC particles, the possibility to affect particle charge may facilitate their utilization in applications where electrostatic interactions are of importance. Moreover, particle modification significantly improved dispersion stability and enabled the preparation of a dispersion containing nanoPCC particles with ASA, a combination typically resulting in aggregation.

Effective stabilization of a given nanoparticle dispersion was noted to be an imperative to obtain a uniform nanoparticle coating. With control of the dispersion stability, submonolayer coatings of the silica nanoparticles were prepared. The coverage of the layers formed when using stabilized nanoPCC dispersions could be tuned by altering the dispersion concentration. Particle stabilization is a prerequisite for both the ability to increase the concentration of the stable dispersions and to prepare a nanoparticle coating with nanoscale thickness. The dispersions containing modified nanoparticles combined with hydrophobic substances, when applied on planar substrates, were able to alter the substrate wetting properties even at very low coverage. Although wetting of a smooth and dense substrate could not be drastically altered with nanoparticle treatment, the effect on a porous paper substrate was more pronounced. Moreover, the water penetration rate into the paper structure was decreased, and the level of hydrophobicity of the paper substrate could be tuned. This is an important factor considering the exploitability of such coating structures in a variety of applications, for example, in printing.

The effect of nanoparticles on the wetting of a planar substrate was examined by combining experimental work with a theoretical model that has not previously been studied. The work demonstrates that the roughness induced by nanoparticles is too low to affect wetting when the droplet size is a few microliters. Evidently the situation is changed if nanoparticle aggregates are used instead of nanoparticles, or if the drop size to nanoparticle size is altered.

This study provides insight on how nanoparticles can be utilized in surface treatments of planar substrates. Although the knowledge gathered in this thesis is mainly of scientific interest, undoubtedly the information can be exploited on a larger scale. The work provides a starting point for rethinking the concept of coatings in regard to

development of low-cost, high-functionality products. The chosen nanoparticle materials relate the work conducted closely to paper surface treatments, but the ability to prepare nanoparticle substrates with tunable coverage yet low thickness provides an interesting premise for treating substrates of other materials as well.

6 References

Ahola, S., Österberg, M. & Laine, J. (2008a). Cellulose nanofibrils - adsorption with poly(amide-amine) epichlorohydrin studied by QCM-D and application as a paper strength additive. *Cellulose* **15**(2), 303-314.

Ahola, S., Salmi, J., Johansson, L.S., Laine, J. & Österberg, M. (2008b). Model films from native cellulose nanofibrils. preparation, swelling, and surface interactions. *Biomacromolecules* **9**(4), 1273-1282.

Ahola, S., Myllytie, P., Österberg, M., Teerinen, T. & Laine, J. (2008c). Effect of polymer adsorption on cellulose nanofibril water binding capacity and aggregation. *Bioresources* **3**(4), 1315-1328.

Alleborn, N. & Raszillier, H. (2004). Spreading and sorption of droplets on layered porous substrates. *J. Colloid Interface Sci.* **280**(2), 449-464.

Andresen, M. & Stenius, P. (2007). Water-in-oil emulsions stabilized by hydrophobized microfibrillated cellulose. *J. Dispersion Sci. Technol.* **28**(6), 837-844.

Ankerfors, C., Lingström, R., Wågberg, L. & Ödberg, L. (2009). A comparison of polyelectrolyte complexes and multilayers: their adsorption behaviour and use for enhancing tensile strength of paper. *Nord. Pulp Pap. Res. J.* **24**(1), 77-86.

Ankerfors, C., Ondaral, S., Wågberg, L. & Ödberg, L. (2010). Using jet mixing to prepare polyelectrolyte complexes: Complex properties and their interaction with silicon oxide surfaces. *J. Colloid Interface Sci.* **351**(1), 88-95.

Argyris, D., Ashby, P.D. & Striolo, A. (2011). Structure and orientation of interfacial water determine atomic force microscopy results: insights from molecular dynamics simulations. *ACS Nano* **5**(3), 2215-2223.

Ariga, K., Lvov, Y., Onda, M., Ichinose, I. & Kunitake, T. (1997). Alternately assembled ultrathin film of silica nanoparticles and linear polycations. *Chem. Lett.* (2), 125-126.

Atalla, R., Beecher, J., Jones, P., Wegner, T., Caron, R., Catchmark, J., Deng, Y., Glasser, W., Gray, D. & Heigler, C. (2005). *Nanotechnology for the forest products industry - vision and technology roadmap*. TAPPI Press, Atlanta, GA.

Aulin, C., Varga, I., Claesson, P.M., Wågberg, L. & Lindström, T. (2008). Buildup of polyelectrolyte multilayers of polyethyleneimine and microfibrillated cellulose studied by in situ dual-polarization interferometry and quartz crystal microbalance with dissipation. *Langmuir* **24**(6), 2509-2518.

Aulin, C., Ahola, S., Josefsson, P., Nishino, T., Hirose, Y., Österberg, M. & Wågberg, L. (2009). Nanoscale cellulose films with different crystallinities and mesostructures-their surface properties and interaction with water. *Langmuir* **25**(13), 7675-7685.

Aulin, C., Gällstedt, M. & Lindström, T. (2010a). Oxygen and oil barrier properties of microfibrillated cellulose films and coatings. *Cellulose* **17**(3), 559-574.

Aulin, C., Johansson, E., Wågberg, L. & Lindström, T. (2010b). Self-organized films from cellulose i nanofibrils using the layer-by-layer technique. *Biomacromolecules* **11**(4), 872-882.

Aveyard, R., Binks, B.P. & Clint, J.H. (2003). Emulsions stabilised solely by colloidal particles. *Adv. Colloid Interface Sci.* **100-102**, 503-546.

Azizi Samir, M.A.S., Alloin, F., Sanchez, J.Y. & Dufresne, A. (2004). Cellulose nanocrystals reinforced poly (oxyethylene). *Polymer* **45**(12), 4149-4157.

Bagwe, R.P., Hilliard, L.R. & Tan, W. (2006). Surface modification of silica nanoparticles to reduce aggregation and nonspecific binding. *Langmuir* **22**(9), 4357-4362.

Beck, S., Bouchard, J. & Berry, R. (2011). Controlling the reflection wavelength of iridescent solid films of nanocrystalline cellulose. *Biomacromolecules* **12**(1), 167-172.

Bergna, H.E. & Roberts, W.O. (2006). *Colloidal silica, fundamentals and applications*. CRC Taylor & Francis, Boca Raton.

Bhushan, B., Jung, Y.C. & Koch, K. (2009a). Micro-, nano-and hierarchical structures for superhydrophobicity, self-cleaning and low adhesion. *Phil. Trans. R. Soc. A* **367**, 1631-1672.

Bhushan, B., Koch, K. & Jung, Y.C. (2009b). Fabrication and characterization of the hierarchical structure for superhydrophobicity and self-cleaning. *Ultramicroscopy* **109**(8), 1029-1034.

Bico, J., Tordeux, C. & Quere, D. (2001). Rough wetting. *Europhys. Lett.* **55**(2), 214-220.

Bico, J., Thiele, U. & Quere, D. (2002). Wetting of textured surfaces. *Colloids Surf., A* **206**(1-3), 41-46.

Biggs, S., Habgood, M., Jameson, G.J. & Yan, Y. (2000). Aggregate structures formed via a bridging flocculation mechanism. *Chem. Eng. J.* **80**(1-3), 13-22.

Binks, B.P. & Lumsdon, S.O. (1999). Stability of oil-in-water emulsions stabilised by silica particles. *Phys. Chem. Chem. Phys.* **1**(12), 3007-3016.

Binks, B.P. & Horozov, T.S. (2005). Aqueous foams stabilized solely by silica nanoparticles. *Angew. Chem., Int. Ed.* **44**(24), 3722-3725.

Binks, B.P., Rodrigues, J.A. & Frith, W.J. (2007). Synergistic interaction in emulsions stabilized by a mixture of silica nanoparticles and cationic surfactant. *Langmuir* **23**(7), 3626-3636.

Binnig, G., Quate, C.F. & Gerber, C. (1986). Atomic force microscope. *Phys. Rev. Lett.* **56**(9), 930-933.

Blomberg, E., Poptoshev, E., Claesson, P.M. & Caruso, F. (2004). Surface interactions during polyelectrolyte multilayer buildup. 1. Interactions and layer structure in dilute electrolyte solutions. *Langmuir* **20**(13), 5432-5438.

Bornside, D.E., Brown, R.A., Ackmann, P.W., Frank, J.R., Tryba, A.A. & Geyling, F.T. (1993). The effects of gas phase convection on mass transfer in spin coating. *J. Appl. Phys.* **73**(2), 585-600.

Bosanquet, C. (1923). LV. On the flow of liquids into capillary tubes. *Philos. Mag.* **45**(267), 525-531.

Braccini, I. & Perez, S. (2001). Molecular basis of Ca^{2+}-induced gelation in alginates and pectins: the egg-box model revisited. *Biomacromolecules* **2**(4), 1089-1096.

Bravo, J., Zhai, L., Wu, Z., Cohen, R.E. & Rubner, M.F. (2007). Transparent superhydrophobic films based on silica nanoparticles. *Langmuir* **23**(13), 7293-7298.

Bucur, C.B., Sui, Z. & Schlenoff, J.B. (2006). Ideal mixing in polyelectrolyte complexes and multilayers: entropy driven assembly. *J. Am. Chem. Soc.* **128**(42), 13690-13691.

Bugner, D. (2002). *Papers and films for ink jet printing*. In: *Handbook of Imaging Materials*, eds. A.S. Diamond & D.S. Weiss, New York.

Buron, C., Filiâtre, C., Membrey, F., Bainier, C., Charraut, D. & Foissy, A. (2007). Effect of substrate on the adsorption of polyelectrolyte multilayers: Study by optical fixed-angle reflectometry and AFM. *Colloids Surf., A* **305**(1-3), 105-111.

Butt, H., Cappella, B. & Kappl, M. (2005). Force measurements with the atomic force microscope: Technique, interpretation and applications. *Surf. Sci. Rep.* **59**(1-6), 1-152.

Cadene, A., Durand-Vidal, S., Turq, P. & Brendle, J. (2005). Study of individual Na-montmorillonite particle size, morphology, and apparent charge. *J. Colloid Interface Sci.* **285**(2), 719-730.

Callies, M. & Quere, D. (2005). On water repellency. *Soft Matter* **1**(1), 55-61.

Carambassis, A. & Rutland, M.W. (1999). Interactions of cellulose surfaces: effect of electrolyte. *Langmuir* **15**(17), 5584-5590.

Caruso, F., Spasova, M., Salgueirino-Maceira, V. & Liz-Marzan, L.M. (2001). Multilayer assemblies of silica-encapsulated gold nanoparticles on decomposable colloid templates. *Adv. Mater.* **13**(14), 1090-1094.

Cassie, A.B.D. & Baxter, S. (1944). Wettability of porous surfaces. *Trans. Faraday Soc.* **40**, 546-551.

Cazabat, A.M. (1987). How does a droplet spread? *Contemp. Phys.* **28**(4), 347-364.

Cazabat, A.M. (1989). The dynamics of wetting. *Nord. Pulp Pap. Res. J.* **4**(2), 146-154.

Cerruti, P., Ambrogi, V., Postiglione, A., Rychly, J., Matisova-Rychla, L. & Carfagna, C. (2008). Morphological and thermal properties of cellulose-montmorillonite nanocomposites. *Biomacromolecules* **9**(11), 3004-3013.

Chang, F.C. & Sposito, G. (1996). The electrical double layer of a disk-shaped clay mineral particle: effects of electrolyte properties and surface charge density. *J. Colloid Interface Sci.* **178**(2), 555-564.

Chen, K.L. & Elimelech, M. (2008). Interaction of fullerene (C_{60}) nanoparticles with humic acid and alginate coated silica surfaces: measurements, mechanisms, and environmental implications. *Environ. Sci. Technol.* **42**(20), 7607-7614.

Chivrac, F., Pollet, E. & Averous, L. (2009). Progress in nano-biocomposites based on polysaccharides and nanoclays. *Mater. Sci. Eng.,R.* **67**(1), 1-17.

Claesson, P.M. & Christenson, H.K. (1988). Very long range attractive forces between uncharged hydrocarbon and fluorocarbon surfaces in water. *J. Phys. Chem.* **92**(6), 1650-1655.

Claesson, P.M., Paulson, O.E.H., Blomberg, E. & Burns, L. (1997). Surface properties of poly(ethylene imine)-coated mica surfaces-salt and pH effects. *Colloids Surf., A* **123-124**, 341-353.

Cosgrove, T. (2005). *Colloid science: principles, methods and applications*. Wiley-Blackwell, Chichester.

Daniel, R.C. & Berg, J.C. (2006). Spreading on and penetration into thin, permeable print media: Application to ink-jet printing. *Adv. Colloid Interface Sci.* **123-126**, 439-469.

Daoud-Mahammed, S., Couvreur, P. & Gref, R. (2007). Novel self-assembling nanogels: Stability and lyophilization studies. *Int. J. Pharm.* **332**(1-2), 185-191.

Decher, G. (1997). Fuzzy nanoassemblies: Toward layered polymeric multicomposites. *Science* **277**(5330), 1232-1237.

Decker, E. & Garoff, S. (1997). Contact line structure and dynamics on surfaces with contact angle hysteresis. *Langmuir* **13**(23), 6321-6332.

Delhom, C.D., White-Ghoorahoo, L.A. & Pang, S.S. (2010). Development and characterization of cellulose/clay nanocomposites. *Compos. B, Eng.* **41B**(6), 475-481.

Delville, A. & Laszlo, P. (1990). The origin of the swelling of clays by water. *Langmuir* **6**(7), 1289-1294.

Derjaguin, B. & Landau, L. (1941). A theory of the stability of strongly charged lyophobic sols and the coalescence of strongly charged particles in electrolytic solution. *Acta Physicochimica URSS* **14**, 633-662.

Domka, L. (1994). Modification estimate of kaolin, chalk, and precipitated calcium carbonate as plastomer and elastomer fillers. *Colloid Polym. Sci.* **272**(10), 1190-1202.

Dong, B.H. & Hinestroza, J.P. (2009). Metal nanoparticles on natural cellulose fibers: electrostatic assembly and in situ synthesis. *ACS Appl. Mater. Interfaces* **1**(4), 797-803.

Du, B. & Johannsmann, D. (2004). Operation of the quartz crystal microbalance in liquids: Derivation of the elastic compliance of a film from the ratio of bandwidth shift and frequency shift. *Langmuir* **20**(7), 2809-2812.

Dubas, S.T. & Schlenoff, J.B. (1999). Factors controlling the growth of polyelectrolyte multilayers. *Macromolecules* **32**(24), 8153-8160.

Ducker, W.A., Senden, T.J. & Pashley, R.M. (1991). Direct measurement of colloidal forces using an atomic force microscope. *Nature* **353**(6341), 239-241.

Eichhorn, S.J., Dufresne, A., Aranguren, M., Marcovich, N.E., Capadona, J.R., Rowan, S.J., Weder, C., Thielemans, W., Toman, M., Renneckar, S., Gindl, W., Veigel, S., Keckes, J., Yano, H., Abe, K., Nogi, M., Nakagaito, A.N., Mangalam, A., Simonsen, J., Benight, A.S., Bismarck, A., Berglund, L.A. & Peijs, T. (2010). Review: current international research into cellulose nanofibres and nanocomposites. *J. Mater. Sci.* **45**(1), 1-33.

Eita, M., Arwin, H., Granberg, H. & Wågberg, L. (2011). Addition of silica nanoparticles to tailor the mechanical properties of nanofibrillated cellulose thin films. *J. Colloid Interface Sci.* **363**(2) 566-572.

Elzbieciak, M., Kolasinska, M., Zapotoczny, S., Krastev, R., Nowakowska, M. & Warszynski, P. (2009). Nonlinear growth of multilayer films formed from weak polyelectrolytes. *Colloids Surf., A* **343**(1-3), 89-95.

Emslie, A.G., Bonner, F.T. & Peck, L.G. (1958). Flow of a viscous liquid on a rotating disk. *J. Appl. Phys.* **29**(5), 858-862.

Enarsson, L. & Wågberg, L. (2007). Kinetics of sequential adsorption of polyelectrolyte multilayers on pulp fibres and their effect on paper strength. *Nord. Pulp Pap. Res. J.* **22**(2), 258-266.

Enarsson, L.E. & Wågberg, L. (2008a). Adsorption kinetics of cationic polyelectrolytes studied with stagnation point adsorption reflectometry and quartz crystal microgravimetry. *Langmuir* **24**(14), 7329-7337.

Enarsson, L.E. & Wågberg, L. (2008b). Polyelectrolyte adsorption on thin cellulose films studied with reflectometry and quartz crystal microgravimetry with dissipation. *Biomacromolecules* **10**(1), 134-141.

Eriksson, M., Torgnysdotter, A. & Wågberg, L. (2006). Surface modification of wood fibers using the polyelectrolyte multilayer technique: effects on fiber joint and paper strength properties. *Ind. Eng. Chem. Res.* **45**(15), 5279-5286.

Eronen, P., Junka, K., Laine, J. & Österberg, M. (2011a). Interaction between water-soluble polysaccharides and native nanofibrillar cellulose thin films. *Bioresources* **6**(4), 4200-4217.

Eronen, P., Heikkinen, S., Österberg, M., Tenkanen, M. & Laine, J. (2011b). Interactions of structurally different hemicelluloses with nanofibrillar cellulose. *Carbohydr. Polym.* **86**(3), 1281-1290.

Eronen, P., Laine, J., Ruokolainen, J. & Österberg, M. (*in press*). Comparison of multilayer formation between different cellulose nano-fibrils and cationic polymers. *J. Colloid Interface Sci.* doi:10.1016/j.jcis.2011.09.028.

Estel, K., Kramer, G. & Schmitt, F.J. (2000). Changes in the interaction characteristics of polyelectrolyte complex covered silica surfaces. *Colloids Surf., A* **161**(1), 193-202.

Evans, D.F. & Wennerström, H. (1999). *The colloidal domain: Where physics, chemistry, biology, and technology meet*. Wiley, New York.

Fang, Y., Al-Assaf, S., Phillips, G.O., Nishinari, K., Funami, T. & Williams, P.A. (2008). Binding behavior of calcium to polyuronates: Comparison of pectin with alginate. *Carbohydr. Polym.* **72**(2), 334-341.

Fatisson, J., Domingos, R.F., Wilkinson, K.J. & Tufenkji, N. (2009). Deposition of TiO_2 nanoparticles onto silica measured using a quartz crystal microbalance with dissipation monitoring. *Langmuir* **25**(11), 6062-6069.

Feng, L., Li, S., Li, Y., Li, H., Zhang, L., Zhai, J., Song, Y., Liu, B., Jiang, L. & Zhu, D. (2002). Super-hydrophobic surfaces: From natural to artificial. *Adv. Mater.* **14**(24), 1857-1860.

Feng, X. & Jiang, L. (2006). Design and creation of superwetting/antiwetting surfaces. *Adv. Mater.* **18**(23), 3063-3078.

Fimbel, P. & Siffert, B. (1986). Interaction of calcium carbonate (calcite) with cellulose fibers in aqueous medium. *Colloids Surf.* **20**(1-2), 1-16.

Fleer, G., Koopal, L. & Lyklema, J. (1972). Polymer adsorption and its effect on the stability of hydrophobic colloids. *Colloid Polym. Sci.* **250**(7), 689-702.

Fleer, G.J., Cohen Stuart, M.A., Scheutjens, J.M.H.M., Cosgrove, T. & Vincent, B. (1993). *Polymers at interfaces*. Chapman & Hall, London.

Foxall, T., Peterson, G.C., Rendall, H.M. & Smith, A.L. (1979). Charge determination at calcium salt/aqueous solution interface. *J. Chem. Soc., Faraday Trans. 1* **75**(5), 1034-1039.

Fritz, G., Schädler, V., Willenbacher, N. & Wagner, N.J. (2002). Electrosteric stabilization of colloidal dispersions. *Langmuir* **18**(16), 6381-6390.

Gane, P.A.C., Schoelkopf, J., Spielmann, D.C., Matthews, G.P. & Ridgway, C.J. (2000). Fluid transport into porous coating structures: Some novel findings. *Tappi J.* **83**(5), 77-78.

Gane, P.A.C. & Rigway, C.J. (2005). A new coating structure strategy for designed absorption and optimised adsorption: A study of the use of novel pigments with nano-

surface features on micro-particles. *Pita Coating Conference: Optimising Quality and Cost in Coated Papers,* Barcelona, Spain.

Gess, J.M. & Rende, D.S. (2005). *Alkenyl Succinic Anhydride*. In: *The sizing of paper*, eds. J.M. Gess & J.M. Rodriguez, TAPPI Press, Atlanta, GA.

Ghule, K., Ghule, A., Chen, B. & Ling, Y. (2006). Preparation and characterization of ZnO nanoparticles coated paper and its antibaterial activity study. *Green Chemistry* **8**(12), 1034-1041.

Goloub, T.P., Koopal, L.K., Bijsterbosch, B.H. & Sidorova, M.P. (1996). Adsorption of cationic surfactants on silica. Surface charge effects. *Langmuir* **12**(13), 3188-3194.

Goodwin, J., Harbron, R. & Reynolds, P. (1990). Functionalization of colloidal silica and silica surfaces via silylation reactions. *Colloid Polym. Sci.* **268**(8), 766-777.

Gu, G., Dang, H., Zhang, Z. & Wu, Z. (2006). Fabrication and characterization of transparent superhydrophobic thin films based on silica nanoparticles. *Appl. Phys. A* **83**(1), 131-132.

Guimond, R., Chabot, B., Law, K.-N. & Daneault, C. (2010). The use of cellulose nanofibres in papermaking. *J. Pulp Pap. Sci.* **36**(1-2), 55-61.

Habibi, Y., Lucia, L.A. & Rojas, O.J. (2010). Cellulose nanocrystals: Chemistry, self-assembly, and applications. *Chem. Rev.* **110**(6), 3479-3500.

Halthur, T.J. & Elofsson, U.M. (2004). Multilayers of charged polypeptides as studied by in situ ellipsometry and quartz crystal microbalance with dissipation. *Langmuir* **20**(5), 1739-1745.

Hamad, W. (2006). On the development and applications of cellulosic nanofibrillar and nanocrystalline materials. *Can. J. Chem. Eng*. **84**(5), 513-519.

Hamaker, H. (1937). The London-van der Waals attraction between spherical particles. *Physica* **4**(10), 1058-1072.

Han, J.T., Zheng, Y., Cho, J.H., Xu, X. & Cho, K. (2005). Stable superhydrophobic organic-inorganic hybrid films by electrostatic self-assembly. *J. Phys. Chem. B* **109**(44), 20773-20778.

Hanarp, P., Sutherland, D.S., Gold, J. & Kasemo, B. (2001). Influence of polydispersity on adsorption of nanoparticles. *J. Colloid Interface Sci.* **241**(1), 26-31.

Henriksson, M., Berglund, L.A., Isaksson, P., Lindström, T. & Nishino, T. (2008). Cellulose nanopaper structures of high toughness. *Biomacromolecules* **9**(6), 1579-1585.

Herrick, F.W., Casebier, R.L., Hamilton, J.K. & Sandberg, K.R. (1983). Microfibrillated cellulose: Morphology and accessibility. *J. Appl. Polym. Sci.: Appl. Polym. Symp*. **37**, 797-813.

Hladnik, A. & Muck, T. (2002). Characterization of pigments in coating formulations for high-end ink-jet papers. *Dyes Pigm.* **54**(3), 253-263.

Holappa, S., Andersson, T., Kantonen, L., Plattner, P. & Tenhu, H. (2003). Soluble polyelectrolyte complexes composed of poly (ethylene oxide)-block-poly (sodium methacrylate) and poly (methacryloyloxyethyl trimethylammonium chloride). *Polymer* **44**(26), 7907-7916.

Holmberg, M., Wigren, R., Erlandsson, R. & Claesson, P.M. (1997). Interactions between cellulose and colloidal silica in the presence of polyelectrolytes. *Colloids Surf., A* **129**, 175-183.

Hsieh, C., Chen, J., Kuo, R., Lin, T. & Wu, C. (2005). Influence of surface roughness on water- and oil-repellent surfaces coated with nanoparticles. *Appl. Surf. Sci.* **240**(1-4), 318-326.

Hu, Y. & Liu, X. (2003). Chemical composition and surface property of kaolins. *Miner. Eng.* **16**(11, Suppl.), 1279-1284.

Hu, Z., Zen, X., Gong, J. & Deng, Y. (2009). Water resistance improvement of paper by superhydrophobic modification with microsized $CaCO_3$ and fatty acid coating. *Colloids Surf., A* **351**(1-3), 65-70.

Hu, Z. & Deng, Y. (2010). Superhydrophobic surface fabricated from fatty acid-modified precipitated calcium carbonate. *Ind. Eng. Chem. Res.* **49**(12), 5625-5630.

Hubbe, M.A. (2006). Paper's resistance to wetting - a review of internal sizing chemicals and their effects. *Bioresources* **2**(1), 106-145.

Huang, Y.C., Fowkes, F.M., Lloyd, T.B. & Sanders, N.D. (1991). Adsorption of calcium ions from calcium chloride solutions onto calcium carbonate particles. *Langmuir* **7**(8), 1742-1748.

Hyde, K., Dong, H. & Hinestroza, J.P. (2007a). Effect of surface cationization on the conformal deposition of polyelectrolytes over cotton fibers. *Cellulose* **14**(6), 615-623.

Hyde, G.K., Park, K.J., Stewart, S.M., Hinestroza, J.P. & Parsons, G.N. (2007b). Atomic layer deposition of Conformal inorganic nanoscale coatings on three-dimensional natural fiber systems: Effect of surface topology on film growth characteristics. *Langmuir* **23**(19), 9844-9849.

Hyväluoma, J., Raiskinmäki, P., Jäsberg, A., Koponen, A., Kataja, M. & Timonen, J. (2006). Simulation of liquid penetration in paper. *Phys. Rev. E.* **73**.

Hänni-Ciunel, K., Findenegg, G.H. & von Klitzing, R. (2007). Water contact angle on polyelectrolyte - coated surfaces: Effects of film swelling and droplet evaporation. *Soft Materials* **5**(2-3), 61-73.

Höök, F., Rodahl, M., Brzezinski, P. & Kasemo, B. (1998a). Energy dissipation kinetics for protein and antibody-antigen adsorption under shear oscillation on a quartz crystal microbalance. *Langmuir* **14**(4), 729-734.

Höök, F., Rodahl, M., Kasemo, B. & Brzezinski, P. (1998b). Structural changes in hemoglobin during adsorption to solid surfaces: Effects of pH, ionic strength, and

ligand binding. *Proceedings of the National Academy of Sciences* **95**(21), 12271-12276.

Iler, R. (1966). Multilayers of colloidal particles. *J. Colloid Interface Sci.* **21**(6), 569-594.

Israelachvili, J.N. & Pashley, R.M. (1983). Molecular layering of water at surfaces and origin of repulsive hydration forces. *Nature* **306**, 249-250.

Israelachvili, J. & Pashley, R. (1984). Measurement of the hydrophobic interaction between two hydrophobic surfaces in aqueous electrolyte solutions. *J. Colloid Interface Sci.* **98**(2), 500-514.

Janhom, S. (2010). Polyethyleneimine/sodium dodecyl sulphate adsorbed silica particles and their adsorption properties. *Colloids Surf., A* **369**(1-3), 186-190.

Jiang, J., Oberdörster, G. & Biswas, P. (2009). Characterization of size, surface charge, and agglomeration state of nanoparticle dispersions for toxicological studies. *J. Nanopart. Res.* **11**(1), 77-89.

Jiang, X., Tong, M., Li, H. & Yang, K. (2010). Deposition kinetics of zinc oxide nanoparticles on natural organic matter coated silica surfaces. *J. Colloid Interface Sci.* **350**(2), 427-434.

Johannsmann, D., Mathauer, K., Wegner, G. & Knoll, W. (1992). Viscoelastic properties of thin films produced with a quartz-crystal resonator. *Phys. Rev. B* **46**(12), 7808-7815.

Johannsmann, D., Reviakine, I. & Richter, R.P. (2009). Dissipation in films of adsorbed nanospheres studied by quartz crystal microbalance (QCM). *Anal. Chem.* **81**(19), 8167-8176.

Juuti, M., Koivunen, K., Silvennoinen, M., Paulapuro, H. & Peiponen, K. (2009). Light scattering study from nanoparticle-coated pigments of paper. *Colloids Surf., A* **352**(1-3), 94-98.

Kallay, N. (2002). Stability of nanodispersions: A model for kinetics of aggregation of nanoparticles. *J. Colloid Interface Sci.* **253**(1), 70-76.

Kamel, S. (2007). Nanotechnology and its applications in lignocellulosic composites. *Express Polym. Lett.* **1**(9), 546-575.

Kamiya, H. & Iijima, M. (2010). Surface modification and characterization for dispersion stability of inorganic nanometer-scaled particles in liquid media. *Sci. Technol. Adv. Mater.* **11**(4).

Kettle, J., Lamminmäki, T. & Gane, P. (2010). A review of modified surfaces for high speed inkjet coating. *Surf. Coat. Technol.* **204**(12-13), 2103-2109.

Kettunen, M., Silvennoinen, R.J., Houbenov, N., Nykänen, A., Ruokolainen, J., Sainio, J., Pore, V., Kemell, M., Ankerfors, M., Lindström, T., Ritala, M., Ras, R.H.A. & Ikkala, O. (2011). Photoswitchable superabsorbency based on nanocellulose aerogels. *Adv. Funct. Mater.* **21**(3), 510-517.

Kim, D.S. & Lee, C.K. (2002). Surface modification of precipitated calcium carbonate using aqueous fluosilicic acid. *Appl. Surf. Sci.* **202**(1-2), 15-23.

Kleimann, J., Gehin-Delval, C., Auweter, H. & Borkovec, M. (2005). Super-stoichiometric charge neutralization in particle-polyelectrolyte systems. *Langmuir* **21**(8), 3688-3698.

Koepenick, M. (2001). Paper innovation ramps up with nano-chemistry. *Pulp Pap. Can.* **102**(1), 17-18, 21.

Koepenick, M. (2003). Nanotech supports grade evolution. *Pulp Pap. Can.* **104**(1), 16.

Koivunen, K., Niskanen, I., Peiponen, K. & Paulapuro, H. (2009). Novel nanostructured PCC fillers. *J. Mater. Sci.* **44**(2), 477-482.

Kolasinska, M. & Warszynski, P. (2005). The effect of support material and conditioning on wettability of PAH/PSS multilayer films. *Bioelectrochemistry* **66**, 65-70.

Kolasinska, M., Zembala, M., Krasowska, M. & Warszynski, P. (2008). Probing of polyelectrolyte monolayers by zeta potential and wettability measurements. *J. Colloid Interface Sci.* **326**, 301-304.

Kontturi, E., Thuene, P.C. & Niemantsverdriet, J.W. (2003). Cellulose model surfaces - simplified preparation by spin coating and characterization by X-ray photoelectron spectroscopy, infrared spectroscopy, and atomic force microscopy. *Langmuir* **19**(14), 5735-5741.

Kontturi, E., Johansson, L.S., Kontturi, K.S., Ahonen, P., Thüne, P.C. & Laine, J. (2007). Cellulose nanocrystal submonolayers by spin coating. *Langmuir* **23**(19), 9674-9680.

Koopmans, T. (1933). The distribution of wave function and characteristic value among the individual electrons of an atom. *Physica* **1**, 104-113.

Korhonen, J., Kettunen, M., Ras, R.H.A. & Ikkala, O. (2011). Hydrophobic nanocellulose aerogels as floating, sustainable, reusable, and recyclable oil absorbents. *ACS Appl. Mater. Interfaces* **3**(6), 1813-1816.

Kotov, N.A., Dekany, I. & Fendler, J.H. (1995). Layer-by-layer self-assembly of polyelectrolyte-semiconductor nanoparticle composite films. *J. Phys. Chem.* **99**(35), 13065-13069.

Kruglyakov, P.M. & Nushtayeva, A.V. (2004). Phase inversion in emulsions stabilized by solid particles. *Adv. Colloid Interface Sci.* **108-109**, 151-158.

Laine, J., Lindström, T., Nordmark, G.G. & Risinger, G. (2000). Studies on topochemical modification of cellulosic fibers. Part 1. Chemical conditions for the attachment of carboxymethyl cellulose onto fibers. *Nord. Pulp Pap. Res. J.* **15**(5), 520-526.

Lan, Q. (2007). Silica nanoparticle dispersions in polymers: Homopolymer versus block copolymer. *J. Polym. Sci., Part B: Polym. Phys.* **45**(16), 2284-2299.

Lavalle, P., Gergely, C., Cuisinier, F., Decher, G., Schaaf, P., Voegel, J. & Picart, C. (2002). Comparison of the structure of polyelectrolyte multilayer films exhibiting a linear and

an exponential growth regime: An in situ atomic force microscopy study. *Macromolecules* **35**(11), 4458-4465.

Lemarchand, C., Couvreur, P., Vauthier, C., Costantini, D. & Gref, R. (2003). Study of emulsion stabilization by graft copolymers using the optical analyzer Turbiscan. *Int. J. Pharm.* **254**(1), 77-82.

Li, L.C. & Tian, Y. (2002). Zeta potential. *Encyclopedia of pharmaceutical technology* **2**, 429-458.

Lifshitz, E. (1956). The theory of molecular attractive forces between solids. *Soviet Phys. JETP* **2**(73).

Lin, Z., Renneckar, S. & Hindman, D.P. (2008). Nanocomposite-based lignocellulosic fibers 1. Thermal stability of modified fibers with clay-polyelectrolyte multilayers. *Cellulose* **15**(2), 333-346.

Lindfors, J., Ahola, S., Kallio, T., Laine, J., Stenius, P. & Danielsson, M. (2005). Spreading and adhesion of ASA on different surfaces present in paper machines. *Nord. Pulp Pap. Res. J.* **20**(4), 453-458.

Lindquist, G.M. & Stratton, R.A. (1976). The role of polyelectrolyte charge density and molecular weight on the adsorption and flocculation of colloidal silica with polyethylenimine. *J. Colloid Interface Sci.* **55**(1), 45-59.

Lingström, R., Wågberg, L. & Larsson, P.T. (2006). Formation of polyelectrolyte multilayers on fibres: Influence on wettability and fibre/fibre interaction. *J. Colloid Interface Sci.* **296**(2), 396-408.

Lingström, R., Notley, S.M. & Wågberg, L. (2007). Wettability changes in the formation of polymeric multilayers on cellulose fibers and their influence on wet adhesion. *J. Colloid Interface Sci.* **314**(1), 1-9.

Liu, A., Walther, A., Ikkala, O., Belova, L. & Berglund, L.A. (2011a). Clay nanopaper with tough cellulose nanofiber matrix for fire retardancy and gas barrier functions. *Biomacromolecules* **12**(3), 633-641.

Liu, Z., Choi, H., Gatenholm, P. & Esker, A.R. (2011b). Quartz crystal microbalance with dissipation monitoring and surface plasmon resonance studies of carboxymethyl cellulose adsorption onto regenerated cellulose surfaces. *Langmuir* **27**(14), 8718-8728.

Liufu, S., Xiao, H. & Li, Y. (2005). Adsorption of cationic polyelectrolyte at the solid/liquid interface and dispersion of nanosized silica in water. *J. Colloid Interface Sci.* **285**(1), 33-40.

Lourenco, C., Teixeira, M., Simões, S. & Gaspar, R. (1996). Steric stabilization of nanoparticles: Size and surface properties. *Int. J. Pharm.* **138**(1), 1-12.

Lowack, K. & Helm, C. (1995). Polyelectrolyte monolayers at the mica/air interface: Mechanically induced rearrangements and monolayer annealing. *Macromolecules* **28**(8), 2912-2921.

Lu, S., Kunjappu, J.T., Somasundaran, P. & Zhang, L. (2008). Adsorption of a double-chain surfactant on an oxide. *Colloids Surf., A* **324**(1-3), 65-70.

Lucas, R. (1918). Rate of capillary ascension of liquids. *Kolloid Z.* **23(15)**

Lvov, Y., Ariga, K., Onda, M., Ichinose, I. & Kunitake, T. (1997). Alternate assembly of ordered multilayers of SiO_2 and other nanoparticles and polyions. *Langmuir* **13**(23), 6195-6203.

Lvov, Y.M., Rusling, J.F., Thomsen, D.L., Papadimitrakopoulos, F., Kawakami, T. & Kunitake, T. (1998). High-speed multilayer film assembly by alternate adsorption of silica nanoparticles and linear polycation. *Chem. Commun.* (11), 1229-1230.

Marmur, A. & Bittoun, E. (2009). When Wenzel and Cassie are right: Reconciling local and global considerations. *Langmuir* **25**(3), 1277-1281.

Martines, E., Seunarine, K., Morgan, H., Gadegaard, N., Wilkinson, C.D.W. & Riehle, M.O. (2005). Superhydrophobicity and superhydrophilicity of regular nanopatterns. *Nano Lett.* **5**(10), 2097-2103.

Maximova, N., Österberg, M., Laine, J. & Stenius, P. (2004). The wetting properties and morphology of lignin adsorbed on cellulose fibres and mica. *Colloids Surf., A* **239**(1-3), 65-75.

McConnell, M.D., Bassani, A.W., Yang, S. & Composto, R.J. (2009). Tunable wetting of nanoparticle-decorated polymer films. *Langmuir* **25**(18), 11014-11020.

Mende, M., Petzold, G. & Buchhammer, H.M. (2002). Polyelectrolyte complex formation between poly (diallyldimethyl-ammonium chloride) and copolymers of acrylamide and sodium-acrylate. *Colloid Polym. Sci.* **280**(4), 342-351.

Mengual, O., Meunier, G., Cayre, I., Puech, K. & Snabre, P. (1999a). TURBISCAN MA 2000: Multiple light scattering measurement for concentrated emulsion and suspension instability analysis. *Talanta* **50**(2), 445-456.

Mengual, O., Meunier, G., Cayre, I., Puech, K. & Snabre, P. (1999b). Characterization of instability of concentrated dispersions by a new optical analyzer: The TURBISCAN MA 1000. *Colloids Surf., A* **152**(1-2), 111-123.

Messina, R., Holm, C. & Kremer, K. (2004). Polyelectrolyte adsorption and multilayering on charged colloidal particles. *J. Polym. Sci. Part B* **42**(19), 3557-3570.

Metin, C.O., Lake, L.W., Miranda, C.R. & Nguyen, Q.P. (2011). Stability of aqueous silica nanoparticle dispersions. *J. Nanopart. Res.* **13**(2), 839-850.

Meyerhofer, D. (1978). Characteristics of resist films produced by spinning. *J. Appl. Phys.* **49**(7), 3993-3997.

Midmore, B. (1998). Preparation of a novel silica-stabilized oil/water emulsion. *Colloids Surf., A* **132**(2-3), 257-265.

Miklavic, S., Woodward, C., Joensson, B. & Åkesson, T. (1990). The interaction of charged surfaces with grafted polyelectrolytes: A Poisson-Boltzmann and Monte Carlo study. *Macromolecules* **23**(18), 4149-4157.

Modaressi, H. & Garnier, G. (2002). Mechanism of wetting and absorption of water droplets on sized paper: Effects of chemical and physical heterogeneity. *Langmuir* **18**(3), 642-649.

Moon, R.J., Frihart, C.R. & Wegner, T. (2006). Nanotechnology applications in the forest products industry. *For. Prod. J.* **56**(5), 4-10.

Moulinet, S., Guthmann, C. & Rolley, E. (2002). Roughness and dynamics of a contact line of a viscous fluid on a disordered substrate. *Eur. Phys. J. E: Soft Matter Biol. Phys.* **8**(4), 437-443.

Myllytie, P. (2009). *Interactions of polymers with fibrillar structure of cellulose fibres: A new approach to bonding and strength in paper*, Doctoral thesis, TKK, Espoo, Finland.

Mörseburg, K. & Chinga-Carrasco, G. (2009). Assessing the combined benefits of clay and nanofibrillated cellulose in layered TMP-based sheets. *Cellulose* **16**(5), 795-806.

Naderi, A. & Claesson, P.M. (2006). Adsorption properties of polyelectrolyte-surfactant complexes on hydrophobic surfaces studied by QCM-D. *Langmuir* **22**(18), 7639-7645.

Neuman, R., Berg, J. & Claesson, P. (1993). Direct measurement of surface forces in papermaking and paper coating systems. *Nord. Pulp Pap. Res. J.* **8**(1), 96-104.

Neumann, D., Raverty, W.D. & Vanderhoek, N. (2005). Nanostructured materials and their use in ink receptor layers. *59th Appita Annual Conference and Exhibition,* Auckland, New Zealand.

Nogi, M., Iwamoto, S., Nakagaito, A.N. & Yano, H. (2009). Optically transparent nanofiber paper. *Adv. Mater.* **21**(16), 1595-1598.

Norgren, M., Notley, S.M., Majtnerova, A. & Gellerstedt, G. (2006). Smooth model surfaces from lignin derivatives. I. Preparation and characterization. *Langmuir* **22**(3), 1209-1214.

Norgren, M., Gärdlund, L., Notley, S.M., Htun, M. & Wågberg, L. (2007). Smooth model surfaces from lignin derivatives. II. Adsorption of polyelectrolytes and PECs monitored by QCM-D. *Langmuir* **23**(7), 3737-3743.

Norrish, K. (1954). The swelling of montmorillonite. *Discuss. Faraday Soc.* **18**, 120-134.

Notley, S.M., Eriksson, M. & Wågberg, L. (2005). Visco-elastic and adhesive properties of adsorbed polyelectrolyte multilayers determined in situ with QCM-D and AFM measurements. *J. Colloid Interface Sci.* **292**(1), 29-37.

Notley, S.M. & Leong, Y. (2010). Interaction between silica in the presence of adsorbed poly(ethyleneimine): Correlation between colloidal probe adhesion measurements and yield stress. *Phys. Chem. Chem. Phys.* **12**(35), 10594-10601.

Ohshima, H. (1995). Electrophoretic mobility of soft particles. *Colloids Surf., A* **103**(3), 249-255.

Okahisa, Y., Yoshida, A., Miyaguchi, S. & Yano, H. (2009). Optically transparent wood-cellulose nanocomposite as a base substrate for flexible organic light-emitting diode displays. *Compos. Sci. Technol.* **69**(11-12), 1958-1961.

Okubo, T. & Suda, M. (1999). Alternate sign reversal in the z potential and synchronous expansion and contraction in the absorbed multilayers of poly(4-vinyl-N-n-butylpyridinium bromide) cations and poly(styrene sulfonate) anions on colloidal silica spheres. *Colloid Polym. Sci.* **277**(9), 813-817.

Olsson, R.T., Azizi Samir, M.A.S., Salazar-Alvarez, G., Belova, L., Ström, V., Berglund, L.A., Ikkala, O., Nogues, J. & Gedde, U.W. (2011). Making flexible magnetic aerogels and stiff magnetic nanopaper using cellulose nanofibrils as templates. *Nat. Nanotechnol.* **5**(8), 584-588.

Olszewska, A., Eronen, P., Johansson, L.S., Malho, J.M., Ankerfors, M., Lindström, T., Ruokolainen, J., Laine, J. & Österberg, M. (2011). The behaviour of cationic nanofibrillar cellulose in aqueous media. *Cellulose* **18**(5), 1213-1226.

Ondaral, S., Wågberg, L. & Enarsson, L. (2006). The adsorption of hyperbranched polymers on silicon oxide surfaces. *J. Colloid Interface Sci.* **301**(1), 32-39.

Pashley, R. & Israelachvili, J. (1984). DLVO and hydration forces between mica surfaces in Mg^{2+}, Ca^{2+}, Sr^{2+}, and Ba^{2+} chloride solutions. *J. Colloid Interface Sci.* **97**(2), 446-455.

Pashley, R. & Quirk, J. (1984). The effect of cation valency on DLVO and hydration forces between macroscopic sheets of muscovite mica in relation to clay swelling. *Colloids Surf.* **9**(1), 1-17.

Patwardhan, S.V., Mukherjee, N. & Clarson, S.J. (2002). Effect of process parameters on the polymer mediated synthesis of silica at neutral pH. *Silicon Chem.* **1**(1), 47-55.

Pham, K.N., Fullston, D. & Sagoe-Crentsil, K. (2007). Surface charge modification of nano-sized silica colloid. *Aust. J. Chem.* **60**(9), 662-666.

Pickering, S.U. (1907). Emulsions. *J. Chem. Soc., Trans.* **91**, 2001-2021.

Plunkett, M.A., Claesson, P.M. & Rutland, M.W. (2002). Adsorption of a cationic polyelectrolyte followed by surfactant-induced swelling, studied with a quartz crystal microbalance. *Langmuir* **18**(4), 1274-1280.

Plunkett, M.A., Wang, Z., Rutland, M.W. & Johannsmann, D. (2003). Adsorption of pNIPAM layers on hydrophobic gold surfaces, measured in situ by QCM and SPR. *Langmuir* **19**(17), 6837-6844.

Pääkkö, M., Ankerfors, M., Kosonen, H., Nykänen, A., Ahola, S., Österberg, M., Ruokolainen, J., Laine, J., Larsson, P.T., Ikkala, O. & Lindström, T. (2007). Enzymatic hydrolysis combined with mechanical shearing and high-pressure homogenization for nanoscale cellulose fibrils and strong gels. *Biomacromolecules* **8**(6), 1934-1941.

Qin, F., Zhou, Y., Shi, J. & Zhang, Y. (2009). A DNA transporter based on mesoporous silica nanospheres mediated with polycation poly (allylamine hydrochloride) coating on mesopore surface. *J. Biomed. Mater. Res., Part A* **90**(2), 333-338.

Quéré, D. (2005). Non-sticking drops. *Rep. Prog. Phys* **68**, 2495-2532.

Radhakrishnan, B., Ranjan, R. & Brittain, W.J. (2006). Surface initiated polymerizations from silica nanoparticles. *Soft Matter* **2**(5), 386-396.

Rahim, M.A., San Choi, W., Lee, H.J., Park, J.B. & Jeon, I.C. (2011). Unusual growth of polyelectrolyte multilayers by introduction of a rugged multilayer template and their unique adsorption behaviors. *Polymer* **52**(14), 3112-3117.

Ren, S., Yang, S., Zhao, Y., Yu, T. & Xiao, X. (2003). Preparation and characterization of an ultrahydrophobic surface based on a stearic acid self-assembled monolayer over polyethyleneimine thin films. *Surf. Sci.* **546**, 64-74.

Ridgway, C.J. & Gane, P.A.C. (2002). Dynamic absorption into simulated porous structures. *Colloids Surf., A* **206**(1-3), 217-239.

Ridgway, C.J. & Gane, P.A.C. (2006). Correlating pore size and surface chemistry during absorption into a dispersed calcium carbonate network structure. *Nord. Pulp Pap. Res. J.* **21**(5), 563-568.

Roberts, J.C. (1997). A review of advances in internal sizing of paper. Cambridge, UK.

Rojas, O.J. (2002). *Adsorption of polyelectrolytes on mica*. In: *Encyclopedia of Surface and Colloid Science*. Marcel Dekker Inc., New York.

Rojas, O.J., Ernstsson, M., Neuman, R.D. & Claesson, P.M. (2002). Effect of polyelectrolyte charge density on the adsorption and desorption behavior on mica. *Langmuir* **18**(5), 1604-1612.

Rong, M.Z., Zhang, M.Q. & Ruan, W.H. (2006). Surface modification of nanoscale fillers for improving properties of polymer nanocomposites: A review. *Mater. Sci. Technol.* **22**(7), 787-796.

Rutland, M.W., Carambassis, A., Willing, G.A. & Neuman, R.D. (1997). Surface force measurements between cellulose surfaces using scanning probe microscopy. *Colloids Surf., A* **123-124**, 369-374.

Ryu, R.Y., Gilbert, R.D. & Khan, S.A. (1999). Influence of cationic additives on the rheological, optical, and printing properties of ink-jet coatings. *Tappi J.* **82**(11), 128-134.

Saarinen, T., Österberg, M. & Laine, J. (2008). Adsorption of polyelectrolyte multilayers and complexes on silica and cellulose surfaces studied by QCM-D. *Colloids Surf., A* **330**(2-3), 134-142.

Saarinen, T., Österberg, M. & Laine, J. (2009). Properties of cationic polyelectrolyte layers adsorbed on silica and cellulose surfaces studied by QCM-D - Effect of polyelectrolyte charge density and molecular weight. *J. Dispersion Sci. Technol.* **30**(6), 969-979.

Sadovoy, A.V., Kiryukhin, M.V., Sukhorukov, G.B. & Antipina, M.N. (2011). Kinetic stability of water-dispersed oil droplets encapsulated in a polyelectrolyte multilayer shell. *Phys. Chem. Chem. Phys.* **13**(9), 4005-4012.

Salmi, J., Österberg, M. & Laine, J. (2007a). The effect of cationic polyelectrolyte complexes on interactions between cellulose surfaces. *Colloids Surf., A* **297**(1-3), 122-130.

Salmi, J., Österberg, M., Stenius, P. & Laine, J. (2007b). Surface forces between cellulose surfaces in cationic polyelectrolyte solutions: The effect of polymer molecular weight and charge density. *Nord. Pulp Pap. Res. J.* **22**(2), 249-257.

Sauerbrey, G. (1959). The use of quartz oscillators for weighing thin layers and for microweighing. *Z. Phys.* **155**, 206-222.

Schoelkopf, J., Gane, P.A.C., Ridgway, C.J. & Matthews, G.P. (2000). Influence of inertia on liquid absorption into paper coating structures. *Nord. Pulp Pap. Res. J.* **15**(5), 422-430.

Schoelkopf, J., Gane, P.A.C., Ridgway, C.J. & Matthews, G.P. (2002). Practical observation of deviation from Lucas-Washburn scaling in porous media. *Colloids Surf., A* **206**(1-3), 445-454.

Schwarz, S., Lunkwitz, K., Kessler, B., Spiegler, U., Killmann, E. & Jaeger, W. (2000). Adsorption and stability of colloidal silica. *Colloids Surf., A* **163**(1), 17-27.

Sehaqui, H., Liu, A., Zhou, Q. & Berglund, L.A. (2010). Fast preparation procedure for large, flat cellulose and cellulose/inorganic nanopaper structures. *Biomacromolecules* **11**(9), 2195-2198.

Sennerfors, T., Bogdanovic, G. & Tiberg, F. (2002). Formation, chemical composition, and structure of polyelectrolyte-nanoparticle multilayer films. *Langmuir* **18**(16), 6410-6415.

Shibuichi, S., Onda, T., Satoh, N. & Tsujii, K. (1996). Super water-repellent surfaces resulting from fractal structure. *J. Phys. Chem.* **100**(50), 19512-19517.

Shiratori, S.S. & Rubner, M.F. (2000). pH-Dependent thickness behavior of sequentially adsorbed layers of weak polyelectrolytes. *Macromolecules* **33**(11), 4213-4219.

Shovsky, A., Bijelic, G., Varga, I., Makuska, R. & Claesson, P.M. (2011). Adsorption characteristics of stoichiometric and nonstoichiometric molecular polyelectrolyte complexes on silicon oxynitride surfaces. *Langmuir* **27**(3), 1044-1050.

Siro, I. & Plackett, D. (2010). Microfibrillated cellulose and new nanocomposite materials: A review. *Cellulose* **17**(3), 459-494.

Solberg, D. & Wågberg, L. (2003). Adsorption and flocculation behavior of cationic polyacrylamide and colloidal silica. *Colloids Surf., A* **219**(1-3), 161-172.

Song, J., Li, Y., Hinestroza, J.P. & Rojas, O.J. (2009). *Tools to probe nanoscale surface phenomena in cellulose thin films: Application in the area of adsorption and friction*. In: *Nanoscience and Technology of Renewable Biomaterials*, eds. L.A. Lucia & O.J. Rojas. Wiley, Chichester.

Spori, D.M., Drobek, T., Zuercher, S., Ochsner, M., Sprecher, C., Muehlebach, A. & Spencer, N.D. (2008). Beyond the lotus effect: Roughness influences on wetting over a wide surface-energy range. *Langmuir* **24**(10), 5411-5417.

Studart, A.R., Amstad, E. & Gauckler, L.J. (2007). Colloidal stabilization of nanoparticles in concentrated suspensions. *Langmuir* **23**(3), 1081-1090.

Sun, Q., Schork, F.J. & Deng, Y. (2007). Water-based polymer/clay nanocomposite suspension for improving water and moisture barrier in coating. *Compos. Sci. Technol.* **67**(9), 1823-1829.

Syverud, K. & Stenius, P. (2009). Strength and barrier properties of MFC films. *Cellulose* **16**(1), 75-85.

Sörensen, M.H., Samoshina, Y., Claesson, P.M. & Alberius, P. (2009). Sustained release of ibuprofen from polyelectrolyte encapsulated mesoporous carriers. *J. Dispersion Sci. Technol.* **30**(6), 892-902

Tammelin, T., Österberg, M., Johansson, L.S. & Laine, J. (2006). Preparation of lignin and extractive model surfaces using spincoating technique - application for QCM-D studies. *Nord. Pulp Pap. Res. J.* **21**(4), 444-450.

Tang, Y., Li, Y., Song, J. & Chen, L. (2006). Surface modification of nanometer calcium carbonate and its effect on dynamic viscoelasticity of paper coatings. *3rd International Symposium on Emerging Technologies of Pulping and Papermaking*, Guangzhou, China.

Taniguchi, T. & Okamura, K. (1998). New films produced from microfibrillated natural fibres. *Polym. Int.* **47**(3), 291-294.

Tehrani-Bagha, A. & Holmberg, K. (2008). Cationic ester-containing Gemini surfactants: Adsorption at Tailor-made surfaces monitored by SPR and QCM. *Langmuir* **24**(12), 6140-6145.

Teisala, H., Tuominen, M., Aromaa, M., Mäkelä, J., Stepien, M., Saarinen, J., Toivakka, M. & Kuusipalo, J. (2010). Development of superhydrophobic coating on paperboard surface using the liquid flame spray. *Surf. Coat. Technol.* **205**(2), 436-445.

Tellechea, E., Johannsmann, D., Steinmetz, N.F., Richter, R.P. & Reviakine, I. (2009). Model-independent analysis of QCM data on colloidal particle adsorption. *Langmuir* **25**(9), 5177-5184.

Tolnai, G., Csempesz, F., Kabai-Faix, M., Kalman, E., Keresztes, Z., Kovacs, A.L., Ramsden, J.J. & Horvoelgyi, Z. (2001). Preparation and characterization of surface-modified silica-nanoparticles. *Langmuir* **17**(9), 2683-2687.

Tougaard, S. (1998). Accuracy of the non-destructive surface nanostructure quantification technique based on analysis of the XPS or AES peak shape. *Surf. Interface Anal.* **26**(4), 249-269.

Tougaard, S. (1996). Surface nanostructure determination by x-ray photoemission spectroscopy peak shape analysis. *J. Vac. Sci. Technol., A* **14**(3), 1415-1423.

Tunc, S. & Duman, O. (2010). Preparation and characterization of biodegradable methyl cellulose/montmorillonite nanocomposite films. *Appl. Clay Sci.* **48**(3), 414-424.

Turbak, A.F., Snyder, F.W. & Sandberg, K.R. (1983). Microfibrillated cellulose, a new cellulose product: Properties, uses, and commercial potential. *J. Appl. Polym. Sci.: Appl. Polym. Symp.* **37**, 815-827.

Ulrich, S., Laguecir, A. & Stoll, S. (2004). Complex formation between a nanoparticle and a weak polyelectrolyte chain: Monte Carlo simulations. *J. Nanopart. Res.* **6**(6), 595-603.

van de Steeg, H.G.M., Cohen Stuart, M.A., De Keizer, A. & Bijsterbosch, B.H. (1992). Polyelectrolyte adsorption: A subtle balance of forces. *Langmuir* **8**(10), 2538-2546.

van Olphen, H. (1977). *An introduction to clay colloid chemistry: For clay technologists, geologists, and soil scientists*. Wiley-Interscience Publication, New York.

Vanerek, A., Alince, B. & van de Ven, T.G.M. (2000). Interaction of calcium carbonate fillers with pulp fibers: Effect of surface charge and cationic polyelectrolytes. *J. Pulp Paper Sci.* **26**(9), 317-322.

Verwey, E.J.W. & Overbeek, J.T.G. (1948). *Theory of the Stability of Lyophobic Colloids*. Elsevier, Amsterdam.

von Bahr, M., Seppänen, R., Tiberg, F. & Zhmud, B. (2004). Dynamic wetting of AKD-sized papers. *J. Pulp Pap. Sci.* **30**(3), 74-81.

Vrancken, K., Possemiers, K., van der Voort, P. & Vansant, E. (1995). Surface modification of silica gels with aminoorganosilanes. *Colloids Surf., A* **98**(3), 235-241.

Walecka, J.A. (1956). Low degree of substitution carboxymethylcelluloses. *Tappi J.* **39**, 458-463.

Wallqvist, V., Claesson, P.M., Swerin, A., Schoelkopf, J. & Gane, P.A.C. (2006). Interaction forces between talc and hydrophobic particles probed by AFM. *Colloids Surf., A* **277**(1-3), 183-190.

Wallqvist, V., Claesson, P.M., Swerin, A., Schoelkopf, J. & Gane, P.A.C. (2007). Interaction forces between talc and pitch probed by atomic force microscopy. *Langmuir* **23**(8), 4248-4256.

Wang, Z., Hauser, P.J., Laine, J. & Rojas, O.J. (2011). Multilayers of low charge density polyelectrolytes on thin films of carboxymethylated and cationic cellulose. *J. Adhes. Sci. Technol.* **6**, 643-660.

Washburn, E.W. (1921). The dynamics of capillary flow. *Phys. Rev.* **17**(3), 273-283.

Wegner, T.H. & Jones, P.E. (2006). Advancing cellulose-based nanotechnology. *Cellulose* **13**(2), 115-118.

Wenzel, R.N. (1936). Resistance of solid surfaces to wetting by water. *J. Ind. Eng. Chem.* **28**, 988-994.

Wilson, P. (2005). *Surface sizing*. In: *The sizing of paper*, eds. J.M. Gess & J.M. Rodriguez, TAPPI Press, Atlanta, GA.

Wågberg, L., Forsberg, S., Johansson, A. & Juntti, P. (2002). Engineering of fibre surface properties by application of the polyelectrolyte multilayer concept. Part I. Modification of paper strength. *J. Pulp Paper Sci.* **28**(7), 222-228.

Wågberg, L., Decher, G., Norgren, M., Lindström, T., Ankerfors, M. & Axnäs, K. (2008). The build-up of polyelectrolyte multilayers of microfibrillated cellulose and cationic polyelectrolytes. *Langmuir* **24**(3), 784-795.

Xhanari, K., Syverud, K. & Stenius, P. (2011). Emulsions stabilized by microfibrillated cellulose: The effect of hydrophobization, concentration and o/w ratio. *J.Dispersion Sci.Technol.* **32**(3), 447-452.

Xia, T., Kovochich, M., Liong, M., Meng, H., Kabehie, S., George, S., Zink, J.I. & Nel, A.E. (2009). Polyethyleneimine coating enhances the cellular uptake of mesoporous silica nanoparticles and allows safe delivery of siRNA and DNA constructs. *ACS Nano* **3**(10), 3273-3286.

Xiao, L., Salmi, J., Laine, J. & Stenius, P. (2009). The effects of polyelectrolyte complexes on dewatering of cellulose suspension. *Nord. Pulp Pap. Res. J.* **24**(2), 148-157.

Xu, D., Hodges, C., Ding, Y., Biggs, S., Brooker, A. & York, D. (2010). Adsorption kinetics of laponite and ludox silica nanoparticles onto a deposited poly (diallyldimethylammonium chloride) layer measured by a quartz crystal microbalance and optical reflectometry. *Langmuir* **26**(23), 18105-18112.

Yan, L., Wang, K., Wu, J. & Ye, L. (2007). Hydrophobicity of model surfaces with closely packed nano- and micro-spheres. *Colloids Surf., A* **296**(1-3), 123-131.

Yano, H., Sugiyama, J., Nakagaito, A.N., Nogi, M., Matsuura, T., Hikita, M. & Handa, K. (2005). Optically transparent composites reinforced with networks of bacterial nanofibers. *Adv. Mater.* **17**(2), 153-155.

Yoon, R.H. & Ravishankar, S. (1996). Long-range hydrophobic forces between mica surfaces in dodecylammonium chloride solutions in the presence of dodecanol. *J. Colloid Interface Sci.* **179**(2), 391-402.

Yoon, R.H., Flinn, D.H. & Rabinovich, Y.I. (1997). Hydrophobic interactions between dissimilar surfaces. *J. Colloid Interface Sci.* **185**(2), 363-370.

Yoshimitsu, Z., Nakajima, A., Watanabe, T. & Hashimoto, K. (2002). Effects of surface structure on the hydrophobicity and sliding behavior of water droplets. *Langmuir* **18**(15), 5818-5822.

Yotsumoto, H. & Yoon, R.H. (1993). Application of extended DLVO theory: II. Stability of silica suspensions. *J. Colloid Interface Sci.* **157**(2), 434-441.

Yüce, M.Y. & Demirel, A.L. (2008). The effect of nanoparticles on the surface hydrophobicity of polystyrene. *Eur. Phys. J. B* **64**(3-4), 493-497.

Zauscher, S. & Klingenberg, D.J. (2000). Normal forces between cellulose surfaces measured with colloidal probe microscopy. *J. Colloid Interface Sci.* **229**(2), 497-510.

Åkesson, T., Woodward, C. & Jönsson, B. (1989). Electric double layer forces in the presence of polyelectrolytes. *J. Chem. Phys.* **91**(4), 2461-2469.

Aalto-DD 12/2012

ISBN 978-952-60-4498-9
ISBN 978-952-60-4499-6 (pdf)
ISSN-L 1799-4934
ISSN 1799-4934
ISSN 1799-4942 (pdf)

Aalto University
School of Chemical Technology
Department of Forest Products Technology
www.aalto.fi

BUSINESS +
ECONOMY

ART +
DESIGN +
ARCHITECTURE

SCIENCE +
TECHNOLOGY

CROSSOVER

**DOCTORAL
DISSERTATIONS**